Connecting via Winsock to STN

Welcome to STN International! Enter x:x

LOGINID:ssspta1644pnh

PASSWORD:
TERMINAL (ENTER 1, 2, 3, OR ?):2

* * * * * * * * * * Welcome to STN International * * * * * * * * * *

NEWS 1		Web Page URLs for STN Seminar Schedule - N. America
NEWS 2		"Ask CAS" for self-help around the clock
NEWS 3	DEC 23	New IPC8 SEARCH, DISPLAY, and SELECT fields in USPATFULL/ USPAT2
NEWS 4	JAN 13	IPC 8 searching in IFIPAT, IFIUDB, and IFICDB
NEWS 5	JAN 13	New IPC 8 SEARCH, DISPLAY, and SELECT enhancements added to INPADOC
NEWS 6	JAN 17	Pre-1988 INPI data added to MARPAT
NEWS 7	JAN 17	IPC 8 in the WPI family of databases including WPIFV
NEWS 8	JAN 30	Saved answer limit increased
NEWS 9	FEB 21	STN AnaVist, Version 1.1, lets you share your STN AnaVist visualization results
NEWS 10	FEB 22	The IPC thesaurus added to additional patent databases on STN
NEWS 11	FEB 22	Updates in EPFULL; IPC 8 enhancements added
NEWS 12	FEB 27	New STN AnaVist pricing effective March 1, 2006
NEWS 13	FEB 28	MEDLINE/LMEDLINE reload improves functionality
NEWS 14	FEB 28	TOXCENTER reloaded with enhancements
NEWS 15	FEB 28	REGISTRY/ZREGISTRY enhanced with more experimental spectral property data
NEWS 16	MAR 01	INSPEC reloaded and enhanced
NEWS 17	MAR 03	Updates in PATDPA; addition of IPC 8 data without attributes
NEWS 18	MAR 08	X.25 communication option no longer available after June 2006
NEWS 19	MAR 22	EMBASE is now updated on a daily basis
NEWS 20	APR 03	New IPC 8 fields and IPC thesaurus added to PATDPAFULL
NEWS 21	APR 03	Bibliographic data updates resume; new IPC 8 fields and IPC thesaurus added in PCTFULL
NEWS 22	APR 04	STN AnaVist $500 visualization usage credit offered
NEWS 23	APR 12	LINSPEC, learning database for INSPEC, reloaded and enhanced
NEWS 24	APR 12	Improved structure highlighting in FQHIT and QHIT display in MARPAT
NEWS 25	APR 12	Derwent World Patents Index to be reloaded and enhanced during second quarter; strategies may be affected

NEWS EXPRESS FEBRUARY 15 CURRENT VERSION FOR WINDOWS IS V8.01a,
CURRENT MACINTOSH VERSION IS V6.0c(ENG) AND V6.0Jc(JP),
AND CURRENT DISCOVER FILE IS DATED 19 DECEMBER 2005.
V8.0 AND V8.01 USERS CAN OBTAIN THE UPGRADE TO V8.01a AT
http://download.cas.org/express/v8.0-Discover/

NEWS HOURS	STN Operating Hours Plus Help Desk Availability
NEWS LOGIN	Welcome Banner and News Items
NEWS IPC8	For general information regarding STN implementation of IPC 8

Enter NEWS followed by the item number or name to see news on that specific topic.

of commercial gateways or other similar uses is prohibited and may result in loss of user privileges and other penalties.

* * * * * * * * * * * * * * * * STN Columbus * * * * * * * * * * * * * * * *

FILE 'HOME' ENTERED AT 08:37:22 ON 20 APR 2006

=> file medline embase biosis scisearch caplus
COST IN U.S. DOLLARS SINCE FILE ENTRY 0.21 TOTAL SESSION 0.21
FULL ESTIMATED COST

FILE 'MEDLINE' ENTERED AT 08:37:31 ON 20 APR 2006

FILE 'EMBASE' ENTERED AT 08:37:31 ON 20 APR 2006

FILE 'BIOSIS' ENTERED AT 08:37:31 ON 20 APR 2006

FILE 'SCISEARCH' ENTERED AT 08:37:31 ON 20 APR 2006

FILE 'CAPLUS' ENTERED AT 08:37:31 ON 20 APR 2006

=> s antibod?
L1 2807410 ANTIBOD?

=> s l1 and framework substitution
L2 14 L1 AND FRAMEWORK SUBSTITUTION

=> dup remove l2
PROCESSING COMPLETED FOR L2
L3 5 DUP REMOVE L2 (9 DUPLICATES REMOVED)

=> d l3 1-5 cbib abs

L3 ANSWER 1 OF 5 MEDLINE on STN DUPLICATE 1
2006116628. PubMed ID: 16151804. Humanization of a recombinant monoclonal **antibody** to produce a therapeutic HER dimerization inhibitor, pertuzumab. Adams Camellia W; Allison David E; Flagella Kelly; Presta Leonard; Clarke Janet; Dybdal Noel; McKeever Kathleen; Sliwkowski Mark X. (Genentech Inc., One DNA Way, South San Francisco, CA 94080, USA.. adams.camellia@gene.com) . Cancer immunology, immunotherapy : CII, (2006 Jun) Vol. 55, No. 6, pp. 717-27. Electronic Publication: 2005-09-03. Journal code: 8605732. ISSN: 0340-7004. Pub. country: Germany: Germany, Federal Republic of. Language: English.

AB Dimerization is essential for activity of human epidermal growth factor receptors (HER1/EGFR, HER2/ErbB2, HER3/ErbB3, and ErbB4) and mediates intracellular signaling events leading to cancer cell proliferation, survival, and resistance to therapy. HER2 is the preferred dimerization partner. Activation of HER signaling pathways may be blocked by inhibition of dimer formation using a monoclonal **antibody** (MAb) directed against the dimerization domain of HER2. The murine MAb 2C4 that specifically binds the HER2 dimerization domain was cloned as a chimeric **antibody**, humanized using a computer-generated model to guide **framework substitutions**, and variants were tested as Fabs. Pharmacokinetics and toxicology were evaluated in rodents and cynomolgus monkeys. Cloning the variable domains of MAb 2C4 into a vector containing human kappa and CH1 domains allowed construction of a mouse-human chimeric Fab. DNA sequencing of the chimeric clone permitted identification of CDR residues. The full-length IgG1 of variant F-10 was

equivalent in binding to chimeric IgG1 and was designated pertuzumab (rhuMAb 2C4; Omnitarg). Pertuzumab pharmacokinetics was best described by a two-compartment model with a distribution phase of <1 day, terminal half-life of approximately 10 days, and volume of distribution of approximately 40 mL/kg that approximates serum volume. With the exception of diarrhea, pertuzumab was generally well tolerated in cynomolgus monkeys. Pertuzumab, a recombinant humanized IgG1 MAb, is the first of a new class of agents known as HER dimerization inhibitors. Inhibition of HER dimerization may be an effective anticancer strategy in tumors with either normal or elevated expression of HER2.

L3 ANSWER 2 OF 5 CAPLUS COPYRIGHT 2006 ACS on STN
1992:56937 Document No. 116:56937 Reshaping a therapeutic CD4 **antibody.** Gorman, Scott D.; Clark, Michael R.; Routledge, Edward G.; Cobbold, Stephen P.; Waldmann, Herman (Dep. Pathol., Univ. Cambridge, Cambridge, CB2 1QP, UK). Proceedings of the National Academy of Sciences of the United States of America, 88(10), 4181-5 (English) 1991. CODEN: PNASA6. ISSN: 0027-8424.

AB An immunosuppressive rat **antibody** (Campath-9) against human CD4 has been reshaped for use in the management of autoimmunity and the prevention of graft rejection. Two different forms of the reshaped **antibody** were produced that derive their heavy chain variable region framework sequences from the human myeloma proteins KOL or NEW. When compared to chimeric form of the CD4 **antibody**, the avidity of the KOL-based reshaped **antibody** was only slightly reduced, whereas that of the NEW-based reshaped **antibody** was very poor. The successful reshaping to the KOL-based framework was by a procedure involving the grafting of human framework sequences onto the cloned rodent variable region by in vitro mutagenesis.

L3 ANSWER 3 OF 5 MEDLINE on STN DUPLICATE 2
80161181. PubMed ID: 6767781. Allelic forms of the immunoglobulin heavy chain variable region. Rudikoff S; Potter M. Journal of immunology (Baltimore, Md. : 1950), (1980 May) Vol. 124, No. 5, pp. 2089-92. Journal code: 2985117R. ISSN: 0022-1767. Pub. country: United States. Language: English.

AB The complete variable region sequence of the heavy chain from a phosphorylcholine-binding myeloma protein of C57/BL allotype has been determined. When this sequence was compared with the germ line-coded heavy chain variable region sequence of BALB/c phosphorylcholine-binding proteins, five differences were observed. Four of the substitutions were located in the framework portion of the variable region and the fifth in the "J" or joining segment. Two of the **framework substitutions** were found at positions 14 and 16. Previous studies have shown that heavy chains from all anti-phosphorylcholine **antibodies** induced in C57/BL mice have the same amino acids at positions 14 and 16 as the C57/BL myeloma protein described in this communication. It has therefore been concluded that these residues are encoded in the C57/BL germ line in contrast to two alternatives in the BALB/c genome. This finding, in addition to the 96% homology found between the C57/BL and BALB/c sequences, suggests that these structures represent allelic forms of an entire variable region.

L3 ANSWER 4 OF 5 MEDLINE on STN DUPLICATE 3
80183857. PubMed ID: 6768828. Structural studies on induced **antibodies** with defined idiotypic specificities. IX. Framework differences in the heavy- and light-chain-variable regions of monoclonal anti-p-azophenylarsonate **antibodies** from A/J mice differing with respect to a cross-reactive idiotype. Estess P; Lamoyi E; Nisonoff A; Capra J D. The Journal of experimental medicine, (1980 Apr 1) Vol. 151, No. 4, pp. 863-75. Journal code: 2985109R. ISSN: 0022-1007. Pub. country: United States. Language: English.

AB Amino terminal amino acid sequence analyses have been performed on the heavy and light chains of induced monoclonal **antibodies** with specificity for the hapten p-azophenylarsonate. Four of the eight

antibodies react with conventional antisera to the previously described A/J anti-arsonate cross-reactive idiotype (CRI). Of the 16 chains analyzed, all but one contain sequence differences in their first framework segment (residues 1-30) that distinguish them from the heavy- and light-chain sequences found in anti-arsonate **antibodies** isolated from A/J serum or ascites fluid. The presence of such framework differences appears to be independent of whether or not the hybridoma **antibodies** bear the CRI. In spite of the **framework substitutions**, all four of the CRI-positive hybridoma **antibodies** have variable (V)-region frameworks that are very similar to each other and to the CRI-positive molecules found in A/J serum. Two of the four CRI-negative molecules are also structurally similar to the serum **antibodies.** Two others, however, are strikingly different from any serum anti-arsonate **antibody** thus far described and appear to reflect a completely separate repertoire of anti-arsonate **antibodies** in the A/J MOUSE. In addition, serological analyses with an anti-idiotypic antiserum generated against a CRI-positive hybridoma product suggest that each monoclonal **antibody** may possess individual antigenic specificities different from the determinant(s) detected with the conventional rabbit anti-CRI. The consistent appearance of **framework substitutions** in what has been thought to be a homogeneous **antibody** population has important implications for our understanding of the generation of **antibody** diversity and for the precise chemical definition of an idiotype.

L3 ANSWER 5 OF 5 CAPLUS COPYRIGHT 2006 ACS on STN
1980:547886 Document No. 93:147886 Primary structural analysis of monoclonal anti-p-azophenylarsonate **antibodies.** Estess, Pila; Capra, J. Donald (Southwestern Med. Sch., Univ. Texas, Dallas, TX, 75235, USA). Progress in Clinical and Biological Research, 42(Membr., Recept., Immune Response), 249-61 (English) 1980. CODEN: PCBRD2. ISSN: 0361-7742.
AB Amino terminal amino acid sequence analyses are presented for the heavy and light chains of induced monoclonal **antibodies** with specificity for the hapten p-azophenylarsonate. Four of the 8 **antibodies** react with conventional antisera to A/J anti-arsonate cross-reactive idiotype (CRI). Of the 16 chains analyzed, all but one contain sequence differences in their first framework segment (residues 1-30) which distinguish them from the heavy and light chain sequences found in anti-arsonate **antibodies** isolated from A/J serum or ascites fluid. The presence of such framework differences appears to be independent of whether or not the hybridoma **antibodies** bear the CRI. In spite of the **framework substitutions**, all 4 of the CRI-pos. hybridoma **antibodies** have V-region frameworks that are very similar to each other and to the CRI-pos. mols. found in A/J serum. Two of the 4 CRI-neg. mols. are also structurally similar to the serum **antibodies.** Two others, however, are strikingly different from any serum anti-arsonate **antibody** thus far described and appear to reflect a completely sep. repertoire of anti-arsonate **antibodies** in the A/J mouse.

```
=> s l1 and VEGF
L4       10295 L1 AND VEGF

=> s l4 and "Y0317"
L5           5 L4 AND "Y0317"

=> dup remove l5
PROCESSING COMPLETED FOR L5
L6           1 DUP REMOVE L5 (4 DUPLICATES REMOVED)

=> d l6 cbib abs

L6   ANSWER 1 OF 1     MEDLINE on STN                    DUPLICATE 1
```

2000013091. PubMed ID: 10543973. Selection and analysis of an optimized anti-**VEGF antibody**: crystal structure of an affinity-matured Fab in complex with antigen. Chen Y; Wiesmann C; Fuh G; Li B; Christinger H W; McKay P; de Vos A M; Lowman H B. (Department of Protein Engineering, Genentech, Inc., 1 DNA Way, South San Francisco, CA 94080, USA.) Journal of molecular biology, (1999 Nov 5) Vol. 293, No. 4, pp. 865-81. Journal code: 2985088R. ISSN: 0022-2836. Pub. country: ENGLAND: United Kingdom. Language: English.

AB The Fab portion of a humanized **antibody** (Fab-12; IgG form known as rhuMAb **VEGF**) to vascular endothelial growth factor (**VEGF**) has been affinity-matured through complementarity-determining region (CDR) mutation, followed by affinity selection using monovalent phage display. After stringent binding selections at 37 degrees C, with dissociation (off-rate) selection periods of several days, high affinity variants were isolated from CDR-H1, H2, and H3 libraries. Mutations were combined to obtain cumulatively tighter-binding variants. The final variant identified here, **Y0317**, contained six mutations from the parental **antibody.** In vitro cell-based assays show that four mutations yielded an improvement of about 100-fold in potency for inhibition of **VEGF**-dependent cell proliferation by this variant, consistent with the equilibrium binding constant determined from kinetics experiments at 37 degrees C. Using X-ray crystallography, we determined a high-resolution structure of the complex between **VEGF** and the affinity-matured Fab fragment. The overall features of the binding interface seen previously with wild-type are preserved, and many contact residues are maintained in precise alignment in the superimposed structures. However, locally, we see evidence for improved contacts between **antibody** and antigen, and two mutations result in increased van der Waals contact and improved hydrogen bonding. Site-directed mutants confirm that the most favorable improvements as judged by examination of the complex structure, in fact, have the greatest impact on free energy of binding. In general, the final **antibody** has improved affinity for several **VEGF** variants as compared with the parental **antibody**; however, some contact residues on **VEGF** differ in their contribution to the energetics of Fab binding. The results show that small changes even in a large protein-protein binding interface can have significant effects on the energetics of interaction.

=> s l1 and improve yield
L7 29 L1 AND IMPROVE YIELD

=> dup remove l7
PROCESSING COMPLETED FOR L7
L8 13 DUP REMOVE L7 (16 DUPLICATES REMOVED)

=> d l8 1-13 cbib abs

L8 ANSWER 1 OF 13 MEDLINE on STN DUPLICATE 1
2006019919. PubMed ID: 16408159. Prokaryotic expression of **antibodies.** Arbabi-Ghahroudi Mehdi; Tanha Jamshid; MacKenzie Roger. (Institute for Biological Sciences, National Research Council of Canada, Ottawa, Ontario.. roger.mackenzie@nrc-cnrc.gc.ca) . Cancer metastasis reviews, (2005 Dec) Vol. 24, No. 4, pp. 501-19. Ref: 193. Journal code: 8605731. ISSN: 0167-7659. Pub. country: Netherlands. Language: English.

AB Maximizing the expression yields of recombinant whole **antibodies** and **antibody** fragments such as Fabs, single-chain Fvs and single-domain **antibodies** is highly desirable since it leads to lower production costs. Various eukaryotic and prokaryotic expression systems have been exploited to accommodate **antibody** expression but Escherichia coli systems have enjoyed popularity, in particular with respect to **antibody** fragments, because of their low cost and

convenience. In many instances, product yields have been less than adequate and intrinsic and extrinsic variables have been investigated in an effort to **improve yields.** This review deals with various aspects of **antibody** expression in E. coli with a particular focus on single-domain **antibodies.**

L8 ANSWER 2 OF 13 MEDLINE on STN DUPLICATE 2

2005077340. PubMed ID: 15607488. Preparation and in vivo evaluation of novel linkers for 211At labeling of proteins. Talanov Vladimir S; Yordanov Alexander T; Garmestani Kayhan; Milenic Diane E; Arora Hans C; Plascjak Paul S; Eckelman William C; Waldmann Thomas A; Brechbiel Martin W. (Radiation Oncology Branch, Center for Cancer Research, National Cancer Institute, National Institutes of Health, Bethesda, MD 20892, USA.) Nuclear medicine and biology, (2004 Nov) Vol. 31, No. 8, pp. 1061-71. Journal code: 9304420. ISSN: 0969-8051. Pub. country: England: United Kingdom. Language: English.

AB The syntheses, radiolabeling, **antibody** conjugation and in vivo evaluation of new linkers for (211)At labeling of monoclonal **antibodies** are described. Syntheses of the N-succinimidyl esters and labeling with (211)At to form succinimidyl 4-methoxymethyl-3-[(211)At]astatobenzoate (9) and succinimidyl 4-methylthiomethyl-3-[(211)At]astatobenzoate (11) from the corresponding bromo-aryl esters is reported. Previously reported succinimidyl N-{4-[(211)At]astatophenethyl}succinamate (SAPS) is employed as a standard of in vivo stability. Each agent is conjugated with Herceptin in parallel with their respective (125)I analogue, succinimidyl 4-methoxymethyl-3-[(125)I]iodobenzoate (10), succinimidyl 4-methylthiomethyl-3-[(125)I]iodobenzoate (12) and succinimidyl N-{4-[(125)I]iodophenethyl}succinamate (SIPS), respectively, for comparative assessment in LS-174T xenograft-bearing mice. With 9 and 11, inclusion of an electron pair donor in the ortho position does not appear to provide in vivo stability comparable to SAPS. Variables in radiolabeling chemistry of these three agents with (211)At are notable. Sequential elimination of acetic acid and oxidizing agent, N-chlorosuccinimide (NCS), from the (211)At radiolabeling protocol for forming SAPS **improves yield**, product purity and consistency. NCS appears to be critical for the radiolabeling of 6 with (211)Atomic Formation of 11, however, is found to require the absence of NCS. Elimination of acetic acid is found to have no effect on radiolabeling efficiency or yield for either of these reactions.

L8 ANSWER 3 OF 13 SCISEARCH COPYRIGHT (c) 2006 The Thomson Corporation on STN

2004:386546 The Genuine Article (R) Number: BY84D. A review of the food/feed safety and benefits of Bacillus thuringiensis protein containing insect-protected crops. Hammond B (Reprint). Monsanto Co, Prod Safety Ctr, 800 N Lindbergh Blvd, St Louis, MO 63167 USA (Reprint); Monsanto Co, Prod Safety Ctr, St Louis, MO 63167 USA. AGRICULTURAL BIOTECHNOLOGY: CHALLENGES AND PROSPECTS (2004) Vol. 866, pp. 103-123. ISSN: 0097-6156. Publisher: AMER CHEMICAL SOC, 1155 SIXTEENTH ST NW, WASHINGTON, DC 20036 USA. Language: English.

ABSTRACT IS AVAILABLE IN THE ALL AND IALL FORMATS

AB Infestation of agricultural crops by insect pests has been traditionally managed through the use of chemical insecticides. An alternative method to control insect pests has been the introduction of insecticidal proteins from Bacillus thuringiensis into agricultural crops by genetic engineering. The introduced insect control proteins have an exemplary safety record having been safely used in agriculture for 40 years as the active ingredients of microbial pesticides. Insect-protected biotech crops control a variety of insect pests such as corn borers, cotton bollworms, and Colorado potato beetles. Season long protection of the crop **improves yield** and reduces reliance on traditional chemical insecticides. Protection of corn plants against insect damage reduces infection by certain fungal pathogens that produce fumonisin mycotoxins that are toxic to various species.

L8 ANSWER 4 OF 13 MEDLINE on STN DUPLICATE 3
2003435074. PubMed ID: 13129388. Improved yield and stability of L49-sFv-beta-lactamase, a single-chain **antibody** fusion protein for anticancer prodrug activation, by protein engineering. McDonagh Charlotte F; Beam Kevin S; Wu Gabrielle J S; Chen Judy H; Chace Dana F; Senter Peter D; Francisco Joseph A. (Seattle Genetics Inc, 21823 30th Drive SE, Bothell, Washington 98021, USA.. cmcdonagh@seagen.com) . Bioconjugate chemistry, (2003 Sep-Oct) Vol. 14, No. 5, pp. 860-9. Journal code: 9010319. ISSN: 1043-1802. Pub. country: United States. Language: English.

AB The L49 single-chain Fv fused to beta-lactamase (L49-sFv-bL) combined with the prodrug C-Mel is an effective anticancer agent against tumor cells expressing the p97 antigen. However, large-scale production of L49-sFv-bL from refolded E. coli inclusion bodies has been problematic due to inefficient refolding and instability of the fusion protein. Sequence analysis of the L49-sFv framework regions revealed three residues in the framework regions at positions L2, H82B, and H91, which are not conserved for their position, occurring in <1% of sequences in Fv sequence databases. One further unusual residue, found in <3% of variable sequences, was observed at position H39. Each unusual residue was mutated to a conserved residue for its position and tested for refolding yield from inclusion bodies following expression in E. coli. The three V(H) single mutants showed improvement in the yield of active protein and were combined to form double and triple mutants resulting in a 7-8-fold increased yield compared to the parental protein. In an attempt to further **improve yield**, the orientation of the triple mutant was reversed to create a bL-L49-sFv fusion protein resulting in a 3-fold increase in expressed inclusion body protein and producing a 20-fold increase in the yield of purified protein compared to the parental protein. The triple mutants in both orientations displayed increased stability in murine plasma and binding affinity was not affected by the introduced mutations. Both triple mutants also displayed potent in vitro cytotoxicity and in vivo antitumor activity against p97 expressing melanoma cells and tumor xenografts, respectively. These results show that a rational protein-engineering approach improved the yield, stability, and refolding characteristics of L49-sFv-bL while maintaining binding affinity and therapeutic efficacy.

L8 ANSWER 5 OF 13 CAPLUS COPYRIGHT 2006 ACS on STN
2002:532626 Document No. 138:373927 Enveloped Virus Inactivation by Caprylate: A Robust Alternative to Solvent-Detergent Treatment in Plasma Derived Intermediates. Korneyeva, M.; Hotta, J.; Lebing, W.; Rosenthal, R. S.; Franks, L.; Petteway, S. R., Jr. (Department of Pathogen Safety and Research, Bayer Biological Products, Research Triangle Park, NC, 27709, USA). Biologicals, 30(2), 153-162 (English) 2002. CODEN: BILSEC. ISSN: 1045-1056. Publisher: Academic Press.

AB Solvent-detergent treatment, although used routinely in plasma product processing to inactivate enveloped viruses, substantially reduces product yield from the human plasma resource. To **improve yields** in plasma product manufacturing, a new viral reduction process has been developed using the fatty acid caprylate. As licensure of plasma products warrants thorough evaluation of pathogen reduction capabilities, the present study examined susceptibility of enveloped viruses to inactivation by caprylate in protein solns. with varied pH and temperature In the immunoglobin-rich solns. from Cohn Fraction II+III, human immunodeficiency virus, Type-1, bovine viral diarrhea virus (BVDV), and pseudorabies virus were inactivated by caprylate concns. of ≥9 mM, ≥12 mM, and ≥9 mM, resp. Compared to solvent-detergent treatment, BVDV inactivation in Fraction II+III solution was significantly faster (20-60 fold) using 16 mM caprylate. Caprylate-mediated inactivation of BVDV was not noticeably affected by temperature within the range chosen manufacturing the Ig product. In Fraction II+III solns., IgG solubility was unaffected by ≤19 mM caprylate. In albumin

solution from Cohn supernatant IV-1, 40 mM caprylate rapidly inactivated BVDV, demonstrating versatility in inactivating enveloped viruses potentially present in other protein solns. These data show that caprylate is a robust enveloped virus inactivating agent for Igs and albumin which may potentially be utilized for other proteins; viral inactivation was not adversely affected by protein content and the buffer composition conditions evaluated. Within the parameters examined, caprylate inactivation of enveloped viruses provided comparable activity or advantages relative to the current, standard solvent-detergent treatment.

L8 ANSWER 6 OF 13 CAPLUS COPYRIGHT 2006 ACS on STN

2001:868666 Document No. 136:15960 Nucleotide sequences encoding plant ramosa 1 protein and uses in meristem identity and branch development in plants. Martienssen, Robert A.; Vollbrecht, Erik (Cold Spring Harbor Laboratory, USA). PCT Int. Appl. WO 2001090343 A2 20011129, 90 pp. DESIGNATED STATES: W: AE, AL, AM, AT, AU, AZ, BA, BB, BG, BR, BY, BZ, CA, CH, CN, CO, CR, CU, CZ, DE, DK, DM, DZ, EE, ES, FI, GB, GD, GE, GH, GM, HR, HU, ID, IL, IN, IS, JP, KE, KG, KP, KR, KZ, LC, LK, LR, LS, LT, LU, LV, MA, MD, MG, MK, MN, MW, MX, MZ, NO, NZ, PL, PT, RO, RU, SD, SE, SG, SI, SK, SL, TJ, TM, TR, TT, TZ, UA, UG, US, UZ, VN, YU, ZA, ZW, AM, AZ, BY, KG, KZ, MD, RU, TJ, TM; RW: AT, BE, BF, BJ, CF, CG, CH, CI, CM, CY, DE, DK, ES, FI, FR, GA, GB, GR, IE, IT, LU, MC, ML, MR, NE, NL, PT, SE, SN, TD, TG, TR. (English). CODEN: PIXXD2. APPLICATION: WO 2001-US16659 20010522. PRIORITY: US 2000-2000/PV206136 20000522.

AB The invention relates to the isolation and characterization of a novel maize gene Romosa 1 (Ra1) responsible for meristem development and inflorescence development including branching. The novel gene, gene product, and regulatory regions may be used to manipulate branching, meristem growth, inflorescence development and arrangement, and ultimately to **improve yield** of plants. The invention includes the novel gene and protein product as well as the use of the same for temporal and spatial expression in transgenic plants to alter plant morphol. and affect yield in plants.

L8 ANSWER 7 OF 13 CAPLUS COPYRIGHT 2006 ACS on STN

2001:713570 Document No. 135:270245 The corn fae2 gene involved in meristem proliferation and inflorescence development and use of the gene and promoter in plant breeding. Jackson, David P.; Taguchi Shiobara, Fumio; Hake, Sarah; Yuan, Zhuang (Cold Spring Harbor Laboratory, USA). PCT Int. Appl. WO 2001070987 A2 20010927, 73 pp. DESIGNATED STATES: W: AE, AL, AM, AT, AU, AZ, BA, BB, BG, BR, BY, BZ, CA, CH, CN, CO, CR, CU, CZ, DE, DK, DM, DZ, EE, ES, FI, GB, GD, GE, GH, GM, HR, HU, ID, IL, IN, IS, JP, KE, KG, KP, KR, KZ, LC, LK, LR, LS, LT, LU, LV, MA, MD, MG, MK, MN, MW, MX, MZ, NO, NZ, PL, PT, RO, RU, SD, SE, SG, SI, SK, SL, TJ, TM, TR, TT, TZ, UA, UG, US, UZ, VN, YU, ZA, ZW, AM, AZ, BY, KG, KZ, MD, RU, TJ, TM; RW: AT, BE, BF, BJ, CF, CG, CH, CI, CM, CY, DE, DK, ES, FI, FR, GA, GB, GR, IE, IT, LU, MC, ML, MR, NE, NL, PT, SE, SN, TD, TG, TR. (English). CODEN: PIXXD2. APPLICATION: WO 2001-US8709 20010319. PRIORITY: US 2000-PV190160 20000317.

AB The invention relates to the isolation and characterization of a novel maize gene (fae2 (fasciated ear 2)) responsible for meristem proliferation and inflorescence development. The novel gene, gene product, and regulatory regions may be used to manipulate meristem growth, inflorescence development and arrangement, and ultimately to **improve yield** of plants. The invention includes the novel gene and protein product as well as the use of the same for temporal and spatial expression in transgenic plants to enhance kernel development, alter plant morphol. and increase yield in plants. The gene was first identified as having an effect on fasciation of ears and the morphol. of the tassel. The gene was cloned after tagging with Mu; two Mu-tagged alleles were identified. The gene has no introns and appears to encode a member of the leucine-rich repeat family of transmembrane receptors.

L8 ANSWER 8 OF 13 EMBASE COPYRIGHT (c) 2006 Elsevier B.V. All rights reserved on STN

2001362150 EMBASE Yield of large-volume blood cultures in patients with early lyme disease. Wormser G.P.; Bittker S.; Cooper D.; Nowakowski J.; Nadelman R.B.; Pavia C.. Dr. G.P. Wormser, Div. of Infectious Diseases, Macy Pavilion, Westchester Medical Center, New York, NY 10595, United States. Journal of Infectious Diseases Vol. 184, No. 8, pp. 1070-1072 15 Oct 2001.
Refs: 12.
ISSN: 0022-1899. CODEN: JIDIAQ
Pub. Country: United States. Language: English. Summary Language: English.
Entered STN: 20011025. Last Updated on STN: 20011025

AB To **improve yield**, 6 3-mL plasma cultures (18 mL total) were established for adult patients with early Lyme disease associated with erythema migrans. Borrelia burgdorferi was recovered from the blood of 22 (44.0%) of 50 evaluable patients. The recovery rate per plasma culture and the frequency of positive results for plasma cultures for individual patients were consistent with a level of spirochetemia of .apprx.0.1 cultivable cell/mL of whole blood. Our findings suggest that, if further improvements in the yield of blood cultures are possible, they probably will depend on enhancing the sensitivity of the culture method rather than increasing the volume of material cultured.

L8 ANSWER 9 OF 13 CAPLUS COPYRIGHT 2006 ACS on STN

2000:774014 Document No. 133:330525 Process for producing natural folded eukaryotic proteins with prokaryotes. (F. Hoffmann-La Roche A.-G., Switz.). Eur. Pat. Appl. EP 1048732 A1 20001102, 40 pp. DESIGNATED STATES: R: AT, BE, CH, DE, DK, ES, FR, GB, GR, IT, LI, LU, NL, SE, MC, PT, IE, SI, LT, LV, FI, RO. (German). CODEN: EPXXDW. APPLICATION: EP 1999-107412 19990426.

AB The title process for producing eukaryotic proteins, especially disulfide bond-containing eukaryotic proteins, comprises creation of a chimeric gene consisting of a prokaryotic signal sequence fused to a gene for the desired protein, expression of the gene in the prokaryote, and removal of the signal peptide and isolation of the protein from the periplasm or culture medium. The culture contains arginine or R2CONRR1 (R,R1 = H, (unsatd.,branched)C1-4-alkyl; R2 = H, NHR1, (unsatd.,branched)C1-3-alkyl). The culture medium may addnl. contain a reducing agent such as glutathione. To further **improve yields**, mol. chaperones such as DnaJ or HSP25 may be coexpressed. Thus, E. coli coexpressing a pelB signal sequence-plasminogen activator chimeric gene and a dnaJ gene was cultured in a medium containing glutathione and arginine hydrochloride. The yield of the plasminogen activator was increased approx. 100-fold by this method. A similar method was used to produced an anti-TSH scFv.

L8 ANSWER 10 OF 13 SCISEARCH COPYRIGHT (c) 2006 The Thomson Corporation on STN

1999:774564 The Genuine Article (R) Number: 243QZ. Monoclonal **antibody** production - Strategies **improve yields** , purity and consistency. Schneider I. GENETIC ENGINEERING NEWS (1 OCT 1999) Vol. 19, No. 17, pp. 13-+. ISSN: 0270-6377. Publisher: MARY ANN LIEBERT INC PUBL, 2 MADISON AVENUE, LARCHMONT, NY 10538 USA. Language: English.

L8 ANSWER 11 OF 13 CAPLUS COPYRIGHT 2006 ACS on STN

1998:210849 Document No. 128:254590 Proteases and their variants having peptide protease inhibitors fused to them and their uses in cleaning compositions. Saunders, Charles Winston; McIver, John McMillan; Armpriester, James Michael; Youngquist, Robert Scott (Procter & Gamble Co., USA). PCT Int. Appl. WO 9813483 A1 19980402, 82 pp. DESIGNATED STATES: W: BR, CA, CN, JP, MX, US; RW: AT, BE, CH, DE, DK, ES, FI, FR, GB, GR, IE, IT, LU, MC, NL, PT, SE. (English). CODEN: PIXXD2. APPLICATION: WO 1997-US16354 19970923. PRIORITY: US 1996-26947 19960924.

AB The present invention relates to fusion proteins of proteases and protease inhibitors. Thus, synthetic genes were constructed encoding protease inhibitors, such as eglin and Streptomyces subtilisin inhibitor (SSI), and

then fused in frame to the cDNAs encoding a protease such as Bacillus amyloliquefaciens subtilisin in a vector construct for expression in Bacillus subtilis. The present invention also relates to compns. comprising such fusion proteins for cleaning, such as dishwashing compns., fabric cleaning composition, oral cleaning compns., such as dentifrices, dentures, chewing gum, and mouthwash, and contact lens cleaning compns. These fusion proteins advantageously **improve yield** of the desired protease, control stoichiometry of the inhibitor protease, produce more stable proteases, and thus more stable formulations, while providing active protease during the cleaning process.

L8 ANSWER 12 OF 13 MEDLINE on STN DUPLICATE 4

1998160398. PubMed ID: 9500762. High-level expression of cockroach allergen, Bla g 4, in Pichia pastoris. Vailes L D; Kinter M T; Arruda L K; Chapman M D. (Department of Medicine, Asthma and Allergic Diseases Center, University of Virginia, Charlottesville 22908, USA.) The Journal of allergy and clinical immunology, (1998 Feb) Vol. 101, No. 2 Pt 1, pp. 274-80. Journal code: 1275002. ISSN: 0091-6749. Pub. country: United States. Language: English.

AB Exposure to cockroach allergens is a risk factor for allergic disease and has been linked to an increase in asthma morbidity among cockroach-sensitive inner-city children. Bla g 4 is a ligand-binding protein (or calycin) that causes IgE **antibody** responses in 40% to 60% of patients allergic to cockroaches. Recombinant Bla g 4 was expressed in Escherichia coli as an 18 kd protein but provided poor yields (only 0.25 mg/L culture). To **improve yields**, Bla g 4 was expressed in the Pichia pastoris yeast system as a 23 kd secreted protein at concentrations of 50 mg allergen/L. By cross-inhibition radioimmunoassay, Bla g 4 expressed in E. coli or P. pastoris provided overlapping inhibition curves. Both allergen preparations bound comparable levels of serum IgE **antibody** and showed similar skin test reactivity in individuals allergic to cockroaches (10[-1] to 10[-3] microg/ml). Deglycosylation of Pichia-expressed Bla g 4 with endoglycosidase F resulted in an 18 to 20 kd doublet, and liquid chromatography-mass spectrometry results suggested that the 20 kd band contained residual sugar residues. Both glycosylated and deglycosylated Pichia Bla g 4 showed comparable inhibition of IgE **antibody** binding in radioimmunoassay. Pichia-produced Bla g 4 had the same antigenic reactivity as that produced in E. coli, and glycosylation had no effect on IgE **antibody** binding. The high yield of Bla g 4 obtained in the Pichia system will facilitate studies on the structure and function of calycin allergens and on the immune response of asthma patients to cockroach allergens.

L8 ANSWER 13 OF 13 MEDLINE on STN DUPLICATE 5

95375258. PubMed ID: 7647323. Comparison of four methods to generate immunoreactive fragments of a murine monoclonal **antibody** OC859 against human ovarian epithelial cancer antigen. Zou Y; Bian M; Yiang Z; Lian L; Liu W; Xu X. (Department of Obstetrics and Gynecology, PUMC Hospital, Beijing.) Chinese medical sciences journal = Chung-kuo i hsueh k'o hsueh tsa chih / Chinese Academy of Medical Sciences, (1995 Jun) Vol. 10, No. 2, pp. 78-81. Journal code: 9112559. ISSN: 1001-9294. Pub. country: China. Language: English.

AB In the present study, four different proteases (pepsin, papain, bromelain and ficin) were screened with a murine monoclonal **antibody** OC859, in order to verify whether different digestion procedures could **improve yield** and stability of the F(ab')2 or Fab fragments. The yields of F(ab')2 or Fab fragments from digestion with pepsin, papain, bromelain and ficin were respectively 20.3 +/- 2.0%, 50.5 +/- 5.0%, 74.4 +/- 2.7% and 82.8 +/- 10.2% of the theoretical maximum. Immunoreactivity in a noncompetitive solid-phase radioimmunoassay (SPRIA) of the fragments generated by the four proteases were respectively 10 +/- 5%, 36 +/- 5%, 60 +/- 6% and 75 +/- 6% of the intact OC859 IgG. These results suggested that the fragmentation of OC859 with ficin gave a higher yield of superior immunoreactive fragments.

=> s l1 and substitution
L9 24271 L1 AND SUBSTITUTION

=> s l9 and improve yield
L10 1 L9 AND IMPROVE YIELD

=> d l10 cbib abs

L10 ANSWER 1 OF 1 CAPLUS COPYRIGHT 2006 ACS on STN
2001:868666 Document No. 136:15960 Nucleotide sequences encoding plant ramosa 1 protein and uses in meristem identity and branch development in plants. Martienssen, Robert A.; Vollbrecht, Erik (Cold Spring Harbor Laboratory, USA). PCT Int. Appl. WO 2001090343 A2 20011129, 90 pp. DESIGNATED STATES: W: AE, AL, AM, AT, AU, AZ, BA, BB, BG, BR, BY, BZ, CA, CH, CN, CO, CR, CU, CZ, DE, DK, DM, DZ, EE, ES, FI, GB, GD, GE, GH, GM, HR, HU, ID, IL, IN, IS, JP, KE, KG, KP, KR, KZ, LC, LK, LR, LS, LT, LU, LV, MA, MD, MG, MK, MN, MW, MX, MZ, NO, NZ, PL, PT, RO, RU, SD, SE, SG, SI, SK, SL, TJ, TM, TR, TT, TZ, UA, UG, US, UZ, VN, YU, ZA, ZW, AM, AZ, BY, KG, KZ, MD, RU, TJ, TM; RW: AT, BE, BF, BJ, CF, CG, CH, CI, CM, CY, DE, DK, ES, FI, FR, GA, GB, GR, IE, IT, LU, MC, ML, MR, NE, NL, PT, SE, SN, TD, TG, TR. (English). CODEN: PIXXD2. APPLICATION: WO 2001-US16659 20010522. PRIORITY: US 2000-2000/PV206136 20000522.
AB The invention relates to the isolation and characterization of a novel maize gene Romosa 1 (Ra1) responsible for meristem development and inflorescence development including branching. The novel gene, gene product, and regulatory regions may be used to manipulate branching, meristem growth, inflorescence development and arrangement, and ultimately to **improve yield** of plants. The invention includes the novel gene and protein product as well as the use of the same for temporal and spatial expression in transgenic plants to alter plant morphol. and affect yield in plants.

=> s l9 and FR region
L11 1 L9 AND FR REGION

=> d l11 cbib abs

L11 ANSWER 1 OF 1 SCISEARCH COPYRIGHT (c) 2006 The Thomson Corporation on STN
1999:773772 The Genuine Article (R) Number: 246AM. Targeting and subsequent selection of somatic hypermutations in the human V chi repertoire. Foster S J; Dorner T; Lipsky P E (Reprint). Univ Texas, SW Med Ctr, Dept Internal Med, Harold C Simmons Arthrit Res Ctr, 5323 Harry Hines Blvd, Dallas, TX 75235 USA (Reprint); Univ Texas, SW Med Ctr, Dept Internal Med, Harold C Simmons Arthrit Res Ctr, Dallas, TX 75235 USA. EUROPEAN JOURNAL OF IMMUNOLOGY (OCT 1999) Vol. 29, No. 10, pp. 3122-3132. ISSN: 0014-2980. Publisher: WILEY-V C H VERLAG GMBH, PO BOX 10 11 61, D-69451 WEINHEIM, GERMANY. Language: English.
ABSTRACT IS AVAILABLE IN THE ALL AND IALL FORMATS
AB The number and distribution of nucleotide **substitutions** in human V kappa J kappa genes were examined using a PCR technique that analyzed nonproductive and productive rearrangements amplified from genomic DNA of individual B cells. The results indicate that the mutational mechanism introduces replacement (R) mutations comparably throughout the length of the V kappa J kappa. rearrangement, but tends to target specific triplets. Moreover, hotspots of mutational activity were identified in complementarity determining regions (CDR). A marked increase in the frequency of R mutations in CDR was noted when productive were compared to nonproductive rearrangements, indicating that these were selected into the expressed repertoire. Of note, amino acids encoded by codons adjacent to hotspots of mutation were also positively selected implying that similar regions were targeted for hypermutation and

subsequent selection. In contrast to the distribution of CDR mutations, R mutations in the framework (**FR**) **regions** tended to be eliminated from productive V kappa J kappa rearrangements, implying that the somatic hypermutational machinery frequently introduced amino acid changes that were deleterious to the structural integrity of the kappa chain protein. The difference in the ratio of R to silent mutations in CDR and FR in the expressed repertoire, therefore, reflects the summation of positive selection of R mutations in the CDR and the elimination of R mutations in the FR. The data indicate that the balance between targeted mutation of V kappa J kappa rearrangements and subsequent selection and elimination governs the pattern of mutations manifest within the expressed kappa repertoire.

=> s l1 and IgE
L12 60211 L1 AND IGE

=> s l12 and substitution
L13 489 L12 AND SUBSTITUTION

=> s l13 and yield
L14 9 L13 AND YIELD

=> dup remove l14
PROCESSING COMPLETED FOR L14
L15 4 DUP REMOVE L14 (5 DUPLICATES REMOVED)

=> d l15 1-4 cbib abs

L15 ANSWER 1 OF 4 CAPLUS COPYRIGHT 2006 ACS on STN
2004:633952 Document No. 141:156117 Methods for producing and improving **yield** of humanized or chimeric **antibodies** and fragments in cell culture. Simmons, Laura (Genentech, Inc., USA). PCT Int. Appl. WO 2004065417 A2 20040805, 161 pp. DESIGNATED STATES: W: AE, AE, AG, AL, AL, AM, AM, AM, AT, AT, AU, AZ, AZ, BA, BB, BG, BG, BR, BR, BW, BY, BY, BZ, BZ, CA, CH, CN, CN, CO, CO, CR, CR, CU, CU, CZ, CZ, DE, DE, DK, DK, DM, DZ, EC, EC, EE, EE, EG, ES, ES, FI, FI, GB, GD, GE, GE, GH, GM, HR, HR, HU, HU, ID, IL, IN, IS, JP, JP, KE, KE, KG, KG, KP, KP, KP, KR, KR, KZ, KZ, KZ, LC, LK, LR, LS, LS, LT, LU, LV, MA, MD, MD, MG, MK, MN, MW, MX, MX, MZ, MZ, NA, NI. (English). CODEN: PIXXD2. APPLICATION: WO 2004-US1844 20040123. PRIORITY: US 2003-2003/PV442484 20030123.
AB The present invention provides methods for producing humanized **antibodies** and increasing the **yield** of **antibodies** and/or antigen binding fragments when produced in cell culture. The **antibodies** are anti-VEGF and anti-**IgE** **antibodies.** In one aspect of the invention, at least one framework region amino acid residue of the variable domain is substituted by a corresponding amino acid from a variable domain consensus sequence subgroup that has the most sequence identity with the HVRI and/or HVR2 amino acid sequence of the variable domain. In another aspect, an amino acid is placed at a position proximal to a cys residue that participates in an intrachain variable domain disulfide bond that corresponds to an amino acid found at that position in a variable domain consensus sequence subgroup that has the most sequence identity with the HVR1 and/or HVR2 amino acid sequence of the variable domain.

L15 ANSWER 2 OF 4 BIOSIS COPYRIGHT (c) 2006 The Thomson Corporation on STN
DUPLICATE 1
2004:398829 Document No.: PREV200400400634. The importance of Lys-352 of human immunoglobulin E in FcepsilonRII/CD23 recognition. Sayers, Ian; Housden, Jonathan E. M.; Spivey, Alan C.; Helm, Birgit A. [Reprint Author]. Krebs Inst Biomolec ResDept Mol Biol and Biotechnol, Univ Sheffield, Sheffield, S Yorkshire, S10 2TN, UK. B.Helm@sheffield.ac.uk. Journal of Biological Chemistry, (August 20 2004) Vol. 279, No. 34, pp. 35320-35325. print. CODEN: JBCHA3. ISSN: 0021-9258. Language: English.

AB The interaction of immunoglobulin E (**IgE**) with its low affinity receptor (FcepsilonRII/CD23) plays a central role in the initiation and regulation of type I hypersensitivity responses. We have previously identified the importance of amino acid residues in the A-B loop of the Cepsilon3 domain of human **IgE** and implicated a region close to the glycosylation site at asparagine 371 as contributing to **IgE** -CD23 interaction. These residues were now targeted by site-directed mutagenesis. The **IgE**-CD23 interaction was assessed by semiquantitative flow cytometry. Replacement of the entire Cepsilon3 A-B loop (residues 341 356) with the homologous rat **IgE** sequence resulted in complete loss of human CD23 recognition, as did replacement of residues 346-353, indicating that class-specific effector residue(s) are contained within these eight amino acids. Lysine 352 within the A-B loop was identified as contributing directly to human CD23 interaction. Mutation to the rodent homologue glycine or glutamate resulted in a significant reduction in binding compared with native **IgE**, whereas conservative **substitution** with arginine effected a small, but statistically significant, enhancement of CD23 binding. Mutation of the Cepsilon3 glycosylation site at asparagine 371 to threonine or glutamine did not significantly affect CD23 recognition. Our results **yield** new insights into the structural basis of the hIgE-CD23 interaction and hold promise for the rational design of drugs that can manipulate **IgE**-mediated regulation of the allergic response.

L15 ANSWER 3 OF 4 MEDLINE on STN DUPLICATE 2

2001408712. PubMed ID: 11228379. Effectiveness and safety of mutant Escherichia coli heat-labile enterotoxin (LT H44A) as an adjuvant for nasal influenza vaccine. Hagiwar Y; Tsuji T; Iwasaki T; Kadowaki S; Asanuma H; Chen Z; Komase K; Suzuki Y; Aizawa C; Kurata T; Tamura S. (Department of Pathology, National Institute of Infectious Diseases, Toyama 1-23-1, Shinjuku-ku, 162-8640, Tokyo, Japan.) Vaccine, (2001 Feb 28) Vol. 19, No. 15-16, pp. 2071-9. Journal code: 8406899. ISSN: 0264-410X. Pub. country: England: United Kingdom. Language: English.

AB The effectiveness and safety of mutant Escherichia coli heat-labile enterotoxin, LT H44A (His to Arg **substitution** at position 44 from the N-terminus of the A1 fragment of the A subunit) as an adjuvant for nasal influenza vaccine were examined. (1) When 0.2 microg of LT H44A, together with 0.2 microg of influenza A/PR/8/34 virus (PR8, H1N1) vaccine, was administered intranasally into BALB/c mice (twice, 4 weeks apart), anti-PR8 hemagglutinin (HA) IgA and IgG **antibody** (Ab) responses were induced at levels that were sufficient to provide either complete protection against infection with a small volume of PR8 virus suspension or partial protection against infection with a lethal dose of the suspension. The dose of the mutant LT and vaccine used here (0.2 microg/ 20 g doses mouse) corresponded to the estimated dose per person, i.e. 0.1 mg/10 kg body weight. (2) Using these vaccination conditions, no additional total **IgE** Ab responses were induced. (3) The mutant was confirmed to be less toxic than the native LT when the toxicity was analyzed either using Y1 adrenal cells in vitro (1/483 EC(50)) or by an ileal loop test. (4) One hundred micrograms of the mutant, administered intranasally or intraperitoneally into guinea-pigs (Heartley strain, 0.3-0.4 kg), caused no body-weight changes 7 days after administration, although 100 microg of the native LT administered intraperitoneally caused death in all guinea-pigs due to diarrhea within 2 days. The intranasal administration of 100 microg of the mutant resulted in almost no pathological changes in the nasal mucosa 3 days after administration. These results suggest that LT H44A, which can be produced in high **yields** in an E. coli culture (about 5 mg/l), could be used as one of the effective and safe adjuvants for nasal influenza vaccine in humans.

L15 ANSWER 4 OF 4 SCISEARCH COPYRIGHT (c) 2006 The Thomson Corporation on STN

2000:265306 The Genuine Article (R) Number: 299EE. The ABA-1 allergen of Ascaris lumbricoides: sequence polymorphism, stage and tissue-specific

expression, lipid binding function, and protein biophysical properties. Xia Y; Spence H J; Moore J; Heaney N; McDermott L; Cooper A; Watson D G; Mei B; Komuniecki R; Kennedy M W (Reprint). Univ Glasgow, Div Infect & Immun, Inst Biomed & Life Sci, Joseph Black Bldg, Glasgow G12 8QQ, Lanark, Scotland (Reprint); Univ Glasgow, Div Infect & Immun, Inst Biomed & Life Sci, Glasgow G12 8QQ, Lanark, Scotland; Univ Glasgow, Dept Chem, Glasgow G12 8QQ, Lanark, Scotland; Univ Strathclyde, Dept Pharmaceut Sci, Glasgow G1 1XW, Lanark, Scotland; Univ Toledo, Dept Biol, Toledo, OH 43606 USA. PARASITOLOGY (FEB 2000) Vol. 120, Part 2, pp. 211-224. ISSN: 0031-1820. Publisher: CAMBRIDGE UNIV PRESS, 110 MIDLAND AVE, PORT CHESTER, NY 10573-9863 USA. Language: English.
ABSTRACT IS AVAILABLE IN THE ALL AND IALL FORMATS

AB The ABA-1 protein of Ascaris lumbricoides (of humans) and Ascaris suum (of pigs) is abundant in the pseudocoelomic fluid of the parasites and also appears to be released by the tissue-parasitic larvae and the adult stages. The genes encoding the polyprotein precursor of ABA-1 (aba-1) were found to be arranged similarly in the two taxa, comprising tandemly repeating units encoding a large polyprotein which is cleaved to **yield** polypeptides of approximately 15 kDa which fall into 2 distinct classes, types A and B. The polyprotein possibly comprises only 10 units. The aba-1 gene of A. lumbricoides is polymorphic, and the majority of **substitutions** observed occur in or near predicted loop regions in the encoded proteins. mRNA for ABA-1 is present in infective larvae within the egg, and in all parasitic stages, but was not detectable in unembryonated eggs. ABA-1 mRNA was confined to the gut of adult parasites, and not in body wall or reproductive tissues. Recombinant protein representing a single A-type unit for the A. lumbricoides aba-1 gene was produced and found to bind retinol (Vitamin A) and a range of fatty acids, including the pharmacologically active lipids lysophosphatidic acid, lysoplatelet activating factor, and there was also evidence of binding to leukotrienes. It failed to bind to any of the anthelmintics screened. Differential Scanning Calorimetry showed that the recombinant protein was highly stable, and unfolded in a single transition at 90.4 degrees C. Analysis of the transition indicated that the protein occurs as a dimer and that the dimer dissociates simultaneously with the unfolding of the monomer units.

```
=> s (simmons l?/au)
L16        1113 (SIMMONS L?/AU)

=> s l16 and humanized antibod?
L17           1 L16 AND HUMANIZED ANTIBOD?

=> d l17 cbib abs
```

L17 ANSWER 1 OF 1 CAPLUS COPYRIGHT 2006 ACS on STN

2004:633952 Document No. 141:156117 Methods for producing and improving yield of humanized or chimeric antibodies and fragments in cell culture. **Simmons, Laura** (Genentech, Inc., USA). PCT Int. Appl. WO 2004065417 A2 20040805, 161 pp. DESIGNATED STATES: W: AE, AE, AG, AL, AL, AM, AM, AM, AT, AT, AU, AZ, AZ, BA, BB, BG, BG, BR, BR, BW, BY, BY, BZ, BZ, CA, CH, CN, CN, CO, CO, CR, CR, CU, CU, CZ, CZ, DE, DE, DK, DK, DM, DZ, EC, EC, EE, EE, EG, ES, ES, FI, FI, GB, GD, GE, GE, GH, GM, HR, HR, HU, HU, ID, IL, IN, IS, JP, JP, KE, KE, KG, KG, KP, KP, KP, KR, KR, KZ, KZ, KZ, LC, LK, LR, LS, LS, LT, LU, LV, MA, MD, MD, MG, MK, MN, MW, MX, MX, MZ, MZ, NA, NI. (English). CODEN: PIXXD2. APPLICATION: WO 2004-US1844 20040123. PRIORITY: US 2003-2003/PV442484 20030123.

AB The present invention provides methods for producing **humanized antibodies** and increasing the yield of antibodies and/or antigen binding fragments when produced in cell culture. The antibodies are anti-VEGF and anti-IgE antibodies. In one aspect of the invention, at least one framework region amino acid residue of the variable domain is substituted by a corresponding amino acid from a variable domain consensus sequence subgroup that has the most sequence identity with the HVRI and/or

HVR2 amino acid sequence of the variable domain. In another aspect, an amino acid is placed at a position proximal to a cys residue that participates in an intrachain variable domain disulfide bond that corresponds to an amino acid found at that position in a variable domain consensus sequence subgroup that has the most sequence identity with the HVR1 and/or HVR2 amino acid sequence of the variable domain.

=> s l16 and improve yields
L18 0 L16 AND IMPROVE YIELDS

=> s l16 and antibod?
L19 20 L16 AND ANTIBOD?

=> dup remove l19
PROCESSING COMPLETED FOR L19
L20 13 DUP REMOVE L19 (7 DUPLICATES REMOVED)

=> d l20 1-13 cbib abs

L20 ANSWER 1 OF 13 CAPLUS COPYRIGHT 2006 ACS on STN
2004:633952 Document No. 141:156117 Methods for producing and improving yield of humanized or chimeric **antibodies** and fragments in cell culture. **Simmons, Laura** (Genentech, Inc., USA). PCT Int. Appl. WO 2004065417 A2 20040805, 161 pp. DESIGNATED STATES: W: AE, AE, AG, AL, AL, AM, AM, AM, AT, AT, AU, AZ, AZ, BA, BB, BG, BG, BR, BR, BW, BY, BY, BZ, BZ, CA, CH, CN, CN, CO, CO, CR, CR, CU, CU, CZ, CZ, DE, DE, DK, DK, DM, DZ, EC, EC, EE, EE, EG, ES, ES, FI, FI, GB, GD, GE, GE, GH, GM, HR, HR, HU, HU, ID, IL, IN, IS, JP, JP, KE, KE, KG, KG, KP, KP, KP, KR, KR, KZ, KZ, KZ, LC, LK, LR, LS, LS, LT, LU, LV, MA, MD, MD, MG, MK, MN, MW, MX, MX, MZ, MZ, NA, NI. (English). CODEN: PIXXD2. APPLICATION: WO 2004-US1844 20040123. PRIORITY: US 2003-2003/PV442484 20030123.
AB The present invention provides methods for producing humanized **antibodies** and increasing the yield of **antibodies** and/or antigen binding fragments when produced in cell culture. The **antibodies** are anti-VEGF and anti-IgE **antibodies.** In one aspect of the invention, at least one framework region amino acid residue of the variable domain is substituted by a corresponding amino acid from a variable domain consensus sequence subgroup that has the most sequence identity with the HVRI and/or HVR2 amino acid sequence of the variable domain. In another aspect, an amino acid is placed at a position proximal to a cys residue that participates in an intrachain variable domain disulfide bond that corresponds to an amino acid found at that position in a variable domain consensus sequence subgroup that has the most sequence identity with the HVR1 and/or HVR2 amino acid sequence of the variable domain.

L20 ANSWER 2 OF 13 BIOSIS COPYRIGHT (c) 2006 The Thomson Corporation on STN
2005:457958 Document No.: PREV200510252426. Soluble forms of EphB4 and EphrinB2 reduce neovascular tuft formation in the mouse model of ROP: Novel targets to inhibit angiogenesis. Zamora, D. O. [Reprint Author]; Davies, M. H.; **Simmons, L.**; Montanaro, M. T.; Planck, S. R.; Rosenbaum, J. T.; Powers, M. R.. Oregon Hlth Sci Univ, Casey Eye Inst, Portland, OR 97201 USA. IOVS, (APR 2004) Vol. 45, No. Suppl. 2, pp. U490. Meeting Info.: Annual Meeting of the Association-for-Research-in-Vision-and-Ophthalmology. Ft Lauderdale, FL, USA. April 24 -29, 2004. Assoc Res Vis & Ophthalmol.
CODEN: IOVSDA. ISSN: 0146-0404. Language: English.
AB Purpose: EphB4 (B4) receptors and their EphrinB2 (B2)ligands are key regulators of cell migration during development and help regulate venule-arteriole boundaries. We hypothesize that these molecules play a role in neovascularization (NV) in the mouse model of oxygen-induced retinopathy and that soluble versions of these molecules can potentially alter the pathologic neovascular responsein this disease.Methods: Mice with a genetic deletion of the TF cytoplasmic tail (TFDeltaCT), PAR2

knock-outs (PAR2-/-), and double mutants (TFDelta CT/ PAR2-/-) were tested for angiogenic potential using an ex vivo aortic ringsprouting assay, in vivo turnout growth assays and a mouse retina developmental vasculature model. **Antibodies** specific for the phosphorylated TF cytoplasmic tail, PAR2, and Factor VIIa, along with various markers of actively proliferating endothelial cells, were also used to determine expression patterns in pathological samples from patients with ocular neovascularization.Results: B4 mRNA was detected in the retinas of control mice at all time points, peaking at P12-P14, and decreasing back to initial levels by P17-P24. Interestingly, exposing mice to O-2 shifted B4's peak expression to P14-P21. By P24, B4 mRNA levels were the same in O-2 and control mouse retinas. In contrast, B2 mRNA remained constant through P7-P24 in both 02 and control mouse retinas. The number of preretinal nuclei in 0, exposed mice was reduced by 66% ($p < 0.05$) in B4 injected eyes and by 69% ($p < 0.05$) in B2 injected eyes, as compared to control injections. There was no apparent alteration of intraretinal vascular development by the injections.Conclusions: B4 and B2 are expressed in the developing mouse retina, with B4'sexpression being altered in O-2 injured retinas. Treatment with either soluble B4 or B2 significantly reduced the extent of O-2 inducedNV These results support the hypothesis that B4 and B2 are regulators of retinal NV during ROP and may serve as novel targets for therapeutic intervention.

L20 ANSWER 3 OF 13 MEDLINE on STN DUPLICATE 1
2004344993. PubMed ID: 15248168. Fatalities caused by TRALI. Holness Leslie; Knippen Maureen A; **Simmons Lois**; Lachenbruch Peter A. (Office of Blood Research and Review, Center for Biologics Evaluation and Research, Food and Drug Administration, Rockville, MD 20852, USA.. Holness@cber.fda.gov) . Transfusion medicine reviews, (2004 Jul) Vol. 18, No. 3, pp. 184-8. Ref: 17. Journal code: 8709027. ISSN: 0887-7963. Pub. country: United States. Language: English.

AB This article includes a retrospective review of fatalities caused by transfusion-related acute lung injury (TRALI) over a 5-year period (from 1997 to 2002) that were reported to the Center for Biologics Evaluation and Research involving 58 recipient deaths and the corresponding 63 blood component donors. Descriptive statistics are presented. Recipient characteristics include age, sex, and admitting diagnosis. Cardiovascular disease, pulmonary disorders, and cancer were the most frequent diagnoses of transfusion recipients. Reported deaths did not appear to be associated with age, sex, reason for transfusion, or transfusion component. Implicated blood component(s) and clinical symptoms at the time of reaction were recorded. Fresh frozen plasma was implicated in one half of the cases, whereas red blood cells played a role in approximately one third. The clinical characteristics described most often in TRALI reports included shortness of breath, frothy sputum, pulmonary infiltrates, and hypoxia. Donor variables included age, sex, parity, and laboratory tests for **antibodies** to HLA and/or antigranulocyte **antibodies.** Laboratory tests showed HLA **antibodies** and/or antigranulocyte **antibodies** were positive in the majority of donors tested. More data are needed to better describe the role of **antibodies** in these reactions. Greater awareness is crucial for the practitioner to be alert for signs and symptoms of TRALI and to be aware of the necessary steps in treatment.

L20 ANSWER 4 OF 13 CAPLUS COPYRIGHT 2006 ACS on STN
2003:173763 Document No. 138:220370 A system comprising separate light and heavy chain translational units for **antibody** expression and assembly. Andersen, Dana C.; **Simmons, Laura C.** (Genentech, Inc., USA). PCT Int. Appl. WO 2003018771 A2 20030306, 73 pp. DESIGNATED STATES: W: AE, AG, AL, AM, AT, AU, AZ, BA, BB, BG, BR, BY, BZ, CA, CH, CN, CO, CR, CU, CZ, DE, DK, DM, DZ, EC, EE, ES, FI, GB, GD, GE, GH, GM, HR, HU, ID, IL, IN, IS, JP, KE, KG, KP, KR, KZ, LC, LK, LR, LS, LT, LU, LV, MA, MD, MG, MK, MN, MW, MX, MZ, NO, NZ, OM, PH, PL, PT, RO, RU, SD, SE, SG, SI, SK, SL, TJ, TM, TN, TR, TT, TZ, UA, UG, US, UZ, VC, VN, YU, ZA, ZM, ZW; RW: AT, BE, BF, BJ, CF, CG, CH, CI, CM, CY, DE, DK, ES, FI,

FR, GA, GB, GR, IE, IT, LU, MC, ML, MR, NE, NL, PT, SE, SN, TD, TG, TR. (English). CODEN: PIXXD2. APPLICATION: WO 2002-US27220 20020826. PRIORITY: US 2001-2001/PV315209 20010827.

AB The present invention provides methods comprising two sep. translational units resp. encoding the light and heavy chains for expression and production of recombinant **antibodies** in a host cell system, such as prokaryotic and eukaryotic expression systems. Particularly contemplated are recombinant systems for temporally separated expression of light chain and heavy chain of **antibodies.** Each translational unit comprises sep. secretion signal selected from STII, OmpA, PhoE, LamB, MBP and PhoA. The light and heavy chain translational units are controlled by different promoters such as phoA, TacI, TacII, lpp, lac-lpp, lac, ara, trp, trc and T7 promoters. The **antibody** products including **antibody** fragments can be used in various aspects of biol. research, diagnosis and medical treatment.

L20 ANSWER 5 OF 13 CAPLUS COPYRIGHT 2006 ACS on STN

2002:595015 Document No. 137:151108 Prokaryotically produced **antibodies** using recombinant vectors comprising two promoter-cistron pairs. **Simmons, Laura C.**; Klimowski, Laura; Reilly, Dorothea E.; Yansura, Daniel G. (Genentech, Inc., USA). PCT Int. Appl. WO 2002061090 A2 20020808, 104 pp. DESIGNATED STATES: W: AE, AG, AL, AM, AT, AU, AZ, BA, BB, BG, BR, BY, BZ, CA, CH, CN, CO, CR, CU, CZ, DE, DK, DM, DZ, EC, EE, ES, FI, GB, GD, GE, GH, GM, HR, HU, ID, IL, IN, IS, JP, KE, KG, KP, KR, KZ, LC, LK, LR, LS, LT, LU, LV, MA, MD, MG, MK, MN, MW, MX, MZ, NO, NZ, PH, PL, PT, RO, RU, SD, SE, SG, SI, SK, SL, TJ, TM, TR, TT, TZ, UA, UG, US, UZ, VN, YU, ZA, ZW; RW: AT, BE, BF, BJ, CF, CG, CH, CI, CM, CY, DE, DK, ES, FI, FR, GA, GB, GR, IE, IT, LU, MC, ML, MR, NE, NL, PT, SE, SN, TD, TG, TR. (English). CODEN: PIXXD2. APPLICATION: WO 2001-US48691 20011213. PRIORITY: US 2000-2000/PV256164 20001214.

AB The present invention provides methods and compns. for improved expression and production of recombinant **antibodies** in prokaryotic expression systems. Particularly contemplated are prokaryotic expression and production of full-length aglycosylated **antibodies.** Sep. cistron expression vectors are uniquely designed to comprise a first promoter-cistron pair for expression of an Ig light chain and a second promoter-cistron pair for expression of an Ig heavy chain, whereby expression of the light chain and heavy chain are independently regulated by sep. promoters. Each cistron within the expression cassette polynucleotide comprises a translation initiation region (TIR) operably linked to the nucleic acid sequence coding for the light chain or heavy chain of the full-length **antibody.** Thus, various expression vectors were made for expression of **antibodies** specific to tissue factor and **antibodies** specific to vascular endothelial cell growth factor. For each vector construction, an expression cassette was cloned into the framework of the Escherichia coli pBR322 at the EcoRI site, and contained at least the following components: (1) a phoA promoter for the control of transcription; (2) a Shine-Dalgarno sequence from the E. coli trp or the heat-stable enterotoxin II gene; and (3) a λt0 terminator to end transcription. To address the problem of inefficient secretion, polycistronic vectors were made with modulated TIR strength combinations for light and heavy chain. Co-expression with Dsb proteins facilitate the proper folding and assembly of the **antibodies.** Functional characterization and pharmacokinetics of anti-(tissue factor) **antibodies** produced in E. coli with those produced in standard CHO cells showed no differences. The **antibody** products of the invention can be used in various aspects of biol. research, diagnosis, and medical treatment.

L20 ANSWER 6 OF 13 MEDLINE on STN DUPLICATE 2

2002272182. PubMed ID: 12009210. Expression of full-length immunoglobulins in Escherichia coli: rapid and efficient production of aglycosylated **antibodies. Simmons Laura C**; Reilly Dorothea; Klimowski Laura; Raju T Shantha; Meng Gloria; Sims Paul; Hong Kyu; Shields Robert L;

Damico Lisa A; Rancatore Patricia; Yansura Daniel G. (Department of Molecular Biology, Genentech, Inc., 1 DNA Way, South San Francisco, CA 94080, USA.) Journal of immunological methods, (2002 May 1) Vol. 263, No. 1-2, pp. 133-47. Journal code: 1305440. ISSN: 0022-1759. Pub. country: Netherlands. Language: English.

AB Many research and clinical applications require large quantities of full-length **antibodies** with long circulating half-lives, and production of these complex multi-subunit proteins has in the past been restricted to eukaryotic hosts. In this report, we demonstrate that efficient secretion of heavy and light chains in a favorable ratio leads to the high-level expression and assembly of full-length IgGs in the Escherichia coli periplasm. The technology described offers a rapid, generally applicable and potentially inexpensive method for the production of full-length therapeutic **antibodies**, as verified by the expression of several humanized IgGs. One E. coli-derived **antibody** in particular, anti-tissue factor IgG1, has been thoroughly evaluated and has all of the expected properties of an aglycosylated **antibody**, including tight binding to antigen and the neonatal receptor. As predicted, the protein lacks binding to C1q and the FcgammaRI receptor, making it an ideal candidate for research purposes and therapeutic indications where effector functions are either not required or are actually detrimental. In addition, a limited chimpanzee study suggests that the E. coli-derived IgG1 retains the long circulating half-life of mammalian cell-derived **antibodies.**

L20 ANSWER 7 OF 13 BIOSIS COPYRIGHT (c) 2006 The Thomson Corporation on STN

2000:135245 Document No.: PREV200000135245. Identification of receptor and antagonist **antibody** epitopes on human Neurturin by alanine scanning mutagenesis. Devaux, B. [Reprint author]; Hongo, J. S. [Reprint author]; Suggett, S. [Reprint author]; Schroeder, K. [Reprint author]; **Simmons, L.**; Tsai, S. P.; Jung, C.; Evangelista, F. [Reprint author]; Moffat, B.; Eigenbrot, C.. Department of Antibody Technologies, Genentech, Inc., South San Francisco, CA, 94080, USA. Society for Neuroscience Abstracts, (1999) Vol. 25, No. 1-2, pp. 1531. print. Meeting Info.: 29th Annual Meeting of the Society for Neuroscience. Miami Beach, Florida, USA. October 23-28, 1999. Society for Neuroscience. ISSN: 0190-5295. Language: English.

L20 ANSWER 8 OF 13 CAPLUS COPYRIGHT 2006 ACS on STN

1994:595902 Document No. 121:195902 **Antibodies** to β-amyloid peptide and pharmaceutical screens for agents inhibiting neurotoxicity of β-amyloid peptide. Becker, Gerald Wayne; Brems, David Nettleship; Chaney, Michael Owen; May, Patrick Cornelious; Rydel, Russel Eugene; **Simmons, Linda Karen**; Tomaselli, Kevin James (Eli Lilly and Co., USA; Athena Neurosciences, Inc.). Eur. Pat. Appl. EP 613007 A2 19940831, 6 pp. DESIGNATED STATES: R: AT, BE, CH, DE, DK, ES, FR, GB, GR, IE, IT, LI, LU, NL, PT, SE. (English). CODEN: EPXXDW. APPLICATION: EP 1994-301170 19940218. PRIORITY: US 1993-21609 19930222.

AB This invention describes a series of assays useful in evaluating the efficacy of agents which inhibit the neurotoxic effects of β-amyloid peptide. These assays employ β-amyloid peptide which is in a predominantly β-sheet conformation. This invention also encompasses **antibodies** having a specificity for β-amyloid peptide which is predominantly in a β-sheet conformation as well as pharmaceutical formulations containing these **antibodies.** These **antibodies** show poor reactivity with β-amyloid peptide which has a great deal of random coil or α-helix secondary structure. Neurotoxicity assays in which Ca levels, tetrazolium dye, or lactate dehydrogenase are measured are described. These 3 assays demonstrated that there is a direct correlation between degree of β-sheet structure in the β-amyloid peptide and its neurotoxicity.

L20 ANSWER 9 OF 13 EMBASE COPYRIGHT (c) 2006 Elsevier B.V. All rights reserved on STN

94263092 EMBASE Document No.: 1994263092. Application of enzymeimmunoassay to

measure oestrone sulphate concentrations in cows' milk during pregnancy. Henderson K.M.; Camberis L.M.; **Simmons L.M.H.**; Starrs W.J.; Hardie A.H.M.. AgResearch, Wallaceville Animal Research Centre, PO Box 40063,Upper Hutt, New Zealand. Journal of Steroid Biochemistry and Molecular Biology Vol. 50, No. 3-4, pp. 189-196 1994.
ISSN: 0960-0760. CODEN: JSBBEZ
Pub. Country: United Kingdom. Language: English. Summary Language: English.
Entered STN: 940921. Last Updated on STN: 940921

AB The characteristics of antigen- and **antibody**-coated enzymeimmunoassay (EIA) formats to measure oestrone sulphate (OS) were studied using a murine monoclonal **antibody** as the primary **antibody.** In an antigen-coated format the most sensitive EIA (9 fmol/well) was achieved using 6-ketoestrone-6-O-carboxymethyloxime (OCMO) coupled to bovine serum albumin (BSA), as the coating antigen, and horseradish peroxidase (HRP), as the enzyme label. In an **antibody** -coated format, comparable sensitivity could be achieved using HRP conjugated to either OCMO, oestrone-3-glucuronide (OG) or oestrone-3-hemisuccinate (OHS) as the steroid 'tracer'. In both the antigen- and **antibody**-coated formats replacing HRP with alkaline phosphatase (AP) markedly aggravated the assay sensitivity. The antigen-coated EIA format was used to measure OS concentrations in cows' milk directly without an initial defatting step, and a progressive increase in OS concentrations in milk as pregnancy progressed was observed. Median OS concentrations rose from 1.1 nmol/l at days 70-99 of pregnancy (n = 44) to 3.2 nmol/l at days 140-160 (n = 92). Oestrone sulphate concentrations in milk from non-pregnant cows (n = 51) ranged from non-detectable to 1.3 nmol/l with a median value of 0.4 nmol/l. Only 5% of cows 120 or more days pregnant had milk OS concentrations within the range of values found in milk from non-pregnant cows. Accurate discrimination of non-pregnant and pregnant cows can thus be achieved on the basis of OS concentrations in milk samples taken at least 120 days after mating/insemination. This EIA for OS may have a role in the dairy industry as an alternative non-invasive means of determining pregnancy status in cows.

L20 ANSWER 10 OF 13 SCISEARCH COPYRIGHT (c) 2006 The Thomson Corporation on STN

1992:724314 The Genuine Article (R) Number: KB651. COMPARISON OF ACELLULAR (B-TYPE) AND WHOLE-CELL PERTUSSIS-COMPONENT DIPHTHERIA-TETANUS-PERTUSSIS VACCINES AS THE 1ST BOOSTER IMMUNIZATION IN 15-MONTH-OLD TO 24-MONTH-OLD CHILDREN. FELDMAN S (Reprint); PERRY C S; ANDREW M; JONES L; MOFFITT J E; ABNEY R; CARLYLE W; FREEMAN E E; HENDRICK J; HOPPER S; RAY M; SISTRUNK W; SMITH W H; STONE L; WELCH P; WOMACK N; MILLER J; THOMPSON R H; **SIMMONS L**; SHERWOOD J A; DENNEY S J; SHAAK C; COOKE D T; MCCASLIN L. UNIV MISSISSIPPI, MED CTR, DEPT PEDIAT, DIV INFECT DIS, 2500 N STATE ST, JACKSON, MS 39216 (Reprint); UNIV MISSISSIPPI, MED CTR, DEPT PREVENT MED, JACKSON, MS 39216. JOURNAL OF PEDIATRICS (DEC 1992) Vol. 121, No. 6, pp. 857-861. ISSN: 0022-3476. Publisher: MOSBY-YEAR BOOK INC, 11830 WESTLINE INDUSTRIAL DR, ST LOUIS, MO 63146-3318. Language: English.
ABSTRACT IS AVAILABLE IN THE ALL AND IALL FORMATS

AB We compared an acellular (B type) pertussis-component diphtheria-tetanuspertussis (DTP-Ac) vaccine containing equal amounts of filamentous hemagglutinin and lymphocytosis-promoting factor with a conventional whole-cell vaccine as the first booster immunization in 162 healthy children 15 to 24 months of age. Fewer local reactions (e.g., erythema, swelling, and tenderness at the injection site) were seen in DTP-Ac vaccine recipients during the first 48 hours of observation. This group also had fewer episodes of lever (greater-than-or-equal-to 38-degrees-C) and other systemic reactions (e.g., irritability, drowsiness, and anorexia). Overall, 57% of the DTP-Ac vaccine recipients had no obvious adverse reactions, in contrast to 5% in the comparison group. At 4 to 8 weeks after vaccination, serum **antibody** responses to filamentous hemagglutinin and lymphocytosis-promoting factor were greater in recipients of the acellular vaccine as determined by an

enzyme-linked immunosorbent assay. We conclude that this B-type acellular vaccine is both immunogenic and much less likely to cause an adverse reaction than a currently licensed whole-cell vaccine, and is suitable for routine booster immunizing doses to protect against pertussis.

L20 ANSWER 11 OF 13 EMBASE COPYRIGHT (c) 2006 Elsevier B.V. All rights reserved on STN
84104508 EMBASE Document No.: 1984104508. Evidence for immunological cross-reaction between sporozoites and blood stages of a human malaria parasite. Hope I.A.; Hall R.; **Simmons Ll. D.**; et al.. Department of Molecular Biology, University of Ediburgh, Edinburgh EH9 3JR, United Kingdom. Nature Vol. 308, No. 5955, pp. 191-194 1984.
CODEN: NATUAS
Pub. Country: United Kingdom. Language: English.
Entered STN: 911210. Last Updated on STN: 911210
AB Malaria parasites (Plasmodium spp.) show a complex pattern of development in the mammalian host and many studies support the view that the surface of the sporozoite, injected by the mosquito, has no antigens in common with the erythrocytic stage of development. For example, immunization with the erythrocytic parasites generates antisera with negligible titre by indirect immunofluorescence to the sporozoite surface. Although monoclonal **antibodies** prepared against erythrocytic stages were reported to show cross-reaction to the sporozoite stage, this appeared to be due to cytoplasmic antigens exposed by the method of sporozoite preparation, and in Plasmodium knowlesi, a cDNA clone coding for the circumsporozoite antigen, the major protein of the sporozoite surface, showed no hydridization to mRNA isolated from the erythrocytic stages. Here, however, we present evidence for an antigenic determinant shared by the sporozoite surface and the erythrocytic stages of the human malaria parasite, P. falciparum. Moreover, our studies show that the antigen(s) elicit a strong immune response in man.

L20 ANSWER 12 OF 13 MEDLINE on STN
72267634. PubMed ID: 4341396. Chickenpox in young anthropoid apes: clinical and laboratory findings. White R J; **Simmons L**; Wilson R B. Journal of the American Veterinary Medical Association, (1972 Sep 15) Vol. 161, No. 6, pp. 690-2. Journal code: 7503067. ISSN: 0003-1488. Pub. country: United States. Language: English.

L20 ANSWER 13 OF 13 MEDLINE on STN
68152398. PubMed ID: 5630778. The Weil-Felix test: a survey of sera from the Manchester area, 1963-66. **Simmons L E.** Monthly bulletin of the Ministry of Health and the Public Health Laboratory Service, (1967 Dec) Vol. 26, pp. 262-5. Journal code: 7502630. ISSN: 0368-881X. Pub. country: ENGLAND: United Kingdom. Language: English.

=>

---Logging off of STN---

=>
Executing the logoff script...

=> LOG Y

COST IN U.S. DOLLARS	SINCE FILE ENTRY	TOTAL SESSION
FULL ESTIMATED COST	140.79	141.00

DISCOUNT AMOUNTS (FOR QUALIFYING ACCOUNTS)	SINCE FILE ENTRY	TOTAL SESSION

CA SUBSCRIBER PRICE -10.50 -10.50

STN INTERNATIONAL LOGOFF AT 08:45:02 ON 20 APR 2006

THE JOURNAL OF BIOLOGICAL CHEMISTRY
Vol. 272, No. 16, Issue of April 18, pp. 10678–10684, 1997
Printed in U.S.A.

Antibody Humanization Using Monovalent Phage Display*

(Received for publication, December 20, 1996, and in revised form, February 7, 1997)

Manuel Baca‡, Leonard G. Presta§, Shane J. O'Connor§, and James A. Wells‡¶

From the Departments of ‡Protein Engineering and §Immunology, Genentech, Inc., South San Francisco, California 94080

Antibody humanization often requires the replacement of key residues in the framework regions with corresponding residues from the parent non-human antibody. These changes are in addition to grafting of the antigen-binding loops. Although guided by molecular modeling, assessment of which framework changes are beneficial to antigen binding usually requires the analysis of many different antibody mutants. Here we describe a phage display method for optimizing the framework of humanized antibodies by random mutagenesis of important framework residues. We have applied this method to humanization of the anti-vascular endothelial growth factor murine monoclonal antibody A4.6.1. Affinity panning of a library of humanized A4.6.1 antibody mutants led to the selection of one variant with greater than 125-fold enhanced affinity for antigen relative to the initial humanized antibody with no framework changes. A single additional mutation gave a further 6-fold improvement in binding. The affinity of this variant, 9.3 nM, was only 6-fold weaker than that of a murine/human chimera of A4.6.1. This method provides a general means of rapidly selecting framework mutations that improve the binding of humanized antibodies to their cognate antigens and may prove an attractive alternative to current methods of framework optimization based on cycles of site-directed mutagenesis.

Monoclonal antibodies (mAbs)[1] have enormous potential as therapeutic agents; however, most mAbs are derived from murine or other non-human sources, which severely limits their clinical efficacy. In addition to the immunogenicity of rodent mAbs when administered to humans (1–3), further limitations arise from weak recruitment of effector function (4, 5) and rapid clearance from serum (6, 7). As a means of circumventing these deficiences, the antigen-binding properties of murine mAbs can be conferred to human antibodies through a process known as antibody "humanization" (4, 8). A humanized antibody contains the amino acid sequences from the six complementarity-determining regions (CDRs) of the parent murine mAb, which are grafted onto a human antibody framework. For this reason, humanization of non-human antibodies is commonly referred to as CDR grafting. The low content of non-human sequence in humanized antibodies (~5%) has proven effective in both reducing the immunogenicity and prolonging the serum half-life in humans (7, 9).

Unfortunately, simple grafting of CDR sequences often yields humanized antibodies that bind antigen much more weakly than the parent murine mAb (4, 10–16), and decreases in affinity of up to several hundredfold have been reported (13–15). To restore high affinity, the antibody must be further engineered to fine tune the structure of the antigen-binding loops. This is achieved by replacing key residues in the framework regions of the antibody variable domains with the matching sequence from the parent murine antibody. These framework residues are usually involved in supporting the conformation of the CDR loops (17), although some framework residues may themselves directly contact the antigen (18). Chothia and Lesk (19) first noted the importance of certain framework residues to CDR conformation, and a comprehensive examination of all framework residues that can affect antigen binding was conducted by Foote and Winter (20). These authors tabulated a list of some 30 "Vernier" residues that can potentially contribute to CDR structure. Although higher antigen affinity would likely result from editing the entire set of Vernier residues within a humanized antibody to match the corresponding parent murine sequence, this is not generally desirable given the increased risk of immunogenicity imposed by adding further elements of murine sequence. Thus, from a therapeutic standpoint it is preferable to confine framework changes to the minimum set that affords a high affinity humanized antibody.

As shown in the literature (4, 10–16), the task of identifying framework residues that affect antigen binding is the most challenging and time-consuming aspect of antibody humanization. Although these critical framework residues are generally derived from the large set proposed by Foote and Winter (20), a small set of changes will usually suffice to optimize binding, although these often differ from one humanized antibody to the next. Whereas a molecular model of the humanized antibody can provide valuable guidance, the proper combination of mutations must be determined by experiment. Typically, this is achieved by preparing a panel of mutants with "suspect" framework residues replaced by their murine counterparts. These variants are each tested for antigen binding, and favorable mutations that enhance affinity are combined into a final variant.

As a means of simplifying antibody humanization, a number of different approaches have been developed. A common method is to select the human framework most homologous in sequence to that of the murine antibody of interest (10–12). In this way, the number of mismatches between the humanized and parent murine framework is minimized, and it becomes less likely that a key framework residue will need to be replaced. However, it should be noted that even a single incorrect framework residue can have a dramatic effect on antigen binding (11). An alternative humanization strategy was originally proposed by Padlan (21): here, rather than grafting the CDRs onto a human framework, the entire murine variable domains

* The costs of publication of this article were defrayed in part by the payment of page charges. This article must therefore be hereby marked "*advertisement*" in accordance with 18 U.S.C. Section 1734 solely to indicate this fact.

¶ To whom correspondence should be addressed: 460 Point San Bruno Blvd., South San Francisco, CA 94080. Tel.: 415-225-1177; Fax: 415-225-3734; E-mail: jaw@gene.com.

[1] The abbreviations used are: mAb, monoclonal antibody; CDR, complementarity-determining region; V_L, light chain variable region; $V_L\kappa I$, kappa light chain variable region subgroup I; V_H, heavy chain variable region; $V_H III$, heavy chain variable region subgroup III; VEGF, vascular endothelial growth factor; MES, 4-morpholineethanesulfonic acid; PBS, phosphate-buffered saline.

are retained and select framework residues are replaced with human sequence. Only those residues on the surface of the antibody framework, as defined by exposure to solvent, are targeted for replacement. These residues are considered unimportant for antigen binding but most likely to contribute to any potential immunogenicity. On the other hand, buried residues are retained as the murine sequence since these are most likely to affect the structure (and thus antigen binding) of the antibody but are of low immunogenicity since they are in effect "hidden" from the immune system. Although this approach has been successfully used to humanize two different murine mAbs (22, 23), it remains to be seen whether these antibodies are indeed nonimmunogenic, since even buried residues can invoke a T-cell immune response if presented as a denatured peptide by a class II major histocompatability complex molecule (24).

In contrast to these other techniques, an alternative approach is to humanize antibodies using only a single human framework, regardless of the sequence of the parent murine antibody. This method has been successfully used to humanize a number of murine antibodies (13–15, 25) using a framework derived from consensus sequences of the most abundant human subclasses, namely $V_L\kappa$ subgroup I ($V_L\kappa$I) and V_H subgroup III (V_HIII) (26). Use of the most common human V_L and V_H frameworks minimizes any potential immunogenicity of the humanized antibody and also eliminates possible idiosyncracies associated with any one particular framework. In addition, this framework has been demonstrated to give good yields of antibody when expressed recombinantly in either *Escherichia coli* or eukaryotic expression systems, an important consideration for antibodies that are to go into large scale development for clinical applications. Based on the collective data from these and other unpublished antibody humanizations, we have observed that the framework residues that most often influence antigen binding are consistently derived from a set of only 11 residues. We have incorporated this information into the design of a random mutagenesis approach to antibody humanization. By randomizing this small set of critical framework residues and by monovalent display of the resultant library of antibody molecules on the surface of filamentous phage (27, 28), optimal framework sequences can be identified via affinity-based selection. Here we describe the application of this approach to the humanization of the murine antibody A4.6.1 (29, 30), an antibody that binds to vascular endothelial growth factor (VEGF).

EXPERIMENTAL PROCEDURES

Construction of Anti-VEGF Phagemid Vector, pMB4-19—The murine anti-VEGF mAb A4.6.1 blocks VEGF receptor binding and has been described previously (29, 30). The first Fab variant of humanized A4.6.1, hu2.0, was constructed by site-directed mutagenesis using a deoxyuridine-containing template of plasmid pAK2 (13) that codes for a human $V_L\kappa$I-$C\kappa_1$ light chain and human V_HIII-$C_H1\gamma_1$ heavy chain Fd fragment. The transplanted A4.6.1 CDR sequences were chosen according to the sequence definition of Kabat *et al.* (26), except for CDR-H1, which we extended to encompass both sequence and structural (19) definitions, *viz.* V_H residues 26–35. The Fab encoding sequence was subcloned into the phagemid vector phGHamg3 (27, 28). This final construct, pMB4-19, encodes the initial humanized A4.6.1 Fab, hu2.0, with the carboxyl terminus of the heavy chain fused precisely to the carboxyl portion of the M13 gene III coat protein. pMB4-19 is similar in construction to pDH188, a previously described plasmid for monovalent display of Fab fragments (31). Notable differences between pMB4-19 and pDH188 include a shorter M13 gene III segment (codons 249–406) and use of an amber stop codon immediately following the antibody heavy chain Fd fragment. This permits expression of both secreted heavy chain or heavy chain-gene III fusions in *supE* suppressor strains of *E. coli*.

Expression and Purification of Humanized A4.6.1 Fab Fragments—*E. coli* strain 34B8, a nonsuppressor, was transformed with phagemid pMB4-19 or variants thereof. Single colonies were grown overnight at 37 °C in 5 mL of 2YT medium containing 50 μg/mL carbenicillin. These cultures were diluted into 200 mL of AP5 medium (32) containing 20 μg/mL carbenicillin and incubated for 26 h at 30 °C. The cells were pelleted at 4000 × *g* and frozen at −20 °C for at least 2 h. Cell pellets were then resuspended in 5 mL of 10 mM Tris-HCl (pH 7.6) containing 1 mM EDTA, shaken at 4 °C for 90 min, and centrifuged at 10,000 × *g* for 15 min. The supernatant was applied to a 1-mL streptococcal protein G-Sepharose column (Pharmacia Biotech Inc.) and washed with 10 mL of 10 mM MES (pH 5.5). The bound Fab fragment was eluted with 2.5 mL of 100 mM acetic acid and immediately neutralized with 0.75 mL of 1 M Tris-HCl, pH 8.0. Fab preparations were buffer-exchanged into PBS and concentrated using Centricon-30 concentrators (Amicon). Typical yields of Fab were ~1 mg/L culture after protein G purification. Purified Fab samples were characterized by electrospray mass spectrometry, and concentrations were determined by amino acid analysis.

Construction of the Anti-VEGF Fab Phagemid Library—The humanized A4.6.1 phagemid library was constructed by site-directed mutagenesis according to the method of Kunkel *et al.* (33). A derivative of pMB4-19 containing TAA stop triplets at V_H codons 24, 37, 67, and 93 was prepared for use as the mutagenesis template (all sequence numbering is according to Kabat *et al.* (26)). This modification was to prevent subsequent background contamination by wild type sequences. The codons targeted for randomization were 4 and 71 (light chain) and 24, 37, 67, 69, 71, 73, 75, 76, 78, 93, and 94 (heavy chain).

To randomize heavy chain codons 67, 69, 71, 73, 75, 76, 78, 93, and 94 with a single mutagenic oligonucleotide, two 126-mer oligonucleotides were first preassembled from 60-mer and 66-mer fragments by template-assisted enzymatic ligation. Briefly, 1.5 nmol of 5′ phosphorylated oligonucleotide 503-1 (GAT TTC AAA CGT CGT NYT ACT WTT TCT AGA GAC AAC TCC AAA AAC ACA BYT TAC CTG CAG ATG AAC) or 503-2 (GAT TTC AAA CGT CGT NYT ACT WTT TCT TTA GAC ACC TCC GCA AGC ACA BYT TAC CTG CAG ATG AAC) were combined with 1.5 nmol of 503-3 (AGC CTG CGC GCT GAG GAC ACT GCC GTC TAT TAC TGT DYA ARG TAC CCC CAC TAT TAT GGG) (randomized codons underlined; N = A/G/T/C; W = A/T; B = G/T/C; D = G/A/T; R = A/G; Y = C/T). 1.5 nmol of template oligonucleotide (CTC AGC GCG CAG GCT GTT CAT CTG CAG GTA), with complementary sequence to the 5′ ends of 503-1/503-2 and the 3′ end of 503-3, was added to hybridize each end of the ligation junction. Taq ligase and ligase buffer (New England Biolabs) were added, and the reaction mixture was subjected to 40 rounds of thermal cycling, (95 °C for 1.25 min, 50 °C for 5 min) to cycle the template oligonucleotide between ligated and unligated junctions. The product 126-mer oligonucleotides were purified on a 6% urea, TBE polyacrylamide gel and extracted from the polyacrylamide in buffer. The two 126-mer products were combined in equal ratio, ethanol precipitated, and finally solubilized in 10 mM Tris-HCl, 1 mM EDTA. The mixed 126-mer oligonucleotide product was designated 504-01.

Randomization of select framework codons (V_L, 4 and 71; V_H, 24, 37, 67, 69, 71, 73, 75, 76, 93, and 94) was effected in two steps. First, V_L randomization was achieved by preparing three additional derivatives of the modified pMB4-19 template. Framework codons 4 and 71 in the light chain were replaced individually or pairwise using the two mutagenic oligonucleotides GCT GAT ATC CAG TTG ACC CAG TCC CCG and TCT GGG ACG GAT TAC ACT CTG ACC ATC. Deoxyuridine-containing template was prepared from each of these new derivatives. Together with the original template, these four constructs coded for each of the four possible light chain framework sequence combinations (see Table I).

Oligonucleotides 504-1, a mixture of two 126-mer oligonucleotides (see above), and CGT TTG TCC TGT GCA RYT TCT GGC TAT ACC TTC ACC AAC TAT GGT ATG AAC TGG RTC CGT CAG GCC CCG GGT AAG were used to randomize heavy chain framework codons using each of the four templates just described. The four libraries were electroporated into *E. coli* XL-1 Blue cells (Stratagene) and combined. The total number of independent transformants was estimated at $>1.2 \times 10^8$, approximately 1500-fold greater than the maximum number of DNA sequences in the library.

Phagemid particles displaying the humanized A4.6.1 Fab fragments were propagated in *E. coli* XL-1 Blue cells. Briefly, cells harboring the randomized pMB4-19 construct were grown overnight at 37 °C in 25 mL of 2YT medium containing 50 μg/mL carbenicillin and approximately 10^{10} M13KO7 helper phage (34). Phagemid stocks were purified from culture supernatants by precipitation with a saline polyethylene glycol solution and resuspended in 100 μL of PBS (~10^{14} phagemid/mL)

Selection of Humanized A4.6.1 Fab Variants—Purified $VEGF^{1-121}$ (100 μL at 10 μg/mL in PBS) was coated onto a microtiter plate well

overnight at 4 °C. The coating solution was discarded and this well, in addition to an uncoated well, was blocked with 6% skim milk for 1 h and washed with PBS containing 0.05% Tween 20. 10 μL of phagemid stock, diluted to 100 μL with 20 mM Tris (pH 7.5) containing 0.1% bovine serum albumin and 0.05% Tween 20, was added to each well. After 2 h the wells were washed and the bound phage eluted with 100 μL of 0.1 M glycine (pH 2.0) and neutralized with 25 μL of 1 M Tris, pH 8.0. An aliquot of this was used to titer the number of phage eluted. The remaining phage eluted from the VEGF-coated well were propagated for use in the next selection cycle. A total of eight rounds of selection was performed, after which time 20 individual clones were selected and sequenced (35).

Determination of VEGF Binding Affinities—Association and dissociation rate constants for binding of humanized A4.6.1 Fab variants to $VEGF^{1-121}$ were measured by surface plasmon resonance (36) on a Pharmacia BIAcore instrument. $VEGF^{1-121}$ was covalently immobilized on the biosensor chip via primary amino groups. Binding of humanized A4.6.1 Fab variants was measured by flowing solutions of Fab in PBS, 0.05% Tween 20 over the chip at a flow rate of 20 μL/min. Following each binding measurement, residual Fab was stripped from the immobilized ligand by washing with 5 μL of 50 mM aqueous HCl at 3 μL/min. Binding profiles were analyzed by nonlinear regression using a simple monovalent binding model (BIAevaluation software version 2.0, Pharmacia).

RESULTS

Construction of Humanized A4.6.1—An initial humanized A4.6.1 Fab fragment was constructed (hu2.0) (Fig. 1) in which the CDRs from A4.6.1 were grafted onto a human $V_L\kappa$I-V_HIII framework. All other residues in hu2.0 were maintained as the human sequence. Binding of this variant to VEGF was so weak that it was undetectable. Based on the relative affinity of other weakly binding humanized A4.6.1 variants (data not shown), the K_d for binding of hu2.0 was estimated at >7 μM. This contrasts with an affinity of 1.6 nM for a chimeric Fab construct consisting of the intact V_L and V_H domains from murine A4.6.1 and human constant domains. Thus, binding of hu2.0 to VEGF was reduced at least 4000-fold relative to the chimera. The absence of detectable VEGF binding by variant hu2.0 highlights the important role of the framework in properly structuring the CDR loops for antigen binding.

Design of Antibody Library—Based on the cumulative results from humanizing a number of murine antibodies onto a human $V_L\kappa$I-V_HIII framework (13–15, 25), we have observed that most framework changes, as required to optimize antigen binding, are limited to some subset of the residues shown in Table I and Fig. 2. We reasoned that this information could serve as the basis for a combinatorial approach to selecting required framework mutations. Accordingly, we designed a combinatorial approach to the humanization of mAb A4.6.1 by randomizing these key framework residues and displaying the resultant library of Fab variants on the surface of filamentous phage.

Each of residues 4 and 71 in the light chain and 24, 37, 67, 78, and 93 from the heavy chain were partially randomized to allow the selection of either the murine A4.6.1, human $V_L\kappa$I-V_HIII sequence, or sequences commonly found in other human and murine frameworks (Table I). Note that randomization of these residues was not confined to a choice between the human $V_L\kappa$I-V_HIII consensus or A4.6.1 framework sequences. Rather, inclusion of additional amino acids commonly found in other human and murine framework sequences allows for the possibility that additional diversity may lead to the selection of tighter binding variants.

Additional heavy chain framework residues were randomized in a binary fashion according to the human V_HIII and murine A4.6.1 framework sequences. Residues V_H 71, 73, 75, and 76 are positioned in a hairpin loop adjacent to the antigen-binding site. The side chains of V_H 71 and 73 are largely buried in canonical antibody structures, and their potential role in

V_L domain

```
                10        20        30        40
A4.6.1  DIQMTQTTSSLSASLGDRVIISCSASQDISNYLNWYQQKP
                **        *   * *
hu2.0   DIQMTQSPSSLSASVGDRVTITCSASQDISNYLNWYQQKP

hu2.10  DIQMTQSPSSLSASVGDRVTITCSASQDISNYLNWYQQKP

                50        60        70        80
A4.6.1  DGTVKVLIYFTSSLHSGVPSRFSGSGSGTDYSLTISNLEP
        **** *                          **    * *
hu2.0   GKAPKLLIYFTSSLHSGVPSRFSGSGSGTDFTLTISSLQP
                                          •
hu2.10  GKAPKLLIYFTSSLHSGVPSRFSGSGSGTDYTLTISSLQP

                90       100
A4.6.1  EDIATYYCQQYSTVPWTFGGGTKLEIK
          *                 *   *
hu2.0   EDFATYYCQQYSTVPWTFGQGTKVEIK

hu2.10  EDFATYYCQQYSTVPWTFGQGTKVEIK
```

V_H domain

```
                10        20        30        40
A4.6.1  EIQLVQSGPELKQPGETVRISCKASGYTFTNYGMNWVKQA
         *   *  ** *   *** * *                 *
hu2.0   EVQLVESGGGLVQPGGSLRLSCAASGYTFTNYGMNWVRQA
                                              •
hu2.10  EVQLVESGGGLVQPGGSLRLSCAASGYTFTNYGMNWIRQA

                50 a      60        70        80
A4.6.1  PGKGLKWMGWINTYTGEPTYAADFKRRFTFSLETSASTAYL
          * *                       * *** ** * *
hu2.0   PGKGLEWVGWINTYTGEPTYAADFKRRFTISRDNSKNTLYL
                                      • • •• •
hu2.10  PGKGLEWVGWINTYTGEPTYAADFKRRFTISLDTSASTVYL

          abc      90       100abcdef       110
A4.6.1  QISNLKNDDTATYFCAKYPHYYGSSHWYFDVWGAGTTVTVSS
         *** ***   * *  *                 *   *
hu2.0   QMNSLRAEDTAVYYCARYPHYYGSSHWYFDVWGQGTLVTVSS
                    •
hu2.10  QMNSLRAEDTAVYYCAKYPHYYGSSHWYFDVWGQGTLVTVSS
```

FIG. 1. **Amino acid sequences of murine A4.6.1 and humanized A4.6.1 variants hu2.0 and hu2.10.** Sequence numbering is according to Kabat *et al.* (26), and mismatches are indicated by *asterisks* (murine A4.6.1 *versus* hu2.0) or *bullets* (hu2.0 *versus* hu2.10). Variant hu2.0 contains only the CDR sequences (*boldface*) from the murine antibody grafted onto a human light chain κ subgroup I-heavy chain subgroup III framework. hu2.10 was the consensus humanized clone obtained from phage sorting experiments. CDRs are defined according to the sequence definition of Kabat *et al.* (26), except for CDR-H1, which is the combined sequence and structural (19) definition.

shaping the conformation of CDR-H2 and CDR-H3 is well known (11, 13, 25, 37). On the other hand, although the side chains of V_H 75 and 76 are exposed to solvent (Fig. 2), it has nevertheless been observed that these two residues can also influence antigen binding (15), presumably due to direct antigen contact in some antibody-antigen complexes. Because of their proximity in sequence and possible interdependence, we randomized V_H 71, 73, 75, and 76 en bloc so that only two possible combinations of this tetrad could be selected: either all human V_HIII or all murine A4.6.1 sequence. Finally, V_H residues 69 and 94 were randomized, but only to represent the V_HIII and A4.6.1 sequences. We have not replaced V_H 69 and 94 in previous antibody humanizations, but because they differ between the V_HIII consensus and A4.6.1 sequences (Fig. 1) and have been noted as potentially important for proper CDR con-

TABLE I
Key framework residues important for antigen binding and targeted for randomization

	Framework residue	Human $V_L\kappa$I, V_HIII consensus residue	Murine A4.6.1 residue	Randomization[a]
V_L	4	Met	Met	Met, Leu
	71	Phe	Tyr	Phe, Tyr
V_H	24	Ala	Ala	Ala, Val, Thr
	37	Val	Val	Val, Ile
	67	Phe	Phe	Phe, Val, Thr, Leu, Ile, Ala
	69	Ile	Phe	Ile, Phe
	71	Arg	Leu	[Arg Asp Lys Asn] [Leu Thr Ala Ser]
	73	Asp	Thr	
	75	Lys	Ala	
	76	Asn	Ser	
	78	Leu	Ala	Leu, Ala, Val, Phe
	93	Ala	Ala	Ala, Val, Leu, Ser, Thr
	94	Arg	Lys	Arg, Lys

[a] Amino acid diversity in phagemid library.
[b] V_H 71, 73, 75, and 76 randomized to yield the all-murine (L71/T73/A75/S76) or all-human (R71/D73/K75/N76) V_HIII tetrad.

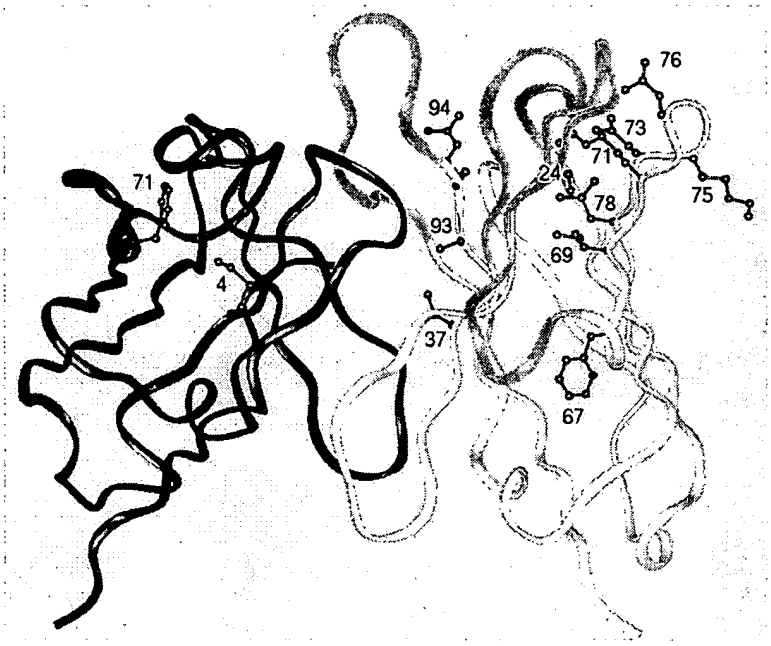

FIG. 2. **Framework residues targeted for randomization.** The V_L backbone trace is in *blue*, V_H is in *yellow*, and *darker coloring* represents the CDR loops. Residues selected for randomization are shown by a *ball and stick* representation and are listed in Table I.

formation (20), we opted to include them in the randomization strategy.

Humanized A4.6.1 Fab Library Displayed on the Surface of Phagemid—A variety of systems have been developed for the functional display of antibody fragments on the surface of filamentous phage (38). These include the display of Fab fragments or single chain variable fragments as fusions to either the gene III or gene VIII coat proteins of M13 bacteriophage. We opted to use a system similar to that described by Garrard *et al.* (31) in which a Fab fragment is monovalently displayed as a gene III fusion (Fig. 3). This system has two notable features: unlike single chain variable fragments, Fab fragments have no tendency to form dimeric species, the presence of which can prevent selection of the tightest binders due to avidity effects. Second, the monovalency of the displayed protein eliminates a second potential source of avidity effects that would otherwise result from the presence of multiple copies of a protein on each phagemid particle (27, 28).

A concern in designing the humanized A4.6.1 phagemid library was that residues targeted for randomization were widely distributed across the V_L and V_H sequences. Limitations in the length of synthetic oligonucleotides require that simultaneous randomization of each of these framework positions can be achieved only through the use of multiple oligonucleotides. However, as the total number of oligonucleotides increases, the efficiency of mutagenesis decreases (*i.e.* the proportion of mutants obtained that incorporate sequence derived from all of the mutagenic oligonucleotides). To circumvent this problem, we incorporated two features into our library construction. The first was to prepare four different mutagenesis templates coding for each of the possible V_L framework combinations. This was simple to do given the limited diversity of the light chain framework (only four different sequences) but was beneficial in that it eliminated the need for two oligonucleotides from the mutagenesis strategy. Second, we preassembled two 126-base oligonucleotides from smaller synthetic fragments. This made possible randomization of V_H codons 67, 69, 71, 73, 75, 76, 93, and 94 with a single long oligonucleotide rather than two smaller ones. The final randomization mutagenesis strategy therefore employed only two oligonucleotides simultaneously onto four different templates.

Selection of Tight Binding Humanized A4.6.1 Fab Variants—Variants from the humanized A4.6.1 Fab phagemid library were selected based on binding to VEGF. Enrichment of functional phagemid, as measured by comparing titers for phage eluted from a VEGF-coated *versus* uncoated microtiter plate well, increased up to the seventh round of affinity panning. After one additional round of sorting, 20 clones were sequenced to identify preferred framework residues selected at each position randomized. These results, summarized in Table II, re-

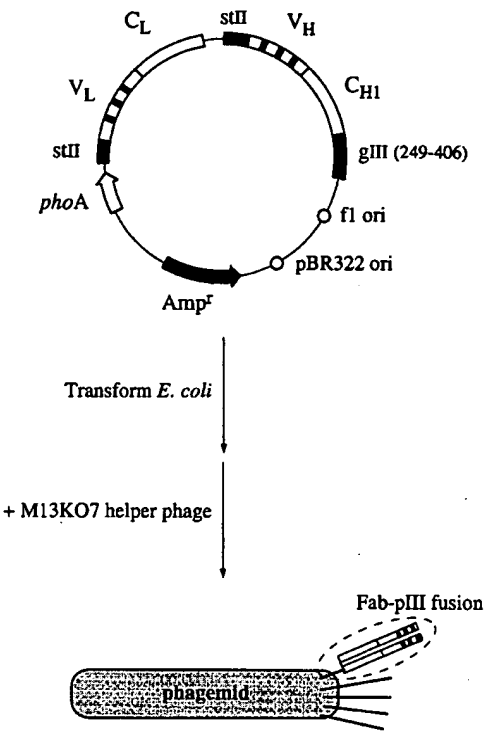

FIG. 3. **Phagemid construct for surface display of Fab-pIII fusions on phage.** The phagemid construct is similar to that described previously (31) and encodes a humanized version of the Fab fragment for antibody A4.6.1 fused to a portion of the M13 gene III coat protein. The fusion protein consists of the Fab joined at the carboxyl terminus of the heavy chain to a single glutamine residue (from suppression of an amber codon in *supE E. coli*) and then the carboxyl-terminal region of the gene III protein (residues 249–406). Transformation into F' *E. coli*, followed by superinfection with M13KO7 helper phage, produces phagemid particles in which a small proportion of these display a single copy of the fusion protein.

vealed strong consensus among the clones selected. Ten out of the 20 clones had the identical DNA sequence, designated hu2.10. Of the 13 framework positions randomized, eight substitutions were selected in hu2.10 (V_L 71 and V_H 37, 71, 73, 75, 76, 78, and 94). Interestingly, residues V_H 37 (Ile) and 78 (Val) were selected neither as the human V_HIII or murine A4.6.1 sequence. This result suggests that some framework positions may benefit from extending the diversity beyond the target human and parent murine framework sequences, although we have not tested this by making the appropriate mutants.

There were four other unique amino acid sequences among the remaining 10 clones analyzed: hu2.1, hu2.2, hu2.6, and hu2.7. All of these clones, in addition to hu2.10, contained identical framework substitutions at positions V_H 37 (Ile), 78 (Val), and 94 (Lys) but retained the human V_HIII consensus sequence at positions 24 and 93. Four clones had lost the light chain coding sequence and did not bind VEGF when tested in a phage enzyme-linked immunosorbent assay (39). We have occasionally noted the loss of heavy or light chain sequence with other Fab phagemid libraries,[2] and these clones are presumably selected for on the basis of enhanced expression. Such artifacts can often be minimized by reducing the number of sorting cycles or by propagating libraries on solid media.

Expression and Binding Affinity of Humanized A4.6.1 Variants—Phage-selected variants hu2.1, hu2.2, hu2.6, hu2.7, and hu2.10 were expressed in *E. coli* using shake flasks, and Fab fragments were purified from periplasmic extracts by protein G affinity chromatography. Recovered yields of Fab for these five clones ranged from 0.2 (hu2.6) to 1.7 mg/L (hu2.1). The affinity of each of these variants for antigen (VEGF) was measured by surface plasmon resonance on a BIAcore instrument (Table III). Analysis of these binding data revealed that the consensus clone hu2.10 possessed the highest affinity for VEGF out of the five variants tested. Thus, our Fab phagemid library was selectively enriched for the tightest binding clone. The calculated K_d for hu2.10 was 55 nM, at least 125-fold tighter than for hu2.0, which contains no framework changes ($K_d > 7$ μM). The other four selected variants all exhibited weaker binding to VEGF, ranging down to a K_d of 360 nM for the weakest (hu2.7). Interestingly, the K_d for hu2.6, 67 nM, was only marginally weaker than that of hu2.10, and yet only one copy of this clone was found among 20 clones sequenced. This may have been due to a lower level of expression and display, as was the case when the soluble Fab of this variant was expressed.

Additional Improvement of Humanized Variant hu2.10—Despite the large improvement in antigen affinity over the initial humanized variant, binding of hu2.10 to VEGF was still 35-fold weaker than that of a chimeric Fab fragment containing the murine A4.6.1 V_L and V_H domains. This considerable difference suggested that further optimization of the humanized framework might be possible through additional mutations. Of the Vernier residues identified by Foote and Winter (20), only residues V_L 46, V_H 2, and V_H 48 differed in the A4.6.1 *versus* human $V_L\kappa$I-V_HIII framework (Fig. 1), but these were not randomized in our phagemid library. A molecular model of the humanized A4.6.1 Fv fragment showed that V_L 46 sits at the V_L-V_H interface and could influence the conformation of CDR-H3. Furthermore, this amino acid is almost always leucine in most $V_L\kappa$ frameworks (26) but is valine in A4.6.1. Accordingly, a Leu → Val substitution was made at this position in the background of hu2.10. Analysis of binding kinetics for this new variant, hu2.10V, indicated a further 6-fold improvement in the K_d for VEGF binding, demonstrating the importance of valine at position V_L 46 in antibody A4.6.1. The K_d for hu2.10V (9.3 nM) was thus within 6-fold that of the chimera. In contrast to V_L 46, no improvement in the binding affinity of hu2.10 was observed for replacement of either V_H 2 or V_H 48 with the corresponding residue from murine A4.6.1.

DISCUSSION

A combinatorial approach to antibody humanization has a distinct advantage over the conventional site-directed mutagenesis-based method in that a much larger pool of mutants can be explored simultaneously, with the best binders being rapidly selected from a phage display library based on relative antigen affinity. We have applied such an approach to humanization of the murine mAb A4.6.1, a neutralizing anti-VEGF antibody known to inhibit mitogenic signaling and potentially useful as an anti-tumor therapeutic (30). A library of framework-randomized variants was sorted, and from this a number of variants were identified that bound VEGF considerably tighter than the straight CDR graft variant hu2.0 (Tables II and III). The tightest binding variant in the final pool was the consensus clone hu2.10, and incorporation of one additional mutation at V_L 46 yielded a humanized A4.6.1 variant with an affinity within 6-fold that of the chimeric Fab.

Although hu2.10V contained nine framework changes, these did not contribute equally to the improvements in antigen binding. The data in Table III provide some insight into the relative contributions that individual framework changes made to antigen binding. As noted previously, a 6-fold improvement in antigen affinity was associated with replacing residue V_L 46 (leucine) with the corresponding amino acid found in A4.6.1 (valine). Interestingly, part of the improvement in affin-

[2] M. Baca and J. A. Wells, unpublished data.

TABLE II

Sequences selected from the humanized A4.6.1 phagemid Fab library

Differences between hu2.0 and murine A4.6.1 antibodies are underlined. The number of identical clones identified for each phage-selected sequence is indicated in parentheses. Dashes in the sequences of phage-selected clones indicate selection of the human $V_L\kappa I$–$V_H III$ framework sequence (*i.e.* as in hu2.0).

Variant	Residue substitutions												
	V_L		V_H										
	4	71	24	37	67	69	71	73	75	76	78	93	94
Murine A4.6.1	M	Y	A	V	F	F	L	T	A	S	A	A	K
hu2.0 (CDR graft)	M	F	A	V	F	I	R	N	K	N	L	A	R
Phage selected clones													
hu2.1 (2)	–	Y	–	I	–	–	–	–	–	–	V	–	K
hu2.2 (2)	L	Y	–	I	–	–	–	–	–	–	V	–	K
hu2.6 (1)	L	–	–	I	T	–	L	T	A	S	V	–	K
hu2.7 (1)	L	–	–	I	–	–	–	–	–	–	V	–	K
hu2.10 (10)	–	Y	–	I	–	–	L	T	A	S	V	–	K

TABLE III

VEGF binding affinity of humanized A4.6.1 Fab variants

k_{on} and k_{off} are association and dissociation rate constants, respectively.

Variant	k_{on}	k_{off}	K_d	$\frac{K_d \text{ mut}}{K_d \text{ (A4.6.1)}}$
	$M^{-1}\,s^{-1}/10^4$	$10^4\,s^{-1}$	nM	
A4.6.1 chimera	5.4	0.85	1.6	
hu2.0	ND	ND	>7000[a]	>4000
Phage selected clones				
hu2.1	0.70	18	260	170
hu2.2	0.47	16	340	210
hu2.6	0.67	4.5	67	40
hu2.7	0.67	24	360	230
hu2.10	0.63	3.5	55	35
hu2.10V[b]	2.0	1.8	9.3	5.8

[a] Too weak to measure; estimate of lower bound.

[b] hu2.10V = hu2.10 with additional framework mutation V_L Leu^{46} → Val. Estimated errors in the BIAcore binding measurements are ±25%.

ity was due to an increase in the association rate constant, suggesting that V_L 46 may play a role in preorganizing the antibody structure into a conformation more suitable for antigen binding. Other mutations that affected antigen affinity were primarily due to changes in the dissociation rate constant for binding. Comparison of hu2.1 and hu2.10 reveals a 5-fold improvement in affinity for substitution of V_H residues 71, 73, 75, and 76 with the A4.6.1 sequence. Conversion of V_L 71 to the A4.6.1 sequence (Phe → Tyr) had negligible effect on binding (hu2.2 *versus* hu2.7), whereas variants with leucine at V_L 4 bound marginally worse (<2-fold) than those with methionine, the naturally occurring residue in both the A4.6.1 and human $V_L\kappa I$ frameworks (hu2.2 *versus* hu2.1). Comparison of other humanized A4.6.1 variants not shown here revealed that the V_H 94 Arg → Lys change resulted in a 5-fold improvement in K_d, either due to direct antigen contact by this residue or to a structural role in maintaining the proper conformation of CDR-H3. Curiously, variant hu2.6 has three sequence differences relative to the consensus clone hu2.10, but nevertheless has a similar K_d. This suggests that these three substitutions have little effect on antigen binding. Although the negligible effect of conservative changes at V_L 4 and 71 concurs with binding data for other variants, it is somewhat surprising that the more drastic change at V_H 67 (Phe → Thr) has little effect on binding.

Recently, Rosok *et al.* (40) reported a combinatorial approach to the humanization of murine mAb BR96. However, the method used in that work differs from that presented here in several key features. For reasons enunciated earlier, we used the same human $V_L\kappa I$-$V_H III$ framework that has been used in previous antibody humanizations (13–15, 25), whereas Rosok *et al.* selected a novel human framework based on homology to the sequence of the parent murine mAb. Furthermore, we humanized the entire framework region (except for CDRs), then randomized only those framework residues that have been empirically found to be important to antigen binding. In contrast, Rosok *et al.* humanized only surface-exposed residues, then randomized the remaining buried residues that differed in sequence between the murine mAb and human template. Thus, the respective sets of residues randomized were almost entirely different, reflecting the use of dissimilar humanization strategies.

We have demonstrated that phage display methods can be readily applied to the humanization of a murine monoclonal antibody. Application to the humanization of mAb A4.6.1 led to selection of a humanized variant that bound VEGF greater than 125-fold tighter than the variant with no framework changes. One additional mutation at V_L 46 within the background of the best phage selected clone was required to improve the affinity to within 6-fold that of murine A4.6.1. It should be noted, however, that V_L 46 does not usually require replacement in antibody humanizations given the overwhelming predominance of leucine at this position in most antibody frameworks (26). Given this consideration, we feel that the general phage method described will usually suffice for the selection of tight binding humanized antibodies. Finally, the success of this humanization, in combination with previous results (13–15, 25), again illustrates the feasibility of using a single human framework as a generic scaffold for humanized antibodies.

Acknowledgments—We thank Marcus Ballinger for assistance with the oligonucleotide preassembly, James Bourell for mass spectrometric analyses, Allan Padua for amino acid analyses, and the oligonucleotide synthesis group.

REFERENCES

1. Jaffers, G. J., Fuller, T. C., Cosimi, A. B., Russell, P. S., Winn, H. J. & Colvin, R. B. (1986) *Transplantation* 41, 572–578
2. Shawler, D. L., Bartholomew, R. M., Smith, L. M. & Dillman, R. O. (1985) *J. Immunol.* 135, 1530–1535
3. Miller, R. A., Oseroff, A. R., Stratte, P. T. & Levy, R. (1983) *Blood* 62, 988–995
4. Riechmann, L., Clark, M., Waldmann, H. & Winter, G. (1988) *Nature* 332,

323–327
5. Junghans, R. P., Waldmann, T. A., Landolfi, N. F., Avdalovic, N. M., Schneider, W. P. & Queen, C. (1990) *Cancer Res.* **50**, 1495–1502
6. Hakimi, J., Chizzonite, R., Luke, D. R., Familletti, P. C., Bailon, P., Kondas, J. A., Pilson, R. S., Lin, P., Weber, D. V., Spence, C., Mondini, L. J., Tsien, W. H., Levin, J. L., Gallati, V. H., Korn, L., Waldmann, T. A., Queen, C. & Benjamin, W. R. (1991) *J. Immunol.* **147**, 1352–1359
7. Stephens, S., Emtage, S., Vetterlein, O., Chaplin, L., Bebbington, C., Nesbitt, A., Sopwith, M., Athwal, D., Novak, C. & Bodmer, M. (1995) *Immunology* **85**, 668–674
8. Jones, P. T., Dear, P. H., Foote, J., Neuberger, M. S. & Winter, G. (1986) *Nature* **321**, 522–525
9. Baselga, J., Tripathy, D., Mendelsohn, J., Baughman, S., Benz, C. C., Dantis, L., Sklarin, N. T., Seidman, A. D., Hudis, C. A., Moore, J., Rosen, P. P., Twaddell, T., Henderson, I. C. & Norton, L. (1996) *J. Clin. Oncol.* **14**, 737–744
10. Queen, C., Schneider, W. P., Selick, H. E., Payne, P. W., Landolfi, N. F., Duncan, J. F., Avdalovic, N. M., Levitt, M., Junghans, R. P. & Waldmann, T. A. (1989) *Proc. Natl. Acad. Sci. U. S. A.* **86**, 10029–10033
11. Kettleborough, C. A., Saldanha, J., Heath, V. J., Morrison, C. J. & Bendig, M. M. (1991) *Protein Eng.* **4**, 773–783
12. Tempest, P. R., Bremner, P., Lambert, M., Taylor, G., Furze, J. M., Carr, F. J. & Harris, W. J. (1991) *Biotechnology* **9**, 266–271
13. Carter, P., Presta, L., Gorman, C. M., Ridgway, J. B., Henner, D., Wong, W. L., Rowland, A. M., Kotts, C., Carver, M. E. & Shepard, H. M. (1992) *Proc. Natl. Acad. Sci. U. S. A.* **89**, 4285–4289
14. Presta, L. G., Lahr, S. J., Shields, R. L., Porter, J. P., Gorman, C. M., Fendly, B. M. & Jardieu, P. M. (1993) *J. Immunol.* **151**, 2623–2632
15. Eigenbrot, C., Gonzalez, T., Mayeda, J., Carter, P., Werther, W., Hotaling, T., Fox, J. & Kessler, J. (1994) *Proteins* **18**, 49–62
16. Pulito, V. L., Roberts, V. A., Adair, J. R., Rothermel, A. L., Collins, A. M., Varga, S. S., Martocello, C., Bodmer, M., Jolliffe, L. K. & Zivin, R. A. (1996) *J. Immunol.* **156**, 2840–2850
17. Chothia, C., Lesk, A. M., Tramontano, A., Levitt, M., Smith-Gill, S. J., Air, G., Sheriff, S., Padlan, E. A., Davies, D., Tulip, W. R., Colman, P. M., Spinelli, S., Alzari, P. M. & Poljak, R. J. (1989) *Nature* **342**, 877–883
18. Mian, I. S., Bradwell, A. R. & Olson, A. J. (1991) *J. Mol. Biol.* **217**, 133–151
19. Chothia, C. & Lesk, A. M. (1987) *J. Mol. Biol.* **196**, 901–917
20. Foote, J. & Winter, G. (1992) *J. Mol. Biol.* **224**, 487–499
21. Padlan, E. A. (1991) *Mol. Immunol.* **28**, 489–498
22. Roguska, M. A., Pedersen, J. T., Keddy, C. A., Henry, A. H., Searle, S. J., Lambert, J. M., Goldmacher, V. S., Blattler, W. A., Rees, A. R. & Guild, B. C. (1994) *Proc. Natl. Acad. Sci. U. S. A.* **91**, 969–973
23. Studnicka, G. M., Soares, S., Better, M., Williams, R. E., Nadell, R. & Horwitz, A. H. (1994) *Protein Eng.* **7**, 805–814
24. Allen, P. M., Matsueda, G. R., Haber, E. & Unanue, E. R. (1985) *J. Immunol.* **135**, 368–373
25. Shalaby, M. R., Shepard, H. M., Presta, L., Rodrigues, M. L., Beverley, P. C., Feldmann, M. & Carter, P. (1992) *J. Exp. Med.* **175**, 217–225
26. Kabat, E. A., Wu, T. T., Perry, H. M., Gottesman, K. S. & Foeller, C. (1991) *Sequences of Proteins of Immunological Interest*, 5th Ed, Public Health Service, National Institutes of Health, Bethesda, MD
27. Bass, S., Green, R. & Wells, J. A. (1990) *Proteins* **8**, 309–314
28. Lowman, H. B., Bass, S. H., Simpson, N. & Wells, J. A. (1991) *Biochemistry* **30**, 10832–10838
29. Kim, K. J., Li, B., Houck, K., Winer, J. & Ferrara, F. (1992) *Growth Factors* **7**, 53–64
30. Kim, K. J., Li, B., Winer, J., Armanini, M., Gillett, N., Phillips, H. S. & Ferrara, N. (1993) *Nature* **362**, 841–844
31. Garrard, L. J., Yang, M., O'Connell, M. P., Kelley, R. F. & Henner, D. J. (1991) *Biotechnology* **9**, 1373–1377
32. Chang, C. N., Rey, M., Bochner, B., Heyneker, H. & Gray, G. (1987) *Gene* **55**, 189–196
33. Kunkel, T. A., Bebenek, K. & McClary, J. (1991) *Methods Enzymol.* **204**, 125–139
34. Vieira, J. & Messing, J. (1987) *Methods Enzymol.* **153**, 3–11
35. Sanger, F., Nicklen, S. & Coulson, A. R. (1977) *Proc. Natl. Acad. Sci. U. S. A.* **74**, 5463–5467
36. Karlsson, R., Michaelsson, A. & Mattsson, L. (1991) *J. Immunol. Methods* **145**, 229–240
37. Tramontano, A., Chothia, C. & Lesk, A. M. (1990) *J. Mol. Biol.* **215**, 175–182
38. Winter, G., Griffiths, A. D., Hawkins, R. E. & Hoogenboom, H. R. (1994) *Annu. Rev. Immunol.* **12**, 433–455
39. Cunningham, B. C., Lowe, D. G., Li, B., Bennett, B. D. & Wells, J. A. (1994) *EMBO J.* **13**, 2508–2515
40. Rosok, M. J., Yelton, D. E., Harris, L. J., Bajorath, J., Hellström, K.-E., Hellström, I., Cruz, G. A., Kristensson, K., Lin, H., Huse, W. D. & Glaser, S. M. (1996) *J. Biol. Chem.* **271**, 22611–22618

Structural Effects of Framework Mutations on a Humanized Anti-Lysozyme Antibody[1]

Margaret A. Holmes,* Timothy N. Buss,* and Jefferson Foote[2]*†

A humanized version of the mouse anti-lysozyme Ab D1.3 was previously constructed as an Fv fragment and its structure was crystallographically determined in the free form and in complex with lysozyme. Here we report five new crystal structures of single-amino acid substitution mutants of the humanized Fv fragment, four of which were determined as Fv-lysozyme complexes. The crystals were isomorphous with the parent forms, and were refined to free *R* values of 28–31% at resolutions of 2.7–2.9 Å. Residue 27 in other Abs has been implicated in stabilizing the conformation of the first complementarity-determining region (CDR) of the H chain, residues 31–35. We find that a Phe-to-Ser mutation at 27 alters the conformation of immediately adjacent residues, but this change is only weakly transmitted to Ag binding residues in the nearby CDR. Residue 71 of the H chain has been proposed to control the relative disposition of H chain CDRs 1 and 2, based on the bulk of its side chain. However, in structures we determined with Val, Ala, or Arg substituted in place of Lys at position 71, no significant change in the conformation of CDRs 1 and 2 was observed. ***The Journal of Immunology,*** **2001, 167: 296–301.**

Humanized Abs are created by replacing the complementarity-determining regions (CDRs)[3] of a human Ab (as defined by Wu and Kabat; Refs. 1, 2) with the corresponding CDRs of a nonhuman Ab (3). This CDR graft transfers the antigenic specificity of the CDR donor molecule, but leaves the new engineered molecule immunologically human, inasmuch as the immunogenicity of humanized Abs in humans is extremely low (4, 5). The first humanized Ab was specific for the hapten nitrophenacetyl. This molecule had been CDR grafted in the H chain only, which was coexpressed with a mouse L chain. The humanized anti-nitrophenacetyl showed 1.5- to 3-fold reduced hapten affinity relative to a control molecule with murine sequences in both chains (3). This finding of altered affinity proved that framework residues can influence the structure of the Ag combining site. Riechmann et al. (4) confirmed this finding in a humanized anti-CD52. The initial humanized construct showed weak avidity. A single Ser-to-Phe mutation at framework residue H27[4] restored avidity to near that of the fully murine control. The importance of framework residues in maintaining the structure of the CDRs and the frequent need for mutational revisions in the framework have since been confirmed many more times during the engineering of humanized Abs to have avidity matching that of their murine antecedents (6).

We developed a humanized anti-lysozyme (HuLys) as a model system for studying structural issues attending the transfer of CDRs from a murine to a human framework (7–9). Thus, murine and human segments for the construction were chosen from among Ab V domains whose structures had been determined. The six CDRs of HuLys come from the murine Ab D1.3, which was raised against hen egg lysozyme (10, 11). The structure of the D1.3 heterodimer of H and L chain V regions (Fv) has been determined at 1.8-Å resolution in both the liganded and unliganded forms (12, 13). The HuLys H chain framework (residues H1–H30, H36–H49, H66–H94, and H103–H113 in the Kabat numbering system) comes from the human myeloma protein NEW, whose structure has been determined at 2.0 Å (14). The κ L chain framework (residues L1–L23, L35–L49, L57–L88, and L98–L108) is a consensus sequence similar to that of the human Bence-Jones protein REI, also determined at 2.0 Å (15).

The crystal structures of the HuLys Fv in free form (16) and complexed with the Ag lysozyme (17) were previously determined at 2.9 and 2.7 Å, respectively (Brookhaven Protein Data Bank accession numbers 1BVL and 1BVK). In this work, we describe crystal structures of a series of single substitution mutants of the HuLys Fv, viz H27S, H71V, H71A, and H71R.

Materials and Methods

Protein engineering

Fvs were expressed in *Escherichia coli* using the pAK19 vector (18), which uses a *phoA* promoter and heat-stable enterotoxin II leader sequence. This vector directs gene products to the periplasm, from which correctly folded, disulfide-oxidized molecules are released after cell harvest. Material used in the present work was released from the periplasm by osmotic shock and purified by affinity chromatography on lysozyme-Sepharose, as described previously (17). Protein concentrations were determined spectrophotometrically, using calculated extinction coefficients (19).

Crystal growth

Crystals of the four mutant complexes were grown in the same way as the native complex crystals (17). Each of the HuLys Fv solutions was mixed with a lysozyme solution in equimolar proportions. The mixtures then sat from several hours to 2 days. PBS was added to dilute the solution, which was centrifuged before use. Protein concentrations ranged from 6.5 to 10.5 mg/ml. The reservoir for vapor diffusion was 0.8 M K_2HPO_4, 0.8 M

*Program in Molecular Medicine, Fred Hutchinson Cancer Research Center, Seattle, WA 98109; and †Department of Immunology, University of Washington, Seattle, WA 98195

Received for publication September 28, 2000. Accepted for publication April 26, 2001.

The costs of publication of this article were defrayed in part by the payment of page charges. This article must therefore be hereby marked *advertisement* in accordance with 18 U.S.C. Section 1734 solely to indicate this fact.

[1] This work was supported by the Department of the Army Breast Cancer Research Program (Grant DAMD 17-97-1-7124).

[2] Address correspondence and reprint requests to Dr. Jefferson Foote, Fred Hutchinson Cancer Research Center, 1100 Fairview Avenue North, C3-168, P.O. Box 19024, Seattle, WA 98109-1024. E-mail address: jfoote@fhcrc.org

[3] Abbreviations used in this paper: CDR, complementarity-determining region; Fv, heterodimer of H and L chain V regions; HuLys, humanized anti-lysozyme; rms, root mean square.

[4] Residues are numbered using the Kabat system and preceded by a chain designator, e.g., H71 for residue 71 in the H chain. The wild-type Fv has Phe at residue H27 and Lys at residue H71; mutant molecules are designated by the substitution, e.g., H71V is an Fv with Val at residue H71.

0022-1767/01/$02.00

Table I. *Data collection*

Structure	H27S Complex		H71V Complex		H71A Complex		H71R Complex		H71V	
Space group	$P4_12_12$		$P4_12_12$		$P4_12_12$		$P4_12_12$		$P4_32_12$	
Fv/asymmetric unit	2		2		2		2		2	
Cell dimensions (Å)	$a=b=97.9$; $c=173.3$		$a=b=96.3$; $c=175.7$		$a=b=97.6$; $c=174.1$		$a=b=97.1$; $c=174.8$		$a=b=146.8$; $c=71.9$	
Resolution (Å)	50.0–2.7	2.75–2.70	50.0–2.7	2.75–2.70	50.0–2.7	2.75–2.70	50.0–2.7	2.75–2.70	50.0–2.9	2.95–2.90
Measured reflections	132,657	>2580	141,035	>3001	108,158	>2271	141,201	>2672	88,937	>1849
Unique reflections	23,047	1060	22,318	1133	21,229	1044	22,707	1025	16,618	751
Completeness (%)	96.3	90.3	95.1	97.5	88.9	90.5	95.6	89.0	92.3	87.0
R value[a]	0.065	0.315	0.067	0.404	0.059	0.310	0.065	0.376	0.075	0.403
Average I/σ_I	10.1	2.6	18.1	2.3	17.4	2.6	16.5	2.3	17.2	2.5

[a] $R = \Sigma\Sigma \mid I_{i,hkl} - \langle I_{hkl}\rangle \mid / \Sigma\Sigma\, I_{i,hkl}$.

NaH_2PO_4, 0.1 M HEPES, pH 6.5. Sitting drops consisting of equal volumes of complex solution and reservoir solution were set up in microbridges.

Crystals of the uncomplexed H71V Fv were grown by macroseeding. The seeds were obtained from a hanging drop vapor diffusion crystallization that used 16 mg/ml protein and a reservoir of 0.74 M sodium citrate, 0.01% NaN_3, pH 6.5. Two rounds of seeding were performed. Each time, a few crystals were removed from the drop and placed in a microbridge in a fresh drop composed of equal volumes of Fv solution (16 mg/ml) and reservoir solution (0.8 M sodium citrate, 0.01% NaN_3, pH 6.5).

Data collection

X-ray diffraction data sets were collected from single crystals at 4°C using an *R* axis detector. The data sets were processed with DENZO and SCALEPACK (20, 21). Details of the processing are given in Table I. Before refinement, the data sets were partitioned into a working set and a test set. The test sets for the complexes contained only reflections that had made up the test set for the refinement of the native complex structure, so as to maintain the independence of the test set (22). The test set for the uncomplexed Fv was created by X-PLOR (23), as the refinement of the native Fv structure did not involve a test set.

Refinement

Refinement of the structure of the HuLys H27S Fv-lysozyme complex began with the model of the native complex with residue H27 changed to Gly. A round of rigid body refinement at 3.5-Å resolution was followed by rounds of positional refinement at 2.7-Å resolution using X-PLOR and model building of the loop containing the mutation. A cycle of torsion angle molecular dynamics refinement was run, followed by more rounds of positional refinement and model building. Omit map density was sufficient to model only one of the two H27 side chains. The refinement was completed with a cycle of individual *B* value refinement with TNT (24) and a cycle of X-PLOR *B* value refinement. Refinement statistics are given in Table II.

Refinement of the structures of the HuLys H71V, H71A, and H71R Fv-lysozyme complexes was more straightforward. The starting model was the native complex with H71 changed to Gly. A round of rigid body refinement at 3.5-Å resolution was followed by a cycle of positional refinement at 2.7-Å resolution, addition of the H71 side chains to the model, and a second cycle of positional refinement. The refinement was completed with one cycle each of individual *B* value refinement with TNT and X-PLOR (Table II). Manual changes of the model, other than placement of the H71 side chain, were needed only for the H71A complex.

Refinement of the structure of the uncomplexed HuLys H71V Fv began with H71 changed to Gly. First, a round of rigid body refinement was conducted at 3.5-Å resolution. Next came two rounds of positional refinement at 2.9 Å, alternating with model-building and addition of the H71 side chains. Group *B* values (1 *B* per residue) were refined with X-PLOR, and a final cycle of positional refinement was performed (Table II).

No solvent molecules are present in any of the models. PROCHECK (25) analyses of the five structures show no residues in disallowed regions other than L51, which is in a γ-turn conformation, as seen in the native and other related structures (26).

Results

H27S structure

The structure of the HuLys Fv mutant H27S was determined as a lysozyme complex in a crystal form identical with the complex structure obtained previously (17). The crystallographic asymmetric unit contains two Fv:Ag complexes, which we designate molecule 1 and molecule 2. Both Fvs superpose well on the corresponding Fvs of the H27F structure, with root mean square (rms) differences in Cα position of 0.5 Å for each of the two complexes. Despite these identical rms differences, two different conformations are present in the two crystallographically independent H27S molecules. Comparing molecule 1 of H27F and H27S, differences in Cα position of up to 2.7 Å occur at residues H23–H29, adjacent to CDR-H1. The overall effect is that in the H27S structure, this portion of the molecule has moved away from the position of the

Table II. *Refinement*

Parameter	H27S Complex	H71V Complex	H71A Complex	H71R Complex	H71V
Resolution (Å)	10.0–2.7	10.0–2.7	10.0–2.7	10.0–2.7	10.0–2.9
Reflections					
Total ($F>2\sigma$)	20,005	19,501	18,592	19,535	14,455
Working set	18,105	17,642	16,805	17,653	13,014
Test set	1,900	1,859	1,787	1,882	1,441
Atoms	5,478	5,486	5,482	5,494	3,484
R value[a]					
Working	0.203	0.202	0.202	0.207	0.225
Free	0.313	0.291	0.291	0.297	0.279
rms deviation from ideality					
Bond lengths (Å)	0.015	0.014	0.015	0.014	0.021
Bond angles (°)	1.8	1.8	1.9	1.8	2.5
PROCHECK analysis					
% in most favored regions	80.9	81.5	80.5	78.8	78.6
Estimated error in atomic position (Å)[b]	0.33	0.34	0.33	0.34	0.37

[a] $R = \Sigma_{hkl} \mid \mid Fobs_{hkl} \mid - \mid Fcalc_{hkl} \mid \mid / \Sigma_{hkl} \mid Fobs_{hkl} \mid$.
[b] Calculated by method of Luzzati (27).

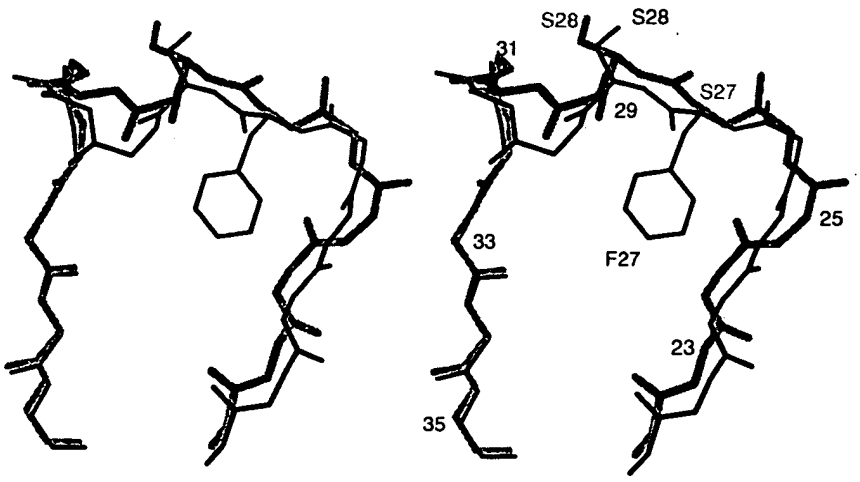

FIGURE 1. Structural effects of different amino acids at position H27, molecule 1. Stereo view of H chain CDR 1 and adjacent peptide segment in H27F (black) and H27S (gray). Atomic coordinates were taken from molecule 1 from the H27F and H27S Fv-lysozyme complex structures. The entire H27S-lysozyme complex was superposed on the H27F-lysozyme complex. The superposed molecules were used for this illustration. Only the peptide backbone from residues H22 to H35 and the side chains from residues H27 and H28 were drawn, to make clear the conformational changes that occur when Ser or Phe is substituted at position H27. Residue H27 in the H27S mutant was modeled as Gly.

Phe side chain present in H27F, toward the H chain N terminus and lysozyme, creating a more open loop (Fig. 1). Residues H74–H76, which pack against CDR-H1, have moved into the space created by this shift. Eight of the Cα shifts larger than twice the rms difference come from residues H23–H29 and H74 and H76. (The others are at chain termini or at locations remote from the combining site.) Modeling of residues H22–H31 was difficult, and the side chain at position H27 could not be fit at all. The possibility exists that this remodeled region is in more than one conformation.

H27S molecule 2 shows a clear difference from the corresponding molecule 2 of the H27F Fv. The Ser and Phe side chains at the substitution site point in opposite directions. As evident in Fig. 2, the phenyl ring of H27F is buried in the interior of the extended loop formed by residues H23–H35, whereas the Ser side chain in H27S points to the aqueous exterior. As predicted (4, 9), substitution of Ser for Phe has created a cavity. Residue Ser H28 in the H27S Fv has shifted so that its main chain and side chain have moved into space occupied by the Phe H27 side chain in the H27F Fv. This large perturbation in backbone conformation extends for several residue positions along the peptide backbone, as is evident in Fig. 2. The shifts of the Cα atoms of residues H23–H31 account for 9 of the 13 shifts greater than twice the rms difference between the mutant and native complexes. A shift at H75 accounts for one more, and the others are at chain termini.

Although the conformation of the loop preceding CDR-H1 differs significantly in H27S and H27F, structural effects on lysozyme binding are small. In the D1.3 complex structure, residue H32 of CDR-H1 makes a weak (3.5 Å) direct contact with lysozyme. Residues H30 and H31 make contact via water molecules (13). In the HuLys H27S structure, the distance for the potential direct contact between H32 and lysozyme is 4.1 Å (molecule 1) or 4.3 Å (molecule 2), similar to the 4.0-Å contact seen in the H27F molecule 1 complex and an increase from the 3.4 Å in the H27F molecule 2 complex, and too large to be important in lysozyme binding (28). Due to the resolution of x-ray data for the HuLys complexes, we have not modeled water molecules, hence we cannot directly compare the Fv-lysozyme interactions involving residues H30 and H31 to the corresponding interactions in D1.3. However, we did compare the positions of the Fv atoms in H27S and H27F involved in these contacts, the carbonyl oxygen atoms of H30 and H31. Both these atoms in H27S molecule 1 have moved 0.8 Å from their positions in H27F. In H27S molecule 2, the backbone Cα atoms of these residues have moved 1.9 Å (H30) and 1.2 Å (H31) from their positions in the H27F complex. The atoms actually forming the contacts, H30 O and H31 O, have moved 1.7 Å and 0.9 Å, respectively. The size of this shift does not necessarily mean that these contacts are broken. The water molecules in the H27S complex presumably could shift position to accommodate the new

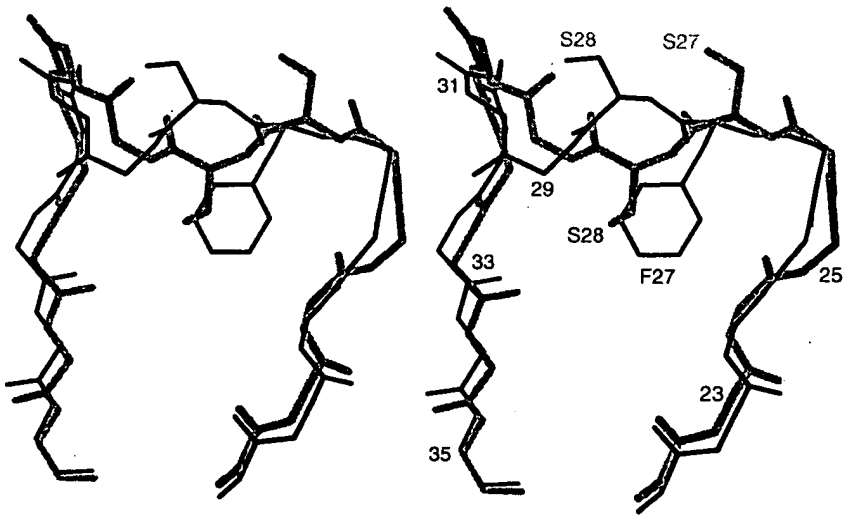

FIGURE 2. Structural effects of different amino acids at position H27, molecule 2. Stereo view of H chain CDR 1 and adjacent peptide segment in H27F (black) and H27S (gray). The illustration was prepared as for Fig. 1, but using atomic coordinates from molecule 2 of the H27F and H27S Fv-lysozyme complex structures.

Table III. *Rms changes in Cα position of H71 mutants relative to H71K*

Mutant	RMS Deviation (Å)	
	Molecule 1	Molecule 2
H71V	0.3	0.3
H71A	0.2	0.2
H71R	0.1	0.1

positions of the protein atoms. The remainder of CDR-H1 in H27S is offset from its location in H27F, with the respective chains back in register by residue H35, the last residue in the CDR.

H71 structures

The size of the side chain at position H71 is thought to control the relative disposition of loops forming CDR-H1 and CDR-H2 (29). Previously published structures of free HuLys Fv and the HuLys-lysozyme complex had Lys in this position. Here we report additional structures with Val, Ala, and Arg at residue H71. All three forms crystallized and were determined as an Fv-lysozyme complex, and a structure of the free H71V Fv was obtained as well.

All the Fv-lysozyme complexes were virtually identical. Superposition of the Cα atoms of the mutant complexes onto the H71K complex gave small rms differences of 0.3 Å or less, as presented in Table III. Twelve Cα atoms in the two H71V molecules have shifts greater than twice the rms differences, and none are near the combining site. Comparing the structures of the H71A and H71K complexes, four Cα atoms have shifts greater than twice the rms difference; three are in the L chain and one is in lysozyme. All are remote from the combining site. The most conservative H71 substitution, arginine for lysine, gave the smallest overall rms difference. However, as for the other H71 mutants, there were moderate shifts of the mutated residue and residues in the nearby segment of polypeptide chain. The Cα atoms of H71 in molecules 1 and 2 moved 0.5 Å and 0.3 Å, respectively, and the preceding Cα atoms in molecule 1, H69 and H70, moved 0.2 Å and 0.4 Å. All other shifts greater than twice the rms distance occurred distant from H71 and from the combining site. Fig. 3 shows superposition of H71 and parts of CDR-H1 and CDR-H2 for the four molecules, taken from the complexed crystal forms. This illustration shows clearly that there is no change in structure of the two CDRs, despite the mutations at H71.

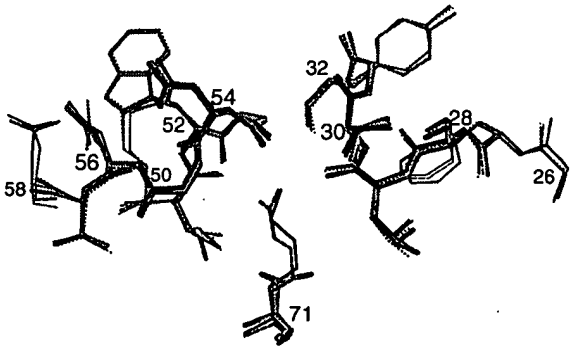

FIGURE 3. Structure of residue H71 and first and second hypervariable loops in four lysozyme-Fv complexes. Conformations of these residues in the two crystallographically independent asymmetric units of all four mutants are essentially identical. This illustration is a composite of superposed molecule 2s seen in H71K (black line), H71V (gray line), H71A (dotted line), and H71R (dashed line). Superpositions were based on H71K molecule 2 and used the Cα atomic coordinates of the residues shown.

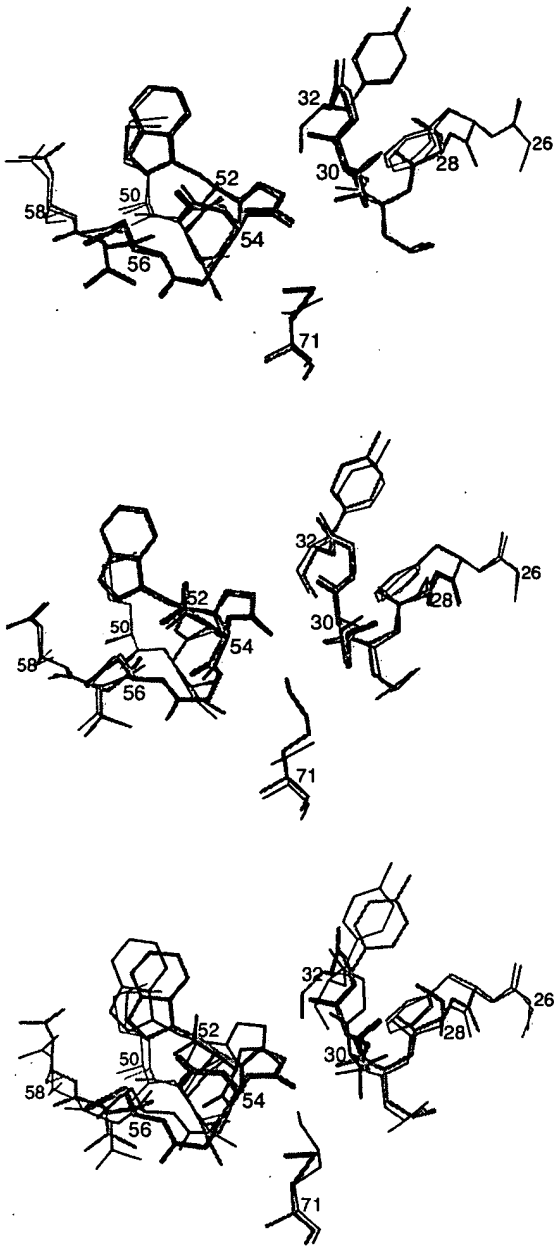

FIGURE 4. Structures of residue H71 and first and second hypervariable loops in unliganded Fv molecules. *Top*, H71V molecule (gray line) 1 superposed on H71K molecule 1 (black line). *Middle*, H71V molecule 2 (gray) superposed on H71K molecule 2 (black). *Bottom*, H71K molecule 2 (gray) superposed on H71K molecule 1 (black).

The structures of uncomplexed H71V and H71K offer another opportunity to test for a mutation-induced conformation change following the Tramontano model. The two unliganded crystal forms of H71K and H71V each have two molecules in the asymmetric unit, hence comprise a total of four independent Fv structures. Molecule 1 of H71K and molecule 1 of H71V superpose almost exactly in the region of the mutation, as evident in Fig. 4, *top*. Molecule 2 of H71K and molecule 2 of H71V superpose similarly well (Fig. 4, *middle*). However, these two pairs represent distinct conformations. The two independent molecules of H71K do not superpose well (Fig. 4, *bottom*), and the same is true for molecule 1 and molecule 2 of H71V. In other words, two Fvs

differing at residue H71, but in identical crystal packing environments, are closer in conformation than two with the same sequence, but in different environments. The two unliganded conformations observed presumably are distinct because of crystal packing interactions, rather than amino acid sequence differences at residue 71. The conformation of H71 and the two loops in the H71K and H71V Fv-lysozyme complexes is intermediate between the two conformations in the unliganded structures, though closer to molecule 2 (rms difference 0.2 Å for the Cα atoms in the illustration superposed on molecule 2 of the H71K complex) than to molecule 1 (0.4 Å rms difference).

Discussion

The role of residues H26–H30 in Ag binding by humanized Abs has been ambiguous. This segment is not considered part of "Kabat" CDR-H1 (residues H31–H35), and these residues rarely contact Ag (30). Other homology- and structure-based definitions of the first Ig H chain CDR have similarly designated residues outside this segment, viz H31–H37 (31), H31–H32 (32), and H30–H35 (33). One exception is the canonical H chain hypervariable loop 1 proposed by Chothia and Lesk (34), extending from H26 to H32. The rationale for this assignment was that the segment forms a loop connecting two β-strands of rather standard geometry. The conservation of particular features in the N-terminal portion of the segment, such as an invariant Gly at position H26, was considered critical for maintaining the backbone conformation of the Ag-contacting C-terminal portion of the H26–H32 loop.

How are conformational changes in CDR-H1 transmitted from the H26–H30 region? Comparison of side-by-side crystal structures of mouse and humanized versions of the same Ab would seem a straightforward way to discover this mechanism, as identical CDR-H1 sequences are abutted in the two cases to H26–H30 regions of separate murine and human origin. However, existing structural data on humanized Abs have been equivocal.

The canonical H26–H32 structure, which the vast majority of Abs adopt (35), is typified by the human H chain NEWM (14, 34). The rat anti-CD52 Ab CAMPATH-1G, with H26–H30 sequence GFTFT, follows this canonical structure precisely (36). The initial humanized form, though based on NEWM frameworks, sequence GSTFS, bound Ag poorly, and probably did not adopt a canonical conformation. The crystallographically studied humanized form, CAMPATH-1H, had higher affinity by virtue of the H26–H30 region being reverted to the rat sequence. Nevertheless, this structure still differed from the canonical conformation at residues H29 and H30. This deviation was attributed to a different interaction with respective side chains at position H71 (Arg in CAMPATH-1G, Val in CAMPATH-1H). A recent structure of the same humanized molecule in complex with an Ag mimotope showed that the H26–H32 loop was once again in the canonical conformation (37).

CDR-H1 of the murine anti-γ-IFN Ab AF2 deviates in conformation from the canonical structure at each position, but is still topologically recognizable as a loop (38). In contrast, the humanized version of AF2, despite having an identical sequence from residue H19–H66, has an α-helical CDR-H1 not seen in any other Ab structure. This unique conformation was attributed to a second structural rearrangement in framework 1 associated with a Pro (mouse) to Ser (humanized) mutation at position H7.

The murine anti-lysozyme Ab D1.3 has a canonical CDR-H1 structure (11). The humanized version of D1.3 whose structure we previously reported (16, 17) has an identical sequence from H26–H35 (7) (H26–H30 sequence GFSLT) and also adopts a canonical CDR-H1 conformation. A kinetic study of HuLys mutants showed that a Ser substitution at residue H27 had only a slightly detrimental effect on Ag affinity (9). This observation was contrary to the profound effect of a Ser-to-Phe mutation in CAMPATH-1H, even though both HuLys and CAMPATH-1H used NEWM framework sequences (4). One possible explanation is that the mutation in HuLys caused no significant structural change. The finding that CDR-H1 of D1.3 contributes little free energy toward lysozyme binding (39) makes plausible an alternative possibility, that the mutation did cause a change in residues H26–H30, but this perturbation was not detectable by kinetic analysis. Crystallographic data presented here favor the latter proposition, made clear in Fig. 1. The HuLys H27S structure shows large changes in backbone conformation in residues H22–H30 in molecule 1 and H26–H30 in molecule 2, but these torsional changes are not transmitted to the nearby Ag binding residues H31 and H32. Translational changes are also not transmitted to these residues, except for a displacement of H31 in molecule 2. Given our findings and the apparent idiosyncrasies observed in other humanized Ab structures, we can only conclude that the conformation of CDR-H1 and the adjacent H26–H30 region are extremely sensitive both to their own sequences and to interactions with adjacent residues. Our understanding of structural determinants of H26–H35 and our ability to rationally manipulate this region remain limited.

Tramontano et al. (29) have articulated a descriptive and predictive model for the structures of the H chain hypervariable loops 1 (Kabat residues H26–H32) and 2 (Kabat residues H52a/53–H55). In this model, the most important determinants of the conformation of hypervariable loop 2 are the length of the loop and specific sequence constraints, with particular canonical structures and conserved residues expected for 3, 4, and 6 residue loops. A further structural determinant is the side chain of residue H71, which is significant in the following way. The position of hypervariable loop 1 is essentially fixed. The position of loop 2 relative to loop 1 is variable, and depends on whether a large side chain at H71 packs between the two loops and separates them or a small side chain at H71 allows loops 1 and 2 to juxtapose.

In HuLys crystal structures with four different side chains at residue H71, the expected conformational rearrangement of the hypervariable loop 2 region is not observed. The absence of a mutation-induced conformation change cannot simply be due to the stabilizing effect of a bound Ag, because the Lys-to-Val mutation in the unliganded crystal forms also does not alter the position of loop 2. The modest (0.4–0.6 kcal/mol) improvement in affinity that accompanied this mutation thus cannot be attributed to relieving an inappropriate displacement of hypervariable loop 2 (9). Our findings do not invalidate the Tramontano model, for which other proof exists, including a specific mutational study of residue H71 in the crystallographically determined Ab B72.3 (40). Our data do demonstrate that a class of exceptions may exist in which the H71 side chain alone does not affect the separation of hypervariable loops 1 and 2. An unknown sequence determinant may override the action of H71, or the compact nature of 3-residue hypervariable loops (H53–H55) may confer less sensitivity to the bulk of the H71 side chain.

The observation that significant conformational changes in the H27S mutant did not lead to much change in Ag affinity, whereas substitutions at H71 gave affinity differences, but no apparent explicatory change in structure illustrates the value of combining structural and kinetic studies.

References

1. Wu, T. T., and E. A. Kabat. 1970. An analysis of the sequences of the variable regions of Bence Jones proteins and myeloma light chains and their implications for antibody complementarity. *J. Exp. Med. 132:211.*
2. Kabat, E. A., T. T. Wu, H. M. Perry, K. S. Gottesman, and K. Coeller. 1991. *Sequences of Proteins of Immunological Interest, 5th Ed.* U.S. Department of

Health and Human Services, Public Health Service, National Institutes of Health, Bethesda, MD.
3. Jones, P. T., P. H. Dear, J. Foote, M. S. Neuberger, and G. Winter. 1986. Replacing the complementarity-determining regions in a human antibody with those from a mouse. *Nature 321:522.*
4. Riechmann, L., M. Clark, H. Waldmann, and G. Winter. 1988. Reshaping human antibodies for therapy. *Nature 332:323.*
5. Stephens, S., S. Emtage, O. Vetterlein, L. Chaplin, C. Bebbington, A. Nesbitt, M. Sopwith, D. Athwal, C. Novak, and M. Bodmer. 1995. Comprehensive pharmacokinetics of a humanized antibody and analysis of residual anti-idiotypic responses. *Immunology 85:668.*
6. Winter, G., and W. J. Harris. 1993. Humanized antibodies. *Immunol. Today 14: 243.*
7. Verhoeyen, M. E., C. Milstein, and G. Winter. 1988. Reshaping human antibodies: grafting an antilysozyme activity. *Science 239:1534.*
8. Riechmann, L., J. Foote, and G. Winter. 1988. Expression of an antibody Fv fragment in myeloma cells. *J. Mol. Biol. 203:825.*
9. Foote, J., and G. Winter. 1992. Antibody residues affecting conformation of the hypervariable loops. *J. Mol. Biol. 224:487.*
10. Mariuzza, R. A., D. L. Jankovíc, G. Boulot, A. G. Amit, P. Saludjian, A. Le Guern, J. C. Mazié, and R. J. Poljak. 1983. Preliminary crystallographic study of the complex between the Fab fragment of a monoclonal anti-lysozyme antibody and its antigen. *J. Mol. Biol. 170:1055.*
11. Amit, A. G., R. A. Mariuzza, S. E. V. Phillips, and R. J. Poljak. 1986. Three-dimensional structure of an antigen-antibody complex at 2.8 Å resolution. *Science 233:747.*
12. Bhat, T. N., G. A. Bentley, T. O. Fischmann, G. Boulot, and R. J. Poljak. 1990. Small rearrangements in structures of Fv and Fab fragments of antibody D1.3 on antigen binding. *Nature 347:483.*
13. Bhat, T. N., G. A. Bentley, G. Boulot, M. I. Green, D. Tello, W. Dall'Acqua, H. Souchon, F. P. Schwarz, R. A. Mariuzza, and R. J. Poljak. 1994. Bound water molecules and conformational stabilization help mediate an antigen-antibody association. *Proc. Natl. Acad. Sci. USA 91:1089.*
14. Saul, F. A., and R. J. Poljak. 1992. Crystal structure of human immunoglobulin fragment Fab New refined at 2.0 Å resolution. *Proteins 14:363.*
15. Epp, O., E. E. Lattman, M. Schiffer, R. Huber, and W. Palm. 1975. The molecular structure of a dimer composed of the variable portions of the Bence-Jones protein REI refined at 2.0 Å resolution. *Biochemistry 14:4943.*
16. Holmes, M. A., and J. Foote. 1997. Structural consequences of humanizing an antibody. *J. Immunol. 158:2192.*
17. Holmes, M. A., T. N. Buss, and J. Foote. 1998. Conformational correction mechanisms aiding antigen recognition by a humanized antibody. *J. Exp. Med. 187: 479.*
18. Carter, P., R. F. Kelley, M. L. Rodrigues, B. Snedecor, M. Covarrubias, M. D. Velligan, W. L. T. Wong, A. M. Rowland, C. E. Kotts, M. E. Carver, et al. 1992. High level *Escherichia coli* expression and production of a bivalent humanized antibody fragment. *Bio/Technology (NY) 10:163.*
19. Perkins, S. J. 1986. Protein volumes and hydration effects. *Eur. J. Biochem. 157:169.*
20. Otwinowski, Z. 1993. Oscillation data reduction program. In *Proceedings of the CCP4 Study Weekend: Data Collection and Processing, January 29–30.* L. Sawyer, N. Isaacs, and S. Bailey, eds. SERC Daresbury Laboratory, Warrington, U.K. pp. 56.
21. Otwinowski, Z., and W. Minor. 1997. Processing of *x*-ray diffraction data collected in oscillation mode. *Methods Enzymol. 276:307.*
22. Kleywegt, G. J., and A. T. Brünger. 1996. Checking your imagination: applications of the free R value. *Structure 4:897.*
23. Brünger, A. T. 1992. *X-PLOR Manual, Version 3.1.* Yale University Press, New Haven, CT.
24. Tronrud, D. E., L. F. TenEyck, and B. W. Matthews. 1987. An efficient general-purpose least-squares refinement program for macromolecular structures. *Acta Crystallogr. A42:489.*
25. Laskowski, R. A., M. W. MacArthur, D. S. Moss, and J. M. Thornton. 1993. PROCHECK: a program to check the stereochemistry of protein structures. *J. Appl. Crystallogr. 26:283.*
26. Milner-White, E. J., B. M. Ross, R. Ismail, K. Belhadj-Mostefa, and R. Poet. 1988. One type of γ-turn, rather than the other gives rise to chain-reversal in proteins. *J. Mol. Biol. 204:777.*
27. Luzzati, V. 1952. Traitment statistique des erreurs dans la determination des structures cristallines. *Acta Crystallogr. 5:802.*
28. Baker, E. N., and R. E. Hubbard. 1984. Hydrogen bonding in globular proteins. *Prog. Biophys. Mol. Biol. 44:97.*
29. Tramontano, A., C. Chothia, and A. M. Lesk. 1990. Framework residue 71 is a major determinant of the position and conformation of the second hypervariable region in the V_H domains of immunoglobulins. *J. Mol. Biol. 215:175.*
30. Padlan, E. O., C. Abergel, and J. P. Tipper. 1995. Identification of specificity-determining residues in antibodies. *FASEB J. 9:133.*
31. Capra, J. D. 1971. Hypervariable region of human immunoglobulin heavy chains. *Nat. New Biol. 230:61.*
32. Novotny, J., R. Bruccoleri, J. Newell, D. Murphy, E. Haber, and M. Karplus. 1983. Molecular anatomy of the antibody binding site. *J. Biol. Chem. 258:14433.*
33. MacCallum, R. M., A. C. R. Martin, and J. M. Thornton. 1996. Antibody-antigen interactions: contact analysis and binding site topography. *J. Mol. Biol. 262:732.*
34. Chothia, C., and A. M. Lesk. 1987. Canonical structures for the hypervariable regions of immunoglobulins. *J. Mol. Biol. 96:901.*
35. Chothia, C., A. M. Lesk, E. Gherardi, I. M. Tomlinson, G. Walter, J. D. Marks, M. B. Llewelyn, and G. Winter. 1992. Structural repertoire of the human V_H segments. *J. Mol. Biol. 227:799.*
36. Cheetham, G. M. T., G. Hale, H. Waldmann, and A. C. Bloomer. 1998. Crystal structures of a rat anti-CD52 (CAMPATH-1) therapeutic antibody Fab fragment and its humanized counterpart. *J. Mol. Biol. 284:85.*
37. James, L. C., G. Hale, H. Waldmann, and A. C. Bloomer. 1999. 1.9 Å structure of the therapeutic antibody CAMPATH-1H Fab in complex with a synthetic peptide antigen. *J. Mol. Biol. 289:293.*
38. Fan, Z. C., L. Shan, B. Z. Goldsteen, L. W. Guddat, A. Thakur, N. F. Landolfi, M. S. Co, M. Vasquez, C. Queen, P. A. Ramsland, and A. B. Edmundson. 1999. Comparison of the three-dimensional structures of a humanized and a chimeric Fab of an anti-γ-interferon antibody. *J. Mol. Recognit. 12:19.*
39. Dall'Acqua, W., E. R. Goldman, E. Eisenstein, and R. A. Mariuzza. 1996. A mutational analysis of the binding of two different proteins to the same antibody. *Biochemistry 35:9667.*
40. Xiang, J., Y. Sha, Z. Jia, L. Prasad, and L. T. J. Delbaere. 1995. Framework residues 71 and 93 of the chimeric B72.3 antibody are major determinants of the conformation of heavy-chain hypervariable loops. *J. Mol. Biol. 253:385.*

Article No. jmbi.1999.3192 available online at http://www.idealibrary.com on IDEAL® J. Mol. Biol. (1999) 293, 865–881

JMB

Selection and Analysis of an Optimized Anti-VEGF Antibody: Crystal Structure of an Affinity-matured Fab in Complex with Antigen

Yvonne Chen[1], Christian Wiesmann[1], Germaine Fuh[1], Bing Li[1], Hans W. Christinger[1], Patrick McKay[2], Abraham M. de Vos[1] and Henry B. Lowman[1]*

[1]*Department of Protein Engineering, Genentech, Inc. 1 DNA Way, South San Francisco, CA 94080, USA*

[2]*Department of Process Sciences, Genentech, Inc. 1 DNA Way, South San Francisco, CA 94080, USA*

**Corresponding author*

The Fab portion of a humanized antibody (Fab-12; IgG form known as rhuMAb VEGF) to vascular endothelial growth factor (VEGF) has been affinity-matured through complementarity-determining region (CDR) mutation, followed by affinity selection using monovalent phage display. After stringent binding selections at 37 °C, with dissociation (off-rate) selection periods of several days, high affinity variants were isolated from CDR-H1, H2, and H3 libraries. Mutations were combined to obtain cumulatively tighter-binding variants. The final variant identified here, Y0317, contained six mutations from the parental antibody. *In vitro* cell-based assays show that four mutations yielded an improvement of about 100-fold in potency for inhibition of VEGF-dependent cell proliferation by this variant, consistent with the equilibrium binding constant determined from kinetics experiments at 37 °C. Using X-ray crystallography, we determined a high-resolution structure of the complex between VEGF and the affinity-matured Fab fragment. The overall features of the binding interface seen previously with wild-type are preserved, and many contact residues are maintained in precise alignment in the superimposed structures. However, locally, we see evidence for improved contacts between antibody and antigen, and two mutations result in increased van der Waals contact and improved hydrogen bonding. Site-directed mutants confirm that the most favorable improvements as judged by examination of the complex structure, in fact, have the greatest impact on free energy of binding. In general, the final antibody has improved affinity for several VEGF variants as compared with the parental antibody; however, some contact residues on VEGF differ in their contribution to the energetics of Fab binding. The results show that small changes even in a large protein-protein binding interface can have significant effects on the energetics of interaction.

Keywords: angiogenesis; humanized antibody-antigen complex; affinity maturation; phage display; X-ray crystallography

Introduction

Angiogenic factors (Folkman & Klagsbrun, 1987), which stimulate endothelial cells leading to new vascularization, have roles in such disease states as cancer, rheumatoid arthritis, and macular degeneration (reviewed by Ferrara, 1995; Folkman, 1995; Iruela-Arispe & Dvorak, 1997). Vascular endothelial growth factor (VEGF), a heparin-binding protein initially identified from pituitary cells (Ferrara & Henzel, 1989), is clearly a key angio-

Abbreviations used: CDR, complementarity-determining region; FR, framework region; HuVEC, human umbilical vein endothelial cell; $K_d^{25°}$, equilibrium dissociation constant determined at 25 °C; mAb, IgG form of monoclonal antibody; PBS, phosphate-buffered saline; SPR, surface plasmon resonance; VEGF, vascular endothelial growth factor; VEGF(109), receptor-binding fragment of VEGF with residues 8-109; VEGF(165), VEGF form with residues 1-165.

E-mail address of the corresponding author: hbl@gene.com

0022-2836/99/440865–17 $30.00/0

genic factor in development as well as in certain disease states, including the growth of solid tumors (reviewed by Ferrara, 1999). A murine monoclonal antibody, A.4.6.1, was found to block VEGF-dependent cell proliferation *in vitro* and to antagonize tumor growth *in vivo* (Kim *et al.*, 1993). The murine mAb was previously humanized in Fab form to yield a variant known as Fab-12 (Presta *et al.*, 1997). Both chimeric and humanized antibodies retained high affinity binding to VEGF, with an apparent equilibrium dissociation constant, $K_d^{25°}$, of 0.9 to 3 nM (Presta *et al.*, 1997; Baca *et al.*, 1997; Muller *et al.*, 1998a). The corresponding full-length IgG form of this antibody, rhumAb VEGF, is being developed as a possible therapeutic agent for the treatment of human solid tumors (Mordenti *et al.*, 1999).

We became interested in obtaining higher affinity variants of Fab-12 in order to test whether affinity improvements of this antibody might improve its potency and efficacy. Phage display of randomized libraries of antibodies and other proteins has been extensively used to engineer proteins with improved affinity and specificity (Lowman *et al.*, 1991; reviewed by Kay & Hoess, 1996; Rader & Barbas, 1997; Griffiths & Duncan, 1998). In particular, a phage-based *in vitro* affinity maturation process has been successful in improving the binding affinity of antibodies previously identified from traditional monoclonal or naive-library sources (e.g. Hawkins *et al.*, 1992; Marks *et al.*, 1992; Barbas *et al.*, 1994; Yang *et al.*, 1995; Schier *et al.*, 1996; Thompson *et al.*, 1996).

In previous work, the humanized anti-VEGF antibody Fab-12 was adapted for improved monovalent phage display through selection of a CDR-L1 variant, designated Y0192 (Muller *et al.*, 1998a). To select target residues for randomization and affinity optimization, we also previously screened all CDR residues, as defined by a combination of the hypervariable (Kabat *et al.*, 1987) and structurally defined (Chothia & Lesk, 1987) CDR residues. Fab variants of Y0192 generated by alanine scanning were analyzed for side-chain contributions to antigen binding (Muller *et al.*, 1998a). In addition, a crystal structure of Fab-12 in complex with the receptor-binding domain of VEGF, VEGF(109), was determined (Muller *et al.*, 1998a). The results of these studies showed that the antigen binding site is almost entirely composed of residues from the heavy chain CDRs, CDR-H1, H2, and H3. Therefore, these CDRs appeared most likely to provide the opportunity for improved binding interactions with antigen.

Here, we describe the selection of an affinity-improved anti-VEGF antibody by phage display and off-rate selection. We show that the affinity-matured antibody binds VEGF with at least 20-fold improved affinity and inhibits VEGF-induced cell proliferation with enhanced potency in a cell-based assay. We also report the crystal structure of an affinity-optimized antibody in complex with VEGF, to our knowledge, representing the first reported structure of an *in vitro* affinity-matured antibody:antigen complex. The structure, together with mutational analysis, shows that subtle changes in the antibody-antigen interface account for improved affinity.

Results

Library design

We used the results of an alanine-scanning analysis, combined with a crystal structure of the wild-type Fab fragment in complex with VEGF (Muller *et al.*, 1998a), to design targeted libraries within the antibody CDRs for random mutagenesis and affinity selection. This strategy enabled us to construct theoretically complete libraries with a small number of residues randomized in each CDR. Although sites remote from the antigen-combining region or buried within the protein could modulate antigen binding affinity indirectly and have in fact been exploited for affinity improvement (Hawkins *et al.*, 1993), clearly residues shown to be important by alanine scanning are useful starting points for binding-affinity optimization (Lowman *et al.*, 1991; Lowman & Wells, 1993). Furthermore, we reasoned that by making mutations at residues of the antibody CDRs which were known to affect antigen binding and were located at or near points of contact in the bound complex, we could minimize the possibility of other indirect effects which might alter stability, immunogenicity, or other properties of the antibody.

Both Ala-scanning and crystallography (Muller *et al.*, 1998a) identified CDR-H3 as the predominant contact segment for VEGF, consistent with the general observation that CDR-H3 is often key to antigen binding (Chothia & Lesk, 1987). Within CDR-H3, residues Y95, P96, H97, Y98, Y99, S100b, H100c, W100d, Y100e, and F100f (numbering is as described by Kabat *et al.* (1987)), all showed effects on binding over a range of twofold to >150-fold when mutated to Ala, and Ala substitution at S100a caused a slight improvement in binding. However, H100c, Y100e, and F100f were found to have little or no direct contact with VEGF and presumed to have indirect effects on binding. On the other hand, Y95 and W100d have significant contacts with VEGF, and Ala substitutions resulted in no detectable binding to VEGF. Therefore, these residues were excluded from optimization. Inspection of the complex structure suggested that substitutions at P96 and Y98 could be disruptive to the antibody structure, while G100, where Ala mutation had little effect, might tolerate further substitutions. We therefore constructed a library (YC81) which fully randomized positions H97, Y99, G100, S100a, and S100b, within CDR-H3.

Significant effects of Ala substitution were also found in CDR-H2. Here, W50, I51, N52, T52a, Y53, T54, T58 alanine mutants all showed >twofold loss in binding affinity, with the greatest residue surface area buried at positions W50, I51, Y53, and

T58 (Muller *et al.*, 1998a). Indeed, W50 along with other aromatic side-chains was observed to form a deep pocket into which a loop of VEGF inserts in the complex, and was excluded from further optimization. Residue I51, on the other hand, showed no direct contact with VEGF and was also excluded. Residue T58 had multiple interactions within the interface, including contacts with VEGF and with the critical W50 of the CDR pocket. Although E56 showed no contact with VEGF and little effect (<twofold) upon alanine substitution, its side-chain lies at the periphery of the interface, near several hydrophobic residues of VEGF. We reasoned that these might be exploited for additional binding interactions. Two CDR-H2 libraries were constructed: YC266, randomizing positions T52a, Y53, T54, and E56; and YC103, randomizing positions N52, T52a, Y53, and T54.

In CDR-H1 G26, Y27, F29, N31, Y32, G33, M34, and N35 were implicated by alanine mutagenesis as important for binding VEGF; however, only N31, Y32, and G33 had significant direct contacts with VEGF. Since Ala substitution of G33 showed reduced binding, larger side-chains seemed less desirable; for this reason, this position was not randomized. Residues 27 (buried in the antibody structure) and T28 and T30 (which are mutually contacting) were included at the end of the H1 loop as possible indirect determinants of binding. Residues 27, 28, and 30-32 were randomized in a library designated YC265.

Framework residues, especially heavy chain residues 71 and 93, normally outside the region of contact with antigen, have also been found to affect antibody binding affinity (Tramontano *et al.*, 1990; Foote & Winter, 1992; Hawkins *et al.*, 1993; Xiang *et al.*, 1995), and sometimes participate in antigen contacts (reviewed by Nezlin, 1998). Therefore, an additional region of the anti-VEGF Fab, within FR-H3 and including position 71, was also targeted for randomization. Since the residue 71-76 region has contacts with CDR-H1 (at F29) and CDR-H2 (at I51 and T52a), these represented potential sites for affinity improvement through secondary effects on the interface residues. Residues L71, T73, and S76 were randomized in this FR-H3 library.

Phage selections

Fab libraries were constructed using a fusion to the g3p minor coat protein in a monovalent phage display (phagemid) vector (Bass *et al.*, 1990; Lowman *et al.*, 1991). For each library, stop codons were introduced by mutagenesis into the Y0192 phage template (Muller *et al.*, 1998a) at each residue position to be randomized. Each stop-codon construct was then used for construction of a fully randomized (using NNS codons) library as described in Materials and Methods. Phage were precipitated from overnight *Escherichia coli* shake-flask cultures and applied to VEGF-coated immunosorbant plates for binding selections. Cycles of selection followed by amplification were carried out essentially as described (Lowman, 1998).

We used an off-rate selection process (see Materials and Methods) similar to previously described procedures (Hawkins *et al.*, 1992; Yang *et al.*, 1995), modified by gradually increasing the selective pressure for binding to antigen during successive cycles of enrichment. The enrichment factor (ratio of displaying phage to non-displaying phage eluted *versus* applied) was used to monitor the stringency of selection at each step (Table 1). As a control, and to obtain a relative measure of affinity improvement, Y0192-phage were subjected to the same procedure at each cycle.

Fab-phage clones were sequenced from several phage-binding selection rounds that showed enrichment for Fab-phage over non-displaying phage. From round 6 of the CDR-H1 library selections, a dominant clone, Y0243-1 was found, having wild-type residues at Y27, T30, and Y32, and substitutions T28D and N31H (Table 2). Additional clones had related sequences, with N31H found in all selectants; Asp or Glu substituting for T28; and Thr, Ser, Gln, or Gly found at position T30.

Table 1. Enrichment factors from phage-displayed Fab libraries

Round	Wash time (hours)	CDR-H1 YC265	CDR-H2 YC266	CDR-H2 YC103	CDR-H3 YC81	FR-H3 YC101	Control Y0192
1	0	8.2	1.7	1.3	3.3	4	1.5
2	1	1.6	25	0.7	10	110	90
3	2	340	880	100	570	2300	22000
4	18	6800	880	5200	3700	600	2700
5	37[a]	210	900	920	1300	480	32
6	47[a]	130	80	100	3500	30	20
7	63[a]	1	1	>3	>25	1	>8

Libraries are designated by CDR region and oligonucleotide label (see the text for details). Library Fab-phage (ampicillin-resistant) were mixed with non-displaying control phage (chloramphenicol-resistant) in each starting pool, and subjected to VEGF binding selection, washing, and elution as described in the text.

The enrichment factor for each library is reported here as the ratio of Amp/Cam colony-forming units in the eluted pool, divided by the ratio of Amp/Cam colony-forming units in the starting pool. Starting phage concentrations were about 10^{12}/ml, except 10^{13}/ml in round 1. The wild-type Fab-phage, Y0192 was included at each round for comparison of enrichment under the particular conditions used.

[a] In some cases, the wash-step included incubation at 37 °C.

Table 2. Anti-VEGF Fab variants selected from a CDR-H1 library (HL-265)

Variant	*n*	Y 27	T 28	T 30	N 31	Y 32	I 34[a]	K_d(Y0192)/ K_d(variant)
Round 6 (HCl)								
Y0243-1	5	Y	D	T	H	Y	M	3.1
Y0243-2	1	Y	E	Q	H	Y	M	
Y0243-3	1	Y	E	T	H	Y	M	
Y0243-4	1	Y	D	G	H	Y	M	
Y0243-5	1	Y	D	S	H	Y	M	
Y0243-6	1	Y	E	S	H	Y	M	
Consensus:		Y	D	T	H	Y	M	3.1

All variants are in the background of Y0192 (Muller *et al.*, 1998a). *n* indicates the number of clones found with identical DNA sequence. The wild-type (Y0192) residue is shown at the top of each column, and the sequence position number is indicated according to Kabat *et al.* (1987).

[a] Position 34 was not randomized, but was changed to Met (as in Fab-12) in this library. The consensus reported here, equivalent to clone Y0243-1, represents the most abundant amino acid residue at each position (including clones with multiple representation ($n > 1$)). K_d(Y0192)/K_d (variant) indicates the fold increase in binding affinity *versus* the wild-type humanized antibody Y0192 (see Table 6).

Clones from two independently constructed CDR-H2 libraries were remarkable in that all sequenced library clones conserved wild-type residues at virtually all positions mutated, except at position Y53, where all clones contained a Trp substitution (Table 3).

Because of the strong enrichment observed from the CDR-H3 library, a number of clones were sequenced from rounds 5 and 7 (Table 4). Of 39 sequenced clones, 37 retained the wild-type residue S100b, and all contained the mutation H97Y. The remaining positions showed greater diversity, even after seven cycles of selection. The dominant clone at round 7, Y0238-3, contained the mutation S100aT (in addition to H97Y), with wild-type residues Y99 and G100. Other substitutions observed included Lys or Arg for Y99 (in 18 of 39 clones), G100N (11 of 39 clones), and a variety of substitutions including Arg, Glu, Gln, and Asn at S100a. In this library, the consensus sequence is represented by the dominant clone, Y0238-1 (Table 4).

Clones from round 6 of the FR-H3 library (Table 5) showed conservation of wild-type residue S76, with wild-type residues or various substitutions at the remaining positions: Val or Ile substituting for L71, and Val or Lys substitutions at T73.

Binding affinity of selected variants

For measurements of binding affinity, we made use of an amber stop codon placed between the genes for the Fab heavy chain and the g3p C-terminal domain, and expressed soluble Fab variants from *E. coli* shake-flask or fermentation cultures. Fab variants purified from protein-G affinity chromatography were characterized for binding affinity using an SPR-based assay on a BIAcore™-2000 instrument. The binding-kinetics assay has been described (Muller *et al.*, 1998a).

Association kinetics (k_{on}) for the wild-type antibody binding to immobilized VEGF are slow (Presta *et al.*, 1997; Baca *et al.*, 1997; Muller *et al.*, 1998a), and none of the variants tested had significantly improved on-rates. On the other hand, dissociation kinetics varied over a range of 10^{-4} s^{-1} to $\leqslant 4 \times 10^{-6}$ s^{-1} at 25 °C (Table 6). Based on measurements of instrumental drift, we could not accurately measure k_{off} (and consequently K_d)

Table 3. Anti-VEGF Fab variants selected from CDR-H2 libraries (HL-266, YC103)

Variant	*n*	N 52[a]	T 52a	Y 53	T 54	G 55[a,b]	E 56[a]	K_d(Y0192)/ K_d(variant)
Round 6 (HCl)								
HL266-A[b]	6	N	T	W	T	G	E	1.3
HL266-E	1	N	T	W	T	G	T	
HL266-I	1	N	T	W	T	G	Q	
YC103-A[b]	7	N	T	W	T	G	E	1.3
YC103-C	1	N	T	W	D	G	E	
Consensus		N	T	W	T	G	E	1.3

All variants are in the background of Y0192 (Muller *et al.*, 1998a). *n* indicates the number of clones found with identical DNA sequence. The wild-type (Y0192) residue is shown at the top of each column, and the sequence position number is indicated according to Kabat *et al.* (1987). The consensus reported here, equivalent to clones HL266A and YC103A, represents the most abundant amino acid at each position (including clones with multiple representation; i.e. $n > 1$). K_d(Y0192)/K_d(variant) indicates the fold increase in binding affinity *versus* the wild-type humanized antibody Y0192 (see Table 6).

[a] Constant positions were position 52 in the HL-266 library and position 56 in the YC103 library.

[b] Equivalent clones are assumed to have equal affinity.

Table 4. Anti-VEGF Fab variants selected from a CDR-H3 library (YC81)

Variant	*n*	H 97	Y 99	G 100	S 100a	S 100b	K_d(Y0192)/K_d(variant)
Round 5 (VEGF)							
Y0228-21	1	Y	R	N	A	S	
Y0228-22	1	Y	T	T	R	S	
Y0228-23	1	Y	E	G	S	S	
Y0228-24	1	Y	R	Q	R	G	
Y0228-26	1	Y	T	G	R	S	
Y0228-27	1	Y	T	N	T	S	
Y0228-28	1	Y	R	K	G	S	
Y0228-29	1	Y	T	G	S	S	
Y0228-30	1	Y	R	S	G	S	
Round 5 (HCl)							
Y0229-20	1	Y	T	N	R	S	
Y0229-21	1	Y	R	N	S	S	
Y0229-22	1	Y	K	E	S	S	
Y0229-23	1	Y	R	D	A	S	
Y0229-24	1	Y	R	Q	K	G	
Y0229-25	1	Y	K	G	G	S	
Y0229-26	1	Y	Y	G	A	S	
Y0229-27	1	Y	R	G	E	S	
Y0229-28	1	Y	R	S	T	S	
Y0238-10[a]	1	Y	R	N	T	S	3.8
Round 7 (HCl)							
Y0238-3	6	Y	Y	G	T	S	≥9.4
Y0238-1	2	Y	R	G	T	S	7.3
Y0238-2	2	Y	I	N	K	S	
Y0238-10[a]	2	Y	R	N	T	S	3.8
Y0238-4	1	Y	Y	N	Q	S	
Y0238-5	1	Y	I	A	K	S	2.1
Y0238-6	1	Y	R	D	N	S	≥5.4
Y0238-7	1	Y	W	G	T	S	
Y0238-8	1	Y	R	Q	N	S	
Y0238-9	1	Y	R	Q	S	S	
Y0238-11	1	Y	K	N	T	S	
Y0238-12	1	Y	I	E	R	S	
Consensus		Y	R	G	T	S	7.3

All variants are in the background of Y0192 (Muller *et al.*, 1998a). The clones are grouped according to the round of selection (5 or 7) and the type of elution (VEGF competition or HCl elution) used for recovery of bound phage. *n*, indicates the number of clones found with identical DNA sequence within each group. The wild-type (Fab-12, or Y0192) residue is shown at the top of each column, and the sequence position number is indicated according to Kabat *et al.* (1987). The consensus reported here, equivalent to clone Y0238-1, represents the most abundant amino acid at each position (including clones with multiple representation (n > 1)). K_d(Y0192)/K_d(variant) indicates the fold increase in binding affinity *versus* the wild-type humanized antibody Y0192 (see Table 6).

[a] One clone was identified at both rounds 5 and 7. Equivalent clones are assumed to have equal affinity.

under these conditions, but instead used the kinetics data to place an upper limit on K_d.

The phage-derived Fab variants tested showed a range of small (within experimental error of about twofold) to significant (>fivefold) improvements in binding affinity over the wild-type (parental phage) antibody Y0192 (Table 6). From the CDR-H1 library, the dominant clone (Y0243-1) showed threefold improved affinity. Variant Y0242-1, the dominant clone in each of three CDR-H2 libraries, showed an affinity equivalent to wild-type within experimental error, and two clones derived from the FR-H3 library (Y0244-1 and Y0244-4) were equivalent or slightly weaker in affinity. Small

Table 5. Anti-VEGF Fab variants selected from a FR-H3 library

Variant	*n*	L 71	T 73	S 76	K_d(Y0192)/K_d(variant)
Round 6 (HCl)					
Y0244-1	1	V	V	S	0.3
Y0244-2	1	L	K	S	
Y0244-3[a]	1	L	V	S	
Y0244-4	1	I	K	S	0.9

All variants are in the background of Y0192 (Muller *et al.*, 1998a). *n*, indicates the number of clones found with identical DNA sequence. The wild-type (Fab-12, or Y0192) residue is shown at the top of each column, and the sequence position number is indicated according to Kabat *et al.* (1987). K_d(Y0192)/K_d(variant) indicates the fold increase in binding affinity *versus* the wild-type humanized antibody Y0192 (see Table 6).

[a] One variant contained a spontaneous mutations, S74W.

Table 6. Binding kinetics of anti-VEGF Fab variants at 25 °C

Variant	$k_{on}/10^4$ (M^{-1} s^{-1})	$k_{off}/10^{-4}$ (s^{-1})	K_d (nM)	K_d(Y0192)/K_d(variant)
Y0192[a]	4.1	1.2	2.9	1
A. *Library-derived*				
Y0238-1	2.6	0.09	0.4	7.3
Y0238-3	1.3	≤0.04[b]	≤0.3[b]	≥9.4[b]
Y0238-5	0.57	0.08	1.4	2.1
Y0238-7	1.1	≤0.06[b]	≤0.5[b]	≥5.4[b]
Y0238-10	1.2	0.09	0.8	3.8
Y0242-1	3.8	0.86	2.3	1.3
Y0243-1	4.8	0.45	0.9	3.1
Y0244-1	3.0	2.7	9.0	0.3
Y0244-4	5.2	1.7	3.3	0.9
B. *Engineered*				
Y0268-1	4.0	0.15	0.38	7.6
Y0313-1	3.5	≤0.05[b]	≤0.15[b]	≥20[b]
Y0192(T28D)	6.8	1.4	2.0	1.4
Y0192(N31H)	4.8	0.37	0.8	3.6
Y0192(H97Y)	2.5	0.045	0.2	14
Y0192(S100aT)	6.8	1.0	1.5	1.9
Y0317	3.6	≤0.05[b]	≤0.14[b]	≥20[b]

Kinetic constants were determined from measurements using a BIAcore™-2000 instrument with a biosensor chip containing immobilized VEGF(109). Measurements were performed at 25 °C. Fab concentrations were calculated from quantitative amino acid analysis. The equilibrium dissociation constant, K_d, is calculated form the ratio of the rate constants, k_{off}/k_{on}. The relative affinity, reported as K_d(Y0192)/K_d(variant) indicates the fold increase in binding affinity versus the wild-type humanized antibody Y0192. Errors in K_d were approximately ±25%. Variant Y0242-1 corresponds to the point mutations Y53W in CDR-H2 of Fab Y0192; for descriptions of the other variants, see Tables 2, 3, 4, 5, and 8.

[a] Data for Y0192 is from Muller *et al.* (1998a,).

[b] In some cases, the dissociation rate constant observed was at or near the limit of detection; therefore, the reported k_{off} and K_d are upper limits, and the relative affinities are an upper limit.

improvements were seen in CDR-H3 variants Y0238-5 and Y0238-10. However, larger improvements (exceeding the limits of measurement (>fivefold to >ninefold)) were observed for the CDR-H3 variants Y0238-1, Y0238-3, and Y0238-7.

All tested variants (in fact all sequenced clones) from the CDR-H3 library contained the mutation H97Y. In the higher affinity group, Gly was conserved at position 100, while the lower affinity variant contained Ala (known to cause 1.8-fold reduction in Y0192 binding; Muller *et al.*, 1998a) or Asn (Table 4). The S100a position, while quite varied among sequenced clones, was changed to Thr in the higher affinity CDR-H3 variants, and Thr or Lys in the lower affinity ones. Substitutions at Y99, though mostly confined to basic or aromatic residues, apparently had little effect since Y0238-1 (representing the consensus CDR-H3 sequence with Y99R) was not significantly different in affinity from Y0238-3, which retained Y99.

Affinity improvements from combinations of CDR mutations

To improve affinity further, several combinations of the phage-selected CDR-H1, H2, and H3 mutations were made by site-directed mutagenesis (Table 7). Among these, the highest affinity was obtained with pY0313-1 (i.e. pY0192 with mutations CDR-H1 (T28D/N31H/I34M) and CDR-H3 (H97Y/S100aT); note I34M is a reversion to Fab-12 wild-type). From BIAcore™ kinetics measurements carried out at 25 °C, this Fab variant had ≥20-fold higher affinity than Y0192 (Table 6).

Addition of the Y53W mutation, which alone produced little or no improvement over Y0192, to Y0313-1 (producing variant Y0268-1) actually reduced binding affinity by >twofold (Table 6).

The final Fab version was constructed by removing the phage-expression enhancing mutations in CDR-L1 from pY0313-1 by site-directed mutagen-

Table 7. Anti-VEGF CDR combination variants

	CDR-L1					CDR-H1			CDR-H2	CDR-H3	
Y0192: Variant	R 24	N 26	E 27	Q 28	L 29	T 28	N 31	I 34	Y 53	H 97	S 100a
Y0313-1	-	-	-	-	-	D	H	M	-	Y	T
Y0268-1	-	-	-	-	-	D	H	M	W	Y	T
Y0317	S	S	Q	D	I	D	H	M	-	Y	T
Fab-12	S	S	Q	D	I	-	-	-	-	-	-

Substitutions are shown relative to Y0192. Fab-12 also contains T221 in the heavy chain. Dashes (-) indicate no substitution. Numbering is according to Kabat *et al.* (1987) for both the light chain (CDR-L1) and heavy chain (CDR-H1, H2, H3).

esis. The M4L substitution was identified during phage-humanization experiments (Baca *et al.*, 1997), and the Leu residue was retained so as to preclude possible oxidation of the Met side-chain. The first libraries were constructed from a Fab-12 phagemid derivative, pY0101, which contained a buried framework mutation, V_L(M4L), as well as a mutation (T221L) at the junction to g3p. Thus the final version, Y0317 (Table 7 and Figure 1) differs from Fab-12 by the following six mutations: V_L(M4L), V_H(T28D/N31H/H97Y/S100aT/T221L).

Each of the CDR mutations in H1 and H3 was tested for its effect on VEGF binding affinity by introducing the corresponding point mutation into the parental Y0192 Fab and measuring binding kinetics. The results (Table 6) show a 14-fold and 3.6-fold improvement with substitution of H97Y or N31H, respectively, into the parental Fab. However, T28D or S100aT had identical affinity to Y0192, within experimental error.

We compared Fab-12 and Y0317 Fab affinities in a solution binding assay, using VEGF competition with [^{125}I]VEGF for binding to Fab. The results showed Fab-12 having $K_d^{25°} = 433$ pM and Y0317 Fab having $K_d^{25°} = 20$ pM, a 22-fold improvement in binding affinity (Figure 2).

Because dissociation kinetics in surface plasmon resonance (SPR) experiments exceeded instrumental capabilities at 25 °C, and in order to assess binding affinity under more physiological conditions, we compared binding affinities of the original humanized antibody Fab-12 with the final variant Y0317 in kinetics experiments at 37 °C. k_{on} and k_{off} were faster for both antibodies than at 25 °C, and k_{off} was clearly measurable above background. Using either immobilized VEGF(109) or immobilized VEGF(165), Y0317 was 120-fold to 140-fold improved in affinity over Fab-12, with a $K_d^{37°}$ of 80-190 pM (Table 8).

VEGF Ala-scan of the Y0317 binding epitope

In order to understand how mutations in the Fab affected binding affinity to VEGF, we also tested VEGF variants for binding to the affinity-improved antibody. For these experiments, we made use of the full-length IgG forms of Fab-12 (known as rhuMab VEGF) and Y0317 (termed Y0317-IgG) produced in CHO cells (V. Chisholm, unpublished results). These VEGF variants were previously used for mapping the parental antibody's binding site on VEGF (Muller *et al.*, 1998a).

In this assay, carried out at 37 °C, VEGF competed with biotin-VEGF with an IC_{50} of 9 nM in binding rhuMab VEGF, compared with an IC_{50} of 1 nM for Y0317-IgG (Table 9). SPR measurements have shown similar affinity improvement of Y0317-IgG over rhuMAb VEGF (H. Lowman, unpublished results).

Alanine mutations of VEGF that affected rhuMab VEGF binding also affected Y0317-IgG. For example, M81A, G88A, and G92A all caused large (100 to >500-fold) losses in binding affinity. And smaller reductions (3 to 30-fold) in binding affinity for both antibodies were seen for I80A, K84A, I91A, E93A, and M94A.

However, significant differences in the magnitude of the effect were observed at certain sites, including Y45A, fourfold reduced in affinity for rhuMAb VEGF *versus* 26-fold for Y0317-IgG; Q89A, 19-fold *versus* sixfold; and M94A, 11-fold versus 25-fold. Most surprisingly, two mutations that led to loss of detectable binding affinity for rhumAb VEGF (>500-fold) had only modest effects (four- to ninefold) on binding to Y0317-IgG. These differences might suggest a shift in the binding epitope of the antibody, and this possibility was addressed with receptor-inhibition assays and structural analysis, both described below.

Inhibition of VEGF activity

Cell-proliferation assays have been described (Fairbrother *et al.*, 1998) for the measurement of VEGF mitogenic activity on human umbilical vein endothelial cells. Here, we compared the potency of Fab-12 and the affinity-improved variants Y0238-3 and Y0313-1.

The results (Figure 3) show both variants Y0238-3 and Y0313-1 inhibit VEGF activity more potently than Y0192 Fab. Comparing the Fab forms, variant Y0313-1 appeared at least 30-fold to 100-fold more potent than the wild-type Fab. In additional experiments, Y0317 activity was similar to that of Y0313-1 (data not shown). It should be noted that the amount of VEGF (0.2 nM) used in this assay is potentially limiting for determination of an accurate IC_{50} for the mutant. For example, if the bind-

Table 8. Binding kinetics of anti-VEGF Fab variants at 37 °C

Variant	Immobilized	$k_{on}/10^4$ (M^{-1} s^{-1})	$k_{off}/10^{-4}$ (s^{-1})	K_d (nM)	K_d(Fab-12)/K_d(variant)
Fab-12	VEGF(109)	5.1	6.6	13 ± 2.2	1
Y0317	VEGF(109)	5.4	0.059	0.11 ± 0.02	120
Fab-12	VEGF(165)	5.5	11	20 ± 3.8	1
Y0317	VEGF(165)	5.3	0.074	0.14 ± 0.05	140

Kinetic constants were determined by injecting Fab solutions onto a BIAcore™-2000 instrument with a biosensor chip containing approximately 190 RU of immobilized VEGF(109) or VEGF(165), as indicated. The equilibrium dissociation constant, K_d, is calculated from the ratio of the rate constants, k_{off}/k_{on}. The relative affinity, reported as K_d(Fab-12)/K_d(variant) indicates the fold increase in binding affinity *versus* the original humanized antibody (Fab-12; Presta *et al.*, 1997) under the specified conditions.

```
Light chain:

            1       10        20        30        40        50
Fab-12      DIQMTQSPSSLSASVGDRVTITCSASQDISNYLNWYQQKPGKAPKVLIYF
Y0192       DIQLTQSPSSLSASVGDRVTITCRANEQLSNYLNWYQQKPGKAPKVLIYF
Y0317.      DIQLTQSPSSLSASVGDRVTITCSASQDISNYLNWYQQKPGKAPKVLIYF

            1       10        20        30        40        50
                    60        70        80        90       100
Fab-12      TSSLHSGVPSRFSGSGSGTDFTLTISSLQPEDFATYYCQQYSTVPWTFGQ
Y0192       TSSLHSGVPSRFSGSGSGTDFTLTISSLQPEDFATYYCQQYSTVPWTFGQ
Y0317       TSSLHSGVPSRFSGSGSGTDFTLTISSLQPEDFATYYCQQYSTVPWTFGQ

                    60        70        80        90       100
                   110       120       130       140       150
Fab-12      GTKVEIKRTVAAPSVFIFPPSDEQLKSGTASVVCLLNNFYPREAKVQWKV
Y0192       GTKVEIKRTVAAPSVFIFPPSDEQLKSGTASVVCLLNNFYPREAKVQWKV
Y0317       GTKVEIKRTVAAPSVFIFPPSDEQLKSGTASVVCLLNNFYPREAKVQWKV

                   110       120       130       140       150
                   160       170       180       190       200
Fab-12      DNALQSGNSQESVTEQDSKDSTYSLSSTLTLSKADYEKHKVYACEVTHQG
Y0192       DNALQSGNSQESVTEQDSKDSTYSLSSTLTLSKADYEKHKVYACEVTHQG
Y0317       DNALQSGNSQESVTEQDSKDSTYSLSSTLTLSKADYEKHKVYACEVTHQG

                   160       170       180       190       200
                   210
Fab-12      LSSPVTKSFNRGEC
Y0192       LSSPVTKSFNRGEC
Y0317       LSSPVTKSFNRGEC

                   210
```

Figure 1 (*legend shown opposite*)

ing affinity (K_d) of the mutant is in fact <0.2 nM, then the IC_{50} in this experiment will appear higher than under conditions of lower VEGF concentration. The result therefore supports the conclusion that the affinity-improved variant is at least 30-fold improved in affinity for VEGF, and that it effectively blocks VEGF activity *in vitro*.

Structure of the complex

In order to compare the structure and binding site of the affinity-improved antibody with that of the parental antibody, we determined the complex structure by X-ray crystallography. Crystals of the complex between the receptor binding domain of VEGF (residues 8 to 109) and the affinity-matured Fab Y0317 were grown as described (see Materials and Methods) and diffracted to a maximum resolution of 2.4 Å. The structure was refined starting from the coordinates of the complex between VEGF and the parent of Fab Y0317, Fab-12 (Muller *et al.*, 1998a), and refined to an *R*-value of 19.9% (R_{free} = 27.4%) for the reflections between 20 Å and 2.4 Å resolution.

Heavy chain:

```
                1       10        20        30        40        50
Fab-12          EVQLVESGGGLVQPGGSLRLSCAASGYTFTNYGMNWVRQAPGKGLEWVGW
Y0192           EVQLVESGGGLVQPGGSLRLSCAASGYTFTNYGINWVRQAPGKGLEWVGW
Y0317           EVQLVESGGGLVQPGGSLRLSCAASGYDFTHYGMNWVRQAPGKGLEWVGW

                1       10        20        30        40        50
                        60        70        80        90       100
Fab-12          INTYTGEPTYAADFKRRFTFSLDTSKSTAYLQMNSLRAEDTAVYYCAKYP
Y0192           INTYTGEPTYAADFKRRFTFSLDTSKSTAYLQMNSLRAEDTAVYYCAKYP
Y0317           INTYTGEPTYAADFKRRFTFSLDTSKSTAYLQMNSLRAEDTAVYYCAKYP

                  a     60        70        80  abc   90     96
                      110       120       130       140       150
Fab-12          HYYGSSHWYFDVWGQGTLVTVSSASTKGPSVFPLAPSSKSTSGGTAALGC
Y0192           HYYGSSHWYFDVWGQGTLVTVSSASTKGPSVFPLAPSSKSTSGGTAALGC
Y0317           YYYGTSHWYFDVWGQGTLVTVSSASTKGPSVFPLAPSSKSTSGGTAALGC

                100abcdef       110       120       130       140
                      160       170       180       190       200
Fab-12          LVKDYFPEPVTVSWNSGALTSGVHTFPAVLQSSGLYSLSSVVTVPSSSLG
Y0192           LVKDYFPEPVTVSWNSGALTSGVHTFPAVLQSSGLYSLSSVVTVPSSSLG
Y0317           LVKDYFPEPVTVSWNSGALTSGVHTFPAVLQSSGLYSLSSVVTVPSSSLG

                      150       160       170       180       190
                      210       220       230
Fab-12          TQTYICNVNHKPSNTKVDKKVEPKSCDKTHT
Y0192           TQTYICNVNHKPSNTKVDKKVEPKSCDKTHL
Y0317           TQTYICNVNHKPSNTKVDKKVEPKSCDKTHL

                      200       210       220
```

Figure 1. Sequence alignment of the original humanized antibody (Fab-12; Presta *et al.*, 1997), the phage-displayed antibody (Y0192; Muller *et al.*, 1998a) and the affinity-improved antibody (Y0317). Sequential numbering of each chain is shown above the sequences; numbering according to Kabat *et al.* (1987) is shown below. CDR regions are underlined. Positions at which Y0317 differs from Fab-12 are indicated with double underlining.

The final model consists of two Fab fragments bound to the symmetrical poles of the VEGF dimer. Only residues 14-107 of each VEGF monomer are well defined in the electron density, and therefore the six N-terminal and the two C-terminal residues of each monomer were omitted from the model. Each Fab light chain comprises residues 1 to 213, with the C-terminal residue disordered, whereas for each heavy chain residues 138 to 143 as well as the six C-terminal residues are absent from the model. As in the parental Fab complex, two out of 1050 residues, namely T51 in the V_L chain of each Fab fragment, are located in the "disallowed regions" (Laskowski *et al.*, 1993) of the Ramachandran plot; 85% of all residues have their main-chain torsion angles in the "most favored"

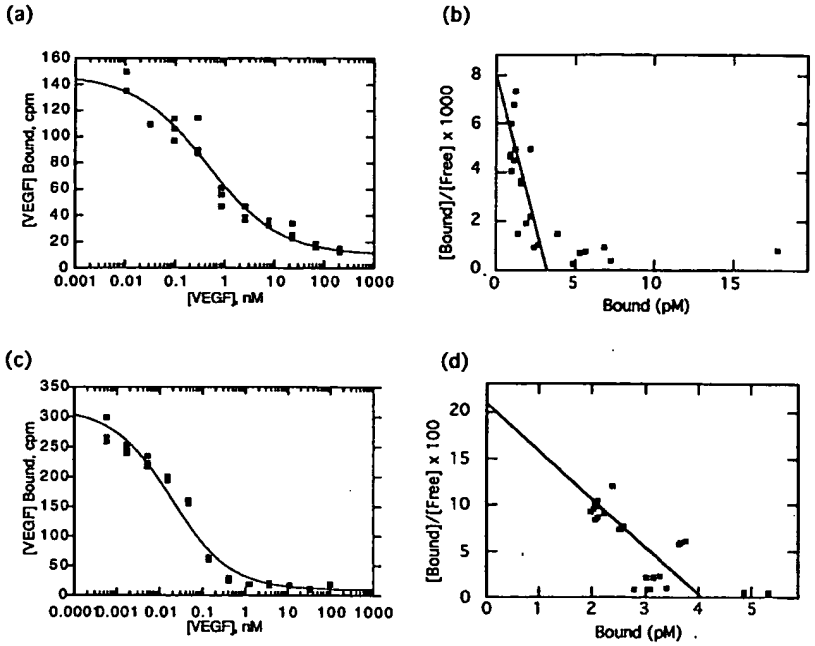

Figure 2. Radiolabeled VEGF binding assay. [^{125}I]VEGF was equilibrated (23 °C) with serial dilutions of unlabeled VEGF and (a) Fab-12 or (c) Y0317. Fabs were captured with an anti-Fab antibody-coated immunosorbant plate. Scatchard analysis (Munson & Rodbard, 1980) with a 1:1 binding model was used to calculate K_d of (b) 433 (±116) pM for Fab-12 and (d) 19.8(±4.3) pM for Y0317.

regions. The average *B*-factor of the model is 51.8 Å^2 and the mobility of the individual domains follows the pattern that was previously observed in the crystal structure of VEGF in complex with the Fab-12, with the constant domain dimer (C_L:C_H1) of one of the Fabs poorly ordered (Muller *et al.*, 1998a).

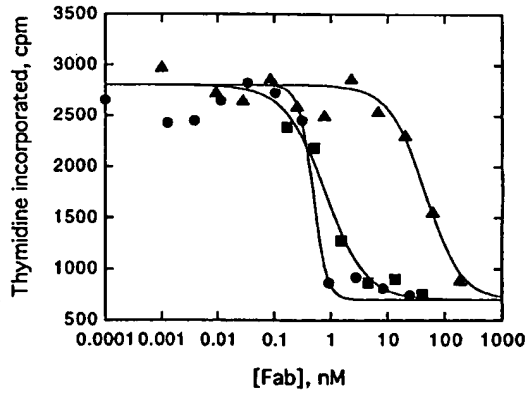

Figure 3. Human umbilical vein endothelial cell (HuVEC) assay of VEGF inhibition. Cells were cultured in the presence of 0.2 nM VEGF and serial dilutions of Fab Y0192 (triangles), Y0238-3 (squares), or Y0313-1 (circles). Cell proliferation was measured by incorporation of [^{3}H]thymidine. Curves show four-parameter fits to the data. Each point represents the mean of three treated wells.

Comparison of the final model with that of the parental Fab-VEGF complex (Muller *et al.*, 1998a) shows that the bound structures are very similar overall (Figure 4(a)) with Y0317 binding to the same site on VEGF as Fab-12 (Figure 4(b)). Side-chains show excellent overlap, and the main-chain structures show very little difference. The most prominent difference in contact residues is at H97Y (Figure 4(c); discussed below), where the tyrosine side-chain packs more favorably with VEGF and a buried water molecule from the parental Fab-VEGF complex is absent in the Y0317-Fab-VEGF complex.

Discussion

Antibody binding selections and affinity improvement

Here we made use of results from alanine-scanning and the previous structure of a humanized antibody-antigen complex to design Fab-phage libraries that randomized the three heavy-chain CDRs as well as one framework region (FR-H3) for improving the binding affinity of an anti-VEGF antibody. Affinity-improved Fab variants were obtained, with the largest effects seen in variants from the CDR-H3 library, although significant improvement was also obtained from mutation of CDR-H1. We therefore combined two mutations from H1 with two from H3, generating a further improved variant, Y0317. By making point mutations, we showed that the 20-fold (Figure 2)

Table 9. Alanine scan of VEGF by ELISA at 37 °C

VEGF(109) variant	IC_{50} (variant)/IC_{50} (VEGF)	
	Fab12-IgG	Y0317-IgG
VEGF(109)	1	1
F17A	1	1
Y21A	1	1
Y45A	4	26
K48A	2	1
Q79A	1	3
I80A	4	5
M81A	>500	930
R82A	>500	4
I83A	>500	9
K84A	3	10
H86A	1	1
Q87A	1	1
G88A	105	87
Q89A	19	6
H90A	1	1
I91A	2	6
G92A	>500	>900
E93A	4	7
M94A	11	25

ELISA assays were carried out using the full-length IgG form of Fab-12 or the IgG form of Y0317 and VEGF(109). Incubation of antibody with VEGF was at 37 °C for five hours. The IC_{50} for inhibition by each Ala mutant was evaluated using a four-parameter equation, and the relative affinities calculated as IC_{50}(mutant VEGF)/IC_{50}(wild-type VEGF). Under these conditions, Fab12-IgG and Y0317-IgG showed IC_{50} values of 9 nM and 1 nM, respectively.

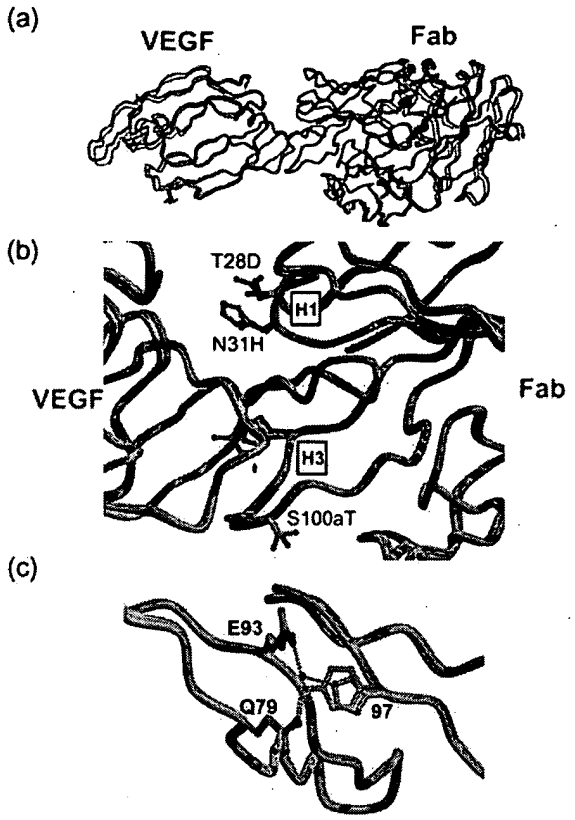

Figure 4. Structure of the affinity-improved Y0317 Fab in complex with VEGF. A superposition of the structure (Muller *et al.*, 1998a) of wild-type humanized antibody Fab-12 (gray) in complex with VEGF (gray) is shown with that of Fab Y0317 (green) in complex with VEGF (yellow). (a) Overall view of the complex, including one Fab molecule bound to one dimer of VEGF (a second Fab molecule is bound at left in the crystal) shows that the binding site for both antibody variants centers on the "80's loop" of VEGF. (b) A view of the four CDR changes between Fab-12 and Y0317 Fab shows that the new D28 and T100a side-chains do not directly contact antigen. However, H31 and Y97 form new contacts. (c) Interactions of H97 and an associated, buried water molecule in the Fab-12 complex, compared with those of Y97 in the Y0317 complex.

to >100-fold (Table 8) affinity improvement in Y0317 can be attributed to two CDR mutations: H97Y and N31H. In fact, H97Y alone improves binding affinty 14-fold.

Despite the relatively slow k_{on} and slow k_{off} of the parental antibody, binding selections described here yielded slower dissociation rates and improved equilibrium dissociation constants. Results of SPR measurements demonstrated that affinity is enhanced mainly through a slower dissociation rate (as opposed to faster association). These results are consistent with the idea of off-rate selection (Hawkins *et al.*, 1992) and with the progressively increased stringency in washing procedures used here (see Materials and Methods and Table 1). Previous binding-optimization efforts have also often yielded larger improvements in k_{off} than in k_{on} (see Lowman & Wells, 1993; Yang *et al.*, 1995; Schier *et al.*, 1996). This may suggest fundamental limitations to the improvements in k_{on} for a given binding site. Even if no conformational changes need occur between free and bound states, the on-rate is limited by the size of the binding interface and the translational and rotational diffusion rates of the binding components (reviewed by Delisi, 1983).

The association rate constants (k_{on}) for both the wild-type Y0192 and the final Y0317 antibodies are relatively slow (about 4×10^4 M^{-1} s^{-1} for both) compared to other antibodies of equal or weaker antigen binding affinity. In fact, the fastest k_{on} identified for any mutant was 6.8×10^4 M^{-1} s^{-1} (Table 6). Typically, k_{on} for antibodies binding to protein antigens, including affinity-matured antibodies, has fallen in the range of 3×10^4 to 1×10^6 M^{-1} s^{-1} (Karlsson *et al.*, 1991; Malmborg *et al.*, 1992; Barbas *et al.*, 1994; Yang *et al.*, 1995; Schier *et al.*, 1996; Wu *et al.*, 1998). In this particular protein-protein interaction, a likely explanation for the slow k_{on} is the high degree of flexibility associated with the binding site both on the Fab and on VEGF. In fact, crystallographic evidence suggests that the "80's loop" region is quite mobile (Muller *et al.*, 1997; Muller *et al.*, 1998b). We are pursuing other strategies to assess whether improvements to k_{on} can be obtained.

The contributions of point mutations in proteins to the free energy of binding or activation are often additive (Wells, 1990). This principle has been used to produce a variety of affinity-improved protein variants based on point or grouped mutations identified by phage display (Lowman & Wells, 1993; Yang *et al.*, 1995) or point-mutant screening (Wu *et al.*, 1998). Considering the initial library selectants Y0238-3 (>ninefold improved in affinity) and Y0243-1 (3.1-fold improved), we would have predicted an improvement of >27-fold for Y0313-1 or Y0317 (Table 7). In fact, a 22-fold improvement is observed (Figure 2) at 25 °C. Addition of the CDR-H1 mutation would be predicted to improve affinity slightly (1.3-fold), but in fact this mutation reduced affinity >twofold (Y0268-1 *versus* Y0313-1; Table 6). Certainly additivity does not always apply, particularly if interacting residues are involved (Wells, 1990). In this case, non-additivity probably results from steric interference between the new Trp in CDR-H2 and the new Tyr in CDR-H3.

To test the energetics of binding by the final Y0317 antibody to VEGF, we made use of a panel of alanine mutants that had been previously constructed for mapping the binding site of the original antibody (Muller *et al.*, 1998a). For these experiments, we made use of the full-length IgG forms of both antibodies. In view of the slow dissociation kinetics for both antibodies, ELISA assays were carried out at 37 °C with incubation for at least five hours to insure that equilibrium was reached. Under these conditions two dramatic differences appear in the Ala-scan of VEGF with respect to Y0317 *versus* Fab-12: both R82A and I83A have small effects on binding in Y0317, but result in large decreases in binding for Fab-12. The reasons for these differences are not clear, but R82 and I83 do have significant surface area (55 Å^2 and 32 Å^2, respectively) buried on binding to VEGF, and make contacts that include residues S100a of CDR-H3 and N52 of CDR-H2 in the wild-type antibody (Muller *et al.*, 1998a).

Structural analysis of the affinity-matured Fab

The structures of a number of antibodies derived from *in vivo* immunization and hybridoma techniques have been determined, in complex with their antigens (reviewed by Nezlin, 1998), and recently, crystallization and preliminary X-ray studies of a chain-shuffled anti-lysozyme scFv antibody in complex with antigen were reported (Küttner *et al.*, 1998). However, to our knowledge, the Y0317 Fab:VEGF structure is the first report of an *in vitro* affinity-matured Fab in complex with antigen. The structural basis of binding affinity improvement is therefore of interest

The Fab fragment of the affinity-matured anti-VEGF antibody Y0317 preserves the structure of the original humanized antibody, Fab-12. Superposition with Fab-12 results in an rmsd of only 0.38 Å for a total of 431 C^{α}-positions, demonstrating the absence of major structural changes between the two molecules. With a total of 1800 Å^2 of solvent-accessible surface buried in each VEGF-Fab interface, the contact area is about 50 Å^2 larger than in the Fab-12 complex. This small increase in buried surface area is mostly due to the exchange of H97 to a tyrosine residue. In the VEGF:Fab-12 complex, H97 buries a solvent-accessible area of 56 Å^2, while the larger tyrosine side-chain of the matured antibody accounts for 86 Å^2 of buried surface. The tyrosine side-chain also affects the hydrogen-bonding pattern and the number of ordered water molecules in the vicinity. In the parental antibody complex, a water molecule near H97 forms two hydrogen bonds to the side-chains of Q79 and E93 of VEGF (Figure 4(c)). In the complex with the affinity-matured Fab, this water molecule is replaced by the hydroxyl group of the newly introduced tyrosine side-chain at position 97. The H97Y mutation therefore not only increases the amount of buried surface area, but also introduces two additional hydrogen bonds between the ligand and Fab-0317 (Figure 4(c)). This is in good agreement with the observation that this single substitution improves VEGF binding affinity by 14-fold (Table 6). We therefore conclude that this single substiution is responsible for the majority of the improvement in binding affinity of Y0317 compared to the parent antibody.

In contrast, despite the availability of the crystal structures of both complexes, it remains uncertain what the structural basis is of the 3.6-fold enhanced binding caused by the N31H mutation. The side-chains of the asparagine and the histidine residues in this position adopt identical conformations in both crystal structures, and the amount of buried surface is not significantly increased in the VEGF:Fab-Y0317 complex. The only difference we can detect is a slight possible improvement in the hydrophobic interactions between the histidine side-chain and the phenyl group of VEGF residue F17, which has rotated slightly compared to the parent complex. It is unclear whether this could contribute to the increased affinity.

Neither of the remaining differences between Fab-12 and Fab-Y0317 has a significant effect on the binding affinity towards VEGF, and the structures show that these residues contribute only marginally to the interface. Some interactions are present between VEGF and the main-chain atoms of the serine and threonine residues in position 100a of the two Fabs, but the side-chains of these residues are not in contact with VEGF. Finally, no contact exist between VEGF and T28 (or D28) of the Fab fragments (the closest point on VEGF to this residue is more than 6 Å distant).

In summary, the analysis and comparison of the two crystal structures are in very good agreement with the results of the binding assays on the various single mutants of the Fab fragments. Although it is not possible to quantify the effects introduced by the amino acid exchanges solely based on the crystal structures, the detailed crystallographic

analysis supports and enables us to interpret the binding data.

Biological implications for antibody inhibition of VEGF

An inhibitory antibody of improved affinity may have improved potency or efficacy in treating diseases associated with VEGF expression. Preceding versions of the anti-VEGF antibody described here, including the murine A4.6.1 (Kim *et al.*, 1993), the humanized version Fab-12 (Presta *et al.*, 1997), as well as Y0192 (Muller *et al.*, 1998a), clearly demonstrated sufficient affinity to effect inhibition of VEGF activity. Here, we show that an affinity-improved variant, Fab Y0317, can inhibit endothelial cell proliferation *in vitro* with least 30-fold greater potency than the parental humanized Fab (Figure 3).

We have limited our optimization strategy to a subset of heavy-chain CDR residues implicated by alanine-scanning and crystallography (Muller *et al.*, 1998a). Furthermore, not all combinations of phage-derived mutations have been tested. One may therefore reasonably ask whether Y0317, with $K_d^{25°} = 20$ pM and $K_d^{37°} = 130$ pM, is the globally optimum variant for binding to this particular epitope (or others) on VEGF. Other affinity optimization efforts have resulted in protein-protein binding affinities in the low picomolar range, from $K_d = 6$ pM to 15 pM (see, e.g. Lowman & Wells, 1993; Schier *et al.*, 1996; Yang *et al.*, 1995). Indeed, we cannot exclude the possibility that higher affinity variants of the A4.6.1 antibody could be produced. However, it seems unlikely that further affinity improvement would greatly enhance biological potency or efficacy because for effective inhibition, the antibody must certainly occupy a significant fraction (perhaps >99 %) of the available (VEGF) binding sites. Serum VEGF concentrations of about 20 pM in normals, and of >300 pM in patients with metastatic carcinoma, have been observed (Kraft *et al.*, 1999). Local or effective concentrations are likely higher. If we conservatively assume the effective concentration of VEGF *in vivo* to be about 400 pM, then 400 pM of even an infinite-affinity Fab would be required to block all sites.

Other factors may limit the improvement in potency of a full-length IgG resulting from an improvement in intrinsic binding affinity of the Fab for antigen. The full-length IgG form of the antibody may benefit from an avidity effect *in vivo*, especially since VEGF is known to associate with proteoglycans on the cell surface (Gitay-Goren *et al.*, 1992). Even in cell-based assays, the IgG form of Fab-12 is a more effective inhibitor than the Fab form (data not shown). Finally, the half-life for dissociation of the affinity-improved antibody is already significant, even on the time-scale of the half-life of clearance for IgG's (days to weeks). The effect of an improved association rate constant for antibody in this system is unknown.

The fact that point (Ala) mutations in the antibody binding site on VEGF sometimes have lesser effects on the binding of Y0317 than on the binding of Fab-12 may suggest that the optimized binding site is more tolerant than the parental one of variations in the antigen. Indeed, Y0317 showed greatly enhanced affinity for murine VEGF over that of Fab-12 (data not shown), though still >100-fold weaker than its affinity for human VEGF. This could provide an advantage against naturally arising VEGF variants.

Materials and Methods

Construction of phage libraries and mutagenesis

A variant of the Fab-12 antibody (a humanized form of murine antibody A4.6.1) was previously identified from phage-displayed Fab libraries for improved expression on phage particles (Muller *et al.*, 1998a). We made use of the plasmid pY0192, a phagemid construct with ampicillin (or carbenicillin) resistance, as the parental ("wild-type") construct for libraries described here. To prevent contamination by wild-type sequence (Lowman *et al.*, 1991; Lowman, 1998), templates with the TAA stop codon at each residue targeted for randomization were prepared from CJ236 *E. coli* cells (Kunkel *et al.*, 1991). Libraries are designated according to the mutagenic oligonucleotides used for their construction: YC265, TCC TGT GCA GCT TCT GGC NNS NNS TTC NNS NNS NNS GGT ATG AAC TGG GTC CG, randomizing residues 27-28, 30-32 in CDR-H1; YC266, GAA TGG GTT GGA TGG ATT AAC NNS NNS NNS GGT NNS CCG ACC TAT GCT GCG G, randomizing residues 52a-54, 56 in CDR-H2; YC103, GAA TGG GTT GGA TGG ATT NNS NNS NNS NNS GGT GAA CCG ACC TAT G, randomizing residues 52-54 in CDR-H2; YC81, C TGT GCA AAG TAC CCG NNS TAT NNS NNS NNS NNS CAC TGG TAT TTC GAC, randomizing residues 97, 99-100b in CDR-H3; and YC101, CGT TTC ACT TTT TCT NNS GAC NNS TCC AAA NNS ACA GCA TAC CTG CAG , randomizing residues 71, 73, and 76 in the "FR-H3" region. An additional library in CDR-H2 was designed to insert three new residues: YC90, GA TGG ATT AAC ACC TAT NNS NNS NNS ACC GGT GAA CCG ACC.

The products of random mutagenesis reactions were electroporated into XL1-Blue *E. coli* cells (Stratagene) and amplified by growing 15-16 hours with M13KO7 helper phage. The complexity of each library, ranging from 2×10^7 to 1.5×10^8 , was estimated based on plating of the initial transformation onto LB plates containing carbenicillin.

Site-directed mutagenesis for point mutations was carried out as above, using appropriate codons to produce the respective mutations, and sequences were confirmed by single-strand DNA sequencing using Sequenase™ (USB).

Phage binding selections

For each round of selection, approximately 10^9-10^{10} phage were screened for binding to plates (Nunc Maxisorp 96-well) coated with 2 μg/ml VEGF(109) in 50 mM carbonate buffer (pH 9.6) and blocked with 5% (w/v) instant milk in 50 mM carbonate buffer, (pH 9.6). Also included were phage prepared from a non-displaying

control phagemid (pCAT), which confers chloramphenicol resistance, as a means of measuring background and enrichment (Lowman & Wells, 1993). Bound phage were eluted with 0.1 M HCl and immediately neutralized with one-third volume of 1 M Tris (pH 8.0). The eluted phage were propagated by infecting XL1 cells for the next selection cycle as described (Lowman, 1998).

In the first cycle, the VEGF plate was incubated with Fab-phage, then was briefly washed to remove bound phage. In the second cycle, binding and washing were followed by a one hour dissociative incubation at room temperature with binding buffer, after which the plate was again washed prior to acid elution. This process was repeated in rounds 3, 4 and 5, except that 1 μM VEGF was included in the dissociative incubation, and the incubation time was increased to 2, 18, and 37 hours, respectively. During these selections, Y0192 phage showed enrichments ranging from 1.5-fold (at the lowest stringency) to 22,000-fold (using a two hour dissociation incubation). However, further increases in stringency (rounds 4-5) resulted in decreasing enrichments for the control phage, with higher enrichments observed for certain libraries, especially the two CDR-H2 libraries and the CDR-H3 library (Table 1).

In cycle 6, a 17 hour dissociative incubation at room temperature was followed by an additional 30 hour incubation at 37 °C (also including VEGF in the buffer). Under these conditions, Y0192-phage showed only slight binding enrichment (20-fold), whereas the CDR-H3 library phage were enriched by 3500-fold. Cycle 7 was carried out with a 63 hour dissociative incubation, after which only small enrichment factors were observed. However, some libraries were continued through eight cycles (with 120 hours of dissociative incubation in the presence of VEGF), after which Fab-phage were still recoverable by acid elution (data not shown).

Purification of Fab

For small-scale preparations, Y0317 Fab and mutants were prepared from *E. coli* shake-flasks as described (Muller *et al.*, 1998a).

For large-scale preparation, whole cell broth was obtained from a ten liter *E. coli* fermentation. The cells were lysed with a Manton-Gaulin homogenizer (two passes at 6000 psi; lysate temperature maintained at 15-25 °C with a heat exchanger). A 5% (v/v) solution of polyethylene imine (PEI), pH 6.0, was added to the lysate to give a final concentration of 0.25% (v/v). The lysate was mixed for 30 minutes at room temperature. The suspension was centrifuged, and the supernatant (containing the Fab) was processed further. The pH of the supernatant was adjusted to 6.0 with 6 M HCl, followed by dilution to a conductivity of 5 mS/cm with purified water. The conditioned supernatant was loaded onto a BakerBond ABx ion-exchange column. Following a wash with the column equilibration buffer, the Fab was eluted with an increasing sodium chloride gradient in the equilibration buffer. Fractions containing the Fab were identified by SDS-PAGE. The BakerBond ABx column fractions were pooled, pH adjusted to 5.5 with 1 M Mes and diluted to a conductivity of 5 mS/cm with purified water. The conditioned BakerBond ABx pool was loaded onto a SP Sepharose HP cation exchange column (Pharmacia). Once again, the Fab was eluted with a sodium chloride-containing gradient. Fractions containing the Fab were identified by SDS-PAGE. The level of purity of Fab (as determined by SDS-PAGE) after this two column purification was >95%.

BIAcore™ binding analysis

The VEGF-binding affinities of Fab fragments were calculated from association and dissociation rate constants measured using a BIAcore™ -2000 surface plasmon resonance system (BIAcore, Inc., Piscataway, NJ). A biosensor chip was activated for covalent coupling of VEGF using *N*-ethyl-*N'*-(3-dimethylaminopropyl)-carbodiimide hydrochloride (EDC) and *N*-hydroxysuccinimide (NHS) according to the supplier's (BIAcore, Inc., Piscataway, NJ) instructions. VEGF(109) or VEGF(165) was buffer-exchanged into 20 mM sodium acetate, pH 4.8 and diluted to approximately 50 μg/ml. Aliquots of VEGF were injected at a flow rate of 2 μl/minute to achieve approximately 700-1400 response units (RU) of coupled protein. A solution of 1 M ethanolamine was injected as a blocking agent.

For kinetics measurements, twofold serial dilutions of Fab were injected in PBS/Tween buffer (0.05% Tween-20 in phosphate-buffered saline) at 25 °C or 37 °C at a flow rate of 10 μl/minute. Equilibrium dissociation constants, K_d values from SPR measurements were calculated as k_{off}/k_{on} (Tables 6 and 8).

Radiolabeled VEGF binding assay

Solution binding affinity of Fabs for VEGF was measured by equilibrating Fab with a minimal concentration of (^{125}I)-labeled VEGF(109) in the presence of a titration series of unlabeled VEGF, then capturing bound VEGF with an anti-Fab antibody-coated plate.

To establish conditions for the assay, microtiter plates (Dynex) were coated overnight with 5 μg/ml of a capturing anti-Fab antibody (Cappel Labs) in 50 mM sodium carbonate (pH 9.6), and subsequently blocked with 2% (w/v) bovine serum albumin in PBS for two to five hours at room temperature (approximately 23 °C). In a non-adsorbant plate (Nunc #269620), 100 pM or 26 pM [^{125}I]VEGF(109) was mixed with serial dilutions of Fab-12 or Fab Y0317, respectively. Fab-12 was incubated overnight; however, the Fab Y0317 incubation was continued for 65 hours to insure that equilibrium was reached. Thereafter, the mixtures were transferred to the capture plate for incubation at room temperature for one hour. The solution was then removed and the plate washed eight times with 0.1% Tween-20 in PBS. When the plates had dried, 150 μl/well of scintillant (MicroScint-20; Packard) was added, and the plates were counted on a Topcount gamma counter (Packard) for ten minutes. Concentrations of each Fab were chosen to give ≤20% of maximal binding.

For competitive binding assays, Dynex plates were coated and blocked as above, and serial threefold dilutions of unlabeled VEGF(109) were made in PBS/Tween buffer in a Nunc plate. [^{125}I]VEGF(109) was added, followed by addition of a fixed concentration of Fab-12 or Fab Y0317. The final concentrations of Fab-12, and Fab Y0317 were 100 pM and 10 pM, respectively. After incubation (as above), bound VEGF was captured and quantified as described above. The binding data was analyzed using a computer program to perform Scatchard analysis (Munson & Rodbard, 1980) for determination of the dissociation binding constants, K_d, for Fab-12 and Fab Y0317.

ELISA assay of VEGF Ala mutants

The binding affinities of VEGF Ala mutants for full-length Fab-12-IgG (known as rhuMAb VEGF) and Y0317-IgG, a full-length IgG form of the improved antibody expressed in CHO cells (V. Chisholm, unpublished results) were measured as previously described (Muller *et al.*, 1997; Muller *et al.*, 1998a) for the murine antibody A4.6.1, except that the temperature was increased to 37 °C, and the incubation time increased to five hours, to insure that equilibrium was reached with the high-affinity antibody.

Cell-based assay of VEGF inhibition

Several versions of the anti-VEGF antibody were tested for their ability to antagonize VEGF(165) induction of the growth of HuVECs (human umbilical vein endothelial cells). The 96-well plates were seeded with 1000 HuVECs per well and fasted in assay medium (F12:DMEM 50:50 supplemented with 1.5% (v/v) dia-filtered fetal bovine serum) for 24 hours.

The concentration of VEGF used for inducing the cells was determined by first titrating to identify the amount of VEGF that can stimulate 80% of maximal DNA synthesis. Fresh assay medium containing fixed amounts of VEGF (0.2 nM final concentration), and increasing concentrations of anti-VEGF Fab or mab were then added. After 40 hours of incubation, DNA synthesis was measured by incorporation of tritiated thymidine. Cells were pulsed with 0.5 μCi per well of [^{3}H]thymidine for 24 hours and harvested for counting, using a TopCount gamma counter.

Crystallization and refinement

The complex between the Fab fragment of affinity-matured, humanized antibody Y0317 Fab and the receptor binding fragment of VEGF (VEGF(109)) was purified and crystallized as described for the analogous complex with the parental humanized Fab-12 fragment (Muller *et al.*, 1998a). The resulting crystals had symmetry consistent with space group $P2_1$ with cell parameters $a = 89.1$ Å, $b = 66.4$ Å, $c = 138.7$ Å, and $\beta = 94.7°$, and were isomorphous with the crystals obtained with the parent complex. A data set was collected from a single frozen crystal at beam line 5.0.2 at the Advanced Light Source, Berkeley, and processed using programs MOSFLM and SCALA (CCP4, 1994). The final data set (R_{merge} = 7.3%) is described in Table 10. Starting with the model of Brookhaven Protein Data Bank entry 1bj1 (Muller *et al.*, 1998a), the structure was refined using the programs X-PLOR (Brünger *et al.*, 1987) and REFMAC (CCP4, 1994). The free *R*-value was monitored using the identical set of reflections sequestered before refinement of parent complex. The differences in the primary structure between Fab-12 and Fab-Y0317 were modeled using the program O (Jones *et al.*, 1991). After correction for anisotropy and application of a bulk solvent correction, the *R*-value reached its final value of 19.9% for all reflections greater than 0.2σ (see Table 10; R_{free} = 27.4%).

Table 10. Crystallographic data and refinement statistics

A. *Data collection*	Overall	Last shell
Resolution range (Å)	30-2.4	2.53-2.40
No. of observations	208,257	22,278
Unique reflections	61,742	8900
Completeness (%)	97.4	96.7
Mean $I/\sigma(I)$	13.6	2.7
R_{sym}	0.073	0.38
B. *Refinement*		
Resolution range (Å)	20-2.4	
No. of reflections	61,689	
No. of atoms	8577	
rmsd bond lengths (Å)	0.013	
rmsd angles (deg.)	1.9	
rmsd improper angles (deg.)	0.92	
rmsd *B*-factors for all bonded atoms, Å^2	3.5	
Number of main-chain torsion angles in disallowed regions of Ramachandran plot[a]	2	

[a] See Laskowski *et al.* (1993).

Protein Data Bank accession number

The coordinates for the VEGF:Y0317 Fab complex have been deposited in the Protein Data Bank, accession number 1cz8.

Acknowledgments

We thank Lyn Deguzman and Tom Zioncheck for providing ^{125}[I]VEGF; Alan Padua and Bill Henzel for quantitative amino acid analysis; James Bourell for mass spectrometry; Vanessa Chisholm and Lynne Krummen for construction of cell lines; and Manuel Baca, Napoleone Ferrara, Yves Muller, Leonard Presta, and James Wells for many helpful discussions.

References

Baca, M., Presta, L. G., O'Connor, S. J. & Wells, J. A. (1997). Antibody humanization using monovalent phage display. *J. Biol. Chem.* **272**, 10678-10684.

Barbas, C. F., III, Hu, D., Dunlop, N., Sawyer, L., Cababa, D., Hendry, R. M., Nara, P. L. & Burton, D. R. (1994). *In vitro* evolution of a neutralizing human antibody to human immunodeficiency virus type 1 to enhance affinity and broaden strain cross-reactivity. *Proc. Natl Acad. Sci. USA*, **91**, 3809-3813.

Bass, S., Greene, R. & Wells, J. A. (1990). Hormone phage: an enrichment method for variant proteins with altered binding properties. *Proteins: Struct. Funct. Genet.* **8**, 309-314.

Brünger, A. T., Kuriyan, J. & Karplus, M. (1987). Crystallographic *R* factor refinement by molecular dynamics. *Science*, **235**, 458-460.

CCP4 (1994). Programs for protein crystallography. *Acta Crystallog. sect. D*, **50**, 760-763.

Chothia, C. & Lesk, A. M. (1987). Canonical structures for the hypervariable reigions of immunoglobulins. *J. Mol. Biol.* **196**, 901-917.

Delisi, C. (1983). Role of diffusion regulation in receptor-ligand interactions. *Methods Enzymol.* **93**, 95-109.

Fairbrother, W. J., Christinger, H. W., Cochran, A. G., Fuh, G., Keenan, C. J., Quan, C., Shriver, S. K., Tom, J. Y., Wells, J. A. & Cunningham, B. C. (1998). Novel peptides selected to bind vascular endothelial growth factor target the receptor-binding site. *Biochemistry*, **37**, 17754-17764.

Ferrara, N. (1995). The role of vascular endothelial growth factor in pathological angiogenesis. *Breast Cancer Res. Treat.* **36**, 127-137.

Ferrara, N. (1999). Vascular endothelial growth factor: molecular and biological aspects. *Curr. Top. Microbiol. Immunol.* **237**, 1-30.

Ferrara, N. & Henzel, W. J. (1989). Pituitary follicular cells secrete a novel heparin-binding growth factor specific for vascular endothelial cells. *Biochem. Biophys. Res. Commun.* **161**, 851-858.

Folkman, J. (1995). Angiogenesis in cancer, vascular, rheumatoid and other disease. *Nature Med.* **1**, 27-31.

Folkman, J. & Klagsbrun, M. (1987). Angiogenic factors. *Science*, **235**, 442-443.

Foote, J. & Winter, G. (1992). Antibody framework residues affecting the conformation of the hypervariable loops. *J. Mol. Biol.* **224**, 487-499.

Gitay-Goren, H., Soker, S., Vlodavsky, I. & Neufeld, G. (1992). The binding of vascular endothelial growth factor to its receptors is dependent on cell-surface-associated heparin-like molecules. *J. Biol. Chem.* **267**, 6093-6098.

Griffiths, A. D. & Duncan, A. R. (1998). Strategies for selection of antibodies by phage display. *Curr. Opin. Biotechnol.* **9**, 102-108.

Hawkins, R. E., Russell, S. J. & Winter, G. (1992). Selection of phage antibodies by binding affinity mimicking affinity maturation. *J. Mol. Biol.* **226**, 889-896.

Hawkins, R. E., Russell, S. J., Baier, M. & Winter, G. (1993). The contribution of contact and non-contact residues of antibody in the affinity of binding to antigen. *J. Mol. Biol.* **234**, 958-964.

Iruela-Arispe, M. L. & Dvorak, H. F. (1997). Angiogenesis: a dynamic balance of stimulators and inhibitors. *Thromb. Haem.* **78**, 672-677.

Jones, T. A., Zhou, J.-Y., Cowan, S. W. & Kjelgaard, M. (1991). Improved methods for building protein models in electron density maps and the location of errors in these models. *Acta Crystallog. sect. A*, **47**, 110-119.

Kabat, E. A., Wu, T. T., Redi-Miller, M., Perry, H. M. & Gottesman, K. S. (1987). *Sequences of Proteins of Immunological Interest*, 4th edit., National Institutes of Health, Bethesda, MD.

Karlsson, R., Michaelsson, A. & Mattsson, L. (1991). Kinetic analysis of monoclonal antibody-antigen interactions with a new biosensor based analytical system. *J. Immunol. Methods*, **145**, 229-240.

Kay, B. K. & Hoess, R. H. (1996). Principles and applications of phage display. In *Phage Display of Peptides and Proteins* (Kay, B. K., Winter, J. & McCafferty, J., eds), pp. 21-34, Academic Press, San Diego.

Kim, K. J., Li, B., Winer, J., Armanini, M., Gillett, N., Phillips, H. S. & Ferrara, N. (1993). Inhibition of vascular endothelial growth factor-induced angiogenesis suppresses tumour growth *in vivo*. *Nature*, **362**, 841-844.

Kraft, A., Weindel, K., Ochs, A., Marth, C., Zmija, J., Schumacher, P., Unger, C., Marmé, D. & Gastl, G. (1999). Vascular endothelial growth factor in the sera and effusions of patients with malignant and nonmalignant disease. *Cancer*, **85**, 178-187.

Kunkel, T. A., Bebenek, K. & McClary, J. (1991). Efficient site-directed mutagenesis using uracil-containing DNA. *Methods Enzymol.* **204**, 125-139.

Küttner, G., Keitel, T., Gießmann, E., Wessner, H., Scholz, C. & Höhne, W. (1998). A phage library-derived single-chain Fv fragment in complex with turkey egg-white lysozyme: characterization, crystallization and preliminary X-ray analysis. *Mol. Immunol.* **35**, 189-194.

Laskowski, R. A., MacArthur, M. W., Moss, D. S. & Thornton, J. M. (1993). Procheck: a program to check the stereochemical quality of protein structures. *J. Appl. Crystallog.* **26**, 283-291.

Lowman, H. B. (1998). Phage display of peptide libraries on protein scaffolds. In *Methods in Molecular Biology, Combinatorial Peptide Library Protocols* (Cabilly, S., ed.), vol. 87, pp. 249-264, Humana Press, Totowa, NJ.

Lowman, H. B. & Wells, J. A. (1993). Affinity maturation of human growth hormone by monovalent phage display. *J. Mol. Biol.* **234**, 564-578.

Lowman, H. B., Bass, S. H., Simpson, N. & Wells, J. A. (1991). Selecting high-affinity binding proteins by monovalent phage display. *Biochemistry*, **30**, 10832-10838.

Malmborg, A.-C., Michaelsson, A., Ohlin, M., Jansson, B. & Borrebaeck, C. A. K. (1992). Real time analysis of antibody-antigen reaction kinetics. *Scan. J. Immunol.* **35**, 643-650.

Marks, J. D., Griffiths, A. D., Malmqvist, M., Clackson, T. P., Bye, J. M. & Winter, G. (1992). By-passing immunization: building high affinity human antibodies by chain shuffling. *Biotechnology*, **10**, 779-783.

Mordenti, J., Thomsen, K., Licko, V., Chen, H., Meng, Y. G. & Ferrara, N. (1999). Efficacy and concentration-response of murine anti-VEGF monoclonal antibody in tumor-bearing mice and extrapolation to humans. *Toxicol. Pathol.* **27**, 14-21.

Muller, Y. A., Li, B., Christinger, H. W., Wells, J. A., Cunningham, B. C. & de Vos, A. M. (1997). Vascular endothelial growth factor: crystal structure and functional mapping of the kinase domain receptor binding site. *Proc. Natl Acad. Sci. USA*, **94**, 7192-7197.

Muller, Y. A., Chen, Y., Christinger, H. W., Li, B., Cunningham, B. C., Lowman, H. B. & de Vos, A. M. (1998a). VEGF and the Fab fragment of a humanized neutralizing antibody: crystal structure of the complex at 2.4 Å resolution and mutational analysis of the interface. *Structure*, **6**, 1153-1167.

Muller, Y. A., Christinger, H. W., Keyt, B. A. & de Vos, A. M. (1998b). The crystal structure of vascular endothelial growth factor (VEGF) refined to 1.93 Å resolution: multiple copy flexibility and receptor binding. *Structure*, **5**, 1325-1338.

Munson, P. & Rodbard, D. (1980). Ligand: a versatile computerized approach for characterization of ligand-binding systems. *Anal. Biochem.* **107**, 220-239.

Nezlin, R. (1998). *The Immunoglobulins: Structure and Function*, pp. 151-204, Academic Press, San Diego.

Presta, L. G., Chen, H., O'Connor, S. J., Chisholm, V., Meng, Y. G., Krummen, L., Winkler, M. & Ferrara, N. (1997). Humanization of a vascular endothelial growth factor monoclonal antibody for the therapy of solid tumors and other disorders. *Cancer Res.* **47**, 4593-4599.

Rader, C. & Barbas, C. F., III (1997). Phage display of combinatorial antibody libraries. *Curr. Opin. Biotechnol.* **8**, 503-508.

Schier, R., McCall, A., Adams, G. P., Marshall, K. W., Merritt, H., Yim, M., Crawford, R. S., Weiner, L. M., Marks, C. & Marks, J. D. (1996). Isolation of picomolar affinity anti-c-erbB-2 single-chain Fv by molecular evolution of the complementarity

determining regions in the center of the antibody binding site. *J. Mol. Biol.* **263**, 551-567.

Thompson, J., Pope, T., Tung, J.-S., Chan, C., Hollis, G., Mark, G. & Johnson, K. S. (1996). Affinity maturation of a high-affinity human monoclonal antibody against the third hypervariable loop of human immunodeficiency virus: use of phage display to improve affinity and broaden strain reactivity. *J. Mol. Biol.* **16**, 77-88.

Tramontano, A., Chothia, C. & Lesk, A. M. (1990). Framework residue 71 is a major determinant of the position and conformation of the second hypervariable region in the VH domains of immunoglobulins. *J. Mol. Biol.* **215**, 175-182.

Wells, J. A. (1990). Additivity of mutational effects in proteins. *Biochemistry*, **29**, 8509-8517.

Wu, H., Beuerlein, G., Nie, Y., Smith, H., Lee, B. A., Hensler, M., Huse, W. D. & Watkins, J. D. (1998). Stepwise *in vitro* affinity maturation of vitaxin, an $\alpha_V\beta_3$-specific humanized mAb. *Proc. Natl Acad. Sci. USA*, **95**, 6037-6042.

Xiang, J., Sha, Y., Jia, Z., Prasad, L. & Delbaere, L. T. (1995). Framework residues 71 and 93 of the chimeric B72.3 antibody are major determinants of the conformation of heavy-chain hypervariable loops. *J. Mol. Biol.* **253**, 385-390.

Yang, W.-P., Green, K., Pinz-Sweeney, S., Briones, A. T., Burton, D. R. & Barbas, C. F., III (1995). CDR walking mutagenesis for the affinity maturation of a potent human anti-HIV-1 antibody into the picomolar range. *J. Mol. Biol.* **254**, 392-403.

Edited by I. A. Wilson

(Received 19 July 1999; received in revised form 7 September 1999; accepted 13 September 1999)

THE JOURNAL OF BIOLOGICAL CHEMISTRY
Vol. 272, No. 19, Issue of May 9, pp. 12430–12436, 1997
Printed in U.S.A.

Identification of Framework Residues in a Secreted Recombinant Antibody Fragment That Control Production Level and Localization in *Escherichia coli**

(Received for publication, December 19, 1996)

Göran Forsberg‡§¶, Margareta Forsgren‡, Maria Jaki‡, Martin Norin‡, Catharina Sterky‡, Åsa Enhörning‡, Kerstin Larsson‡, Monica Ericsson‡, and Per Björk§

From the ‡Department of Biology and Biotechnology, Pharmacia and Upjohn, 112 87 Stockholm, Sweden and §Lund Research Centre, Pharmacia and Upjohn, Box 724, 220 07 Lund, Sweden

The monoclonal antibody 5T4, directed against a human tumor-associated antigen, was expressed as a secreted Fab superantigen fusion protein in *Escherichia coli*. The product is a putative agent for immunotherapy of non-small cell lung cancer. During fermentation, most of the fusion protein leaked out from the periplasm to the growth medium at a level of approximately 40 mg/liter. This level was notably low compared with similar products containing identical C_H1, C_L, and superantigen moieties, and the Fv framework was therefore engineered. Using hybrid molecules, the light chain was found to limit high expression levels. Substituting five residues in V_L increased the level almost 15 times, exceeding 500 mg/liter in the growth medium. Here, the substitutions Phe-10 → Ser, Thr-45 → Lys, Thr-77 → Ser, and Leu-78 → Val were most powerful. In addition, replacing four V_H residues diminished cell lysis during fermentation. Thereby the product was preferentially located in the periplasm instead of the growth medium, and the total yield was more than 700 mg/liter. All engineered products retained a high affinity for the tumor-associated antigen. It is suggested that at least some of the identified framework residues generally have to be replaced to obtain high level production of recombinant Fab products in *E. coli*.

Antibody-based therapies are currently evaluated for treatment of several severe diseases such as cancer (1), viral infections, and autoimmunity. Recent technological improvements have made it possible to clone and produce large amounts of intact recombinant monoclonal antibodies or antibody fragments (2, 3). Using phage display technologies, high affinity antibodies can be obtained without prior immunization (4, 5). For production purposes *Escherichia coli* is a very useful host (reviewed in Ref. 6). Correctly folded Fab has been secreted at levels exceeding 1 g/liter (7) and single chain Fv molecules at slightly lower levels (8). Systems involving inclusion body formation and *in vitro* refolding have also been described (9, 10). Consequently, there are effective tools to obtain both these molecules and a variety of clinical applications.

Recently, a concept for cancer therapy using recombinant fusion proteins of tumor-reactive Fab fragment and immunostimulatory bacterial superantigens was presented (11, 12). Superantigens, such as the staphylococcal enterotoxin A (SEA),[1] activate cytotoxic and cytokine-producing T-lymphocytes. Antibody-targeted SEA can initiate a powerful T cell attack against tumor cells *in vivo* (12, 13).

Here *E. coli* production of the 5T4Fab-moiety fused to a genetically engineered superantigen chimera (14),[2] 5T4Fab-SEch, is investigated. The murine antibody 5T4 is directed against a trophoblast-related antigen found on several solid tumor types including carcinomas in lung, breast, colon, and ovary (16, 17). The 5T4Fab-SEch has a high affinity for the antigen and targets T cells to several cancer cell lines. However, when produced as a secreted fusion protein in *E. coli*, the production level is 5–10-fold lower compared with several similar products. To investigate the molecular components behind this phenomenon, several amino acid residues in the Fv framework were altered. Significantly, by replacing only a few light chain residues the level of active product increased, while heavy chain substitutions affected the product distribution between growth medium and periplasmic space.

EXPERIMENTAL PROCEDURES

Materials—Restriction endonucleases and *Taq* polymerase were from Boehringer Mannheim or New England Biolabs (Beverly, MA). The recombinant work was carried out mainly as described (18) in the *E. coli* strain HB101. Plasmid preparation was performed with Wizard® Midipreps DNA purification system (Promega, Madison, WI) from bacteria grown in LB medium with 50 μg/ml kanamycin. Oligonucleotides were synthesized on an ABI 392 DNA/RNA synthesizer (Applied Biosystems, Foster City, CA). Antibodies against murine κ chain were obtained from Bio-Zac (Stockholm, Sweden) and horseradish peroxidase-conjugated antibodies against SEA from Toxin Technology (Sarasota, FL).

Cloning, Engineering, and Insertion into an E. coli Expression Vector of 5T4 Fv—The Fv-encoding portions of 5T4 were cloned from the 5T4 hybridoma obtained from Dr. Peter Stern (CRCT, Paterson Inst. for Cancer Research, Manchester, UK). The cDNA was made from total RNA using the GeneAmp RNA PCR kit (Perkin-Elmer). The coding regions of the entire variable domains and parts of the signal sequences as well as the constant domains of the heavy and light chains were amplified by PCR. All PCR products and DNA linkers were sequenced on an ABI 373A DNA sequencer (Applied Biosystems) as recommended by the supplier. The oligonucleotides 5′-CAATTTTCTTGTCCACCTTGGTGC-3′ and 5′-ACTAGTCGACATGGGATGGAGCTITATCATI(C/T)TCTT-3′ were used for the heavy chain resulting in a 553-base pair fragment, while 5′-ACTAGTCGACATGGGCITCAAGATGGAGTCACA(G/T)(A/T)(C/T)(C/T)C(A/T)GG-3′ and 5′-GCGCCGTCTAGAATTAACACTCATTCCTGTTGAA-3′ were used for the light chain yielding a 724-base pair fragment. For each chain three separate clones were

* The costs of publication of this article were defrayed in part by the payment of page charges. This article must therefore be hereby marked "*advertisement*" in accordance with 18 U.S.C. Section 1734 solely to indicate this fact.

¶ To whom correspondence should be addressed. Tel.: 46-46-19-11-54; Fax: 46-46-19-11-34; E-mail: goran.forsberg@eu.pnu.com.

[1] The abbreviations used are: SEA, staphylococcal enterotoxin A; PCR, polymerase chain reaction; SEch, staphylococcal enterotoxin chimera; IPTG, isopropyl-β-D-thiogalactopyranoside; HPLC, high pressure liquid chromatography; CDR, complementarity-determining region.

[2] Antonsson, P., Gjörloff Wingren, A., Hansson, J., Kalland, T., Varga, M., and Dohlsten, M. (1997) *J. Immunol.*, in press.

sequenced and found to be identical. DNA fragments suitable for insertion into the expression vector (12) were obtained in a second PCR step. To assemble a Fab-expression plasmid, the variable regions of 5T4 were fused to sequences coding for the constant regions of the murine IgG1/k antibody C242 (12) and lacking the interchain disulfide bond. A region coding for a hybrid between SEA and staphylococcal enterotoxin E, SEA/E-BDEG,[2] with the substitution Asp-227 → Ala in the major histocompatibility complex II binding site (14), was connected to the C terminus of the heavy chain via a Gly-Gly-Pro linker. The 5T4 Fv sequence is shown in Fig. 1. All 5T4 mutants were made as one-chain constructs and combined with the partner chain in the expression plasmid. The point mutations coding for Phe-10 → Ser, Ile-63 → Ser, and Tyr-67 → Ser, as well as the heavy chain mutations were introduced by PCR while Thr-45 → Lys, Phe-73 → Leu, Thr-77 → Ser, Leu-78 → Val, and Leu-83 → Ala used synthesized oligonucleotide linkers. Gene segments containing the various point mutations were also combined (Table I). All constructs were verified by DNA sequencing.

Expression of 5T4Fab-SEch in the Fermenter—The products were expressed in the *E. coli* K-12 strain UL 635 (*xyl*-7, *ara*-14, $T4^R$, Δ*ompT*) using a plasmid with a kanamycin resistance gene and lacUV5 promoter. Bacteria from frozen stock were incubated at 25 °C for approximately 21 h in shaker flasks containing (per liter) 2.5 g of $(NH_4)_2SO_4$, 4.45 g of KH_2PO_4, 11.85 g of K_2HPO_4, 0.5 g of sodium citrate, 1 g of $MgSO_4 \cdot 7H_2O$, 11 g of glucose monohydrate, 0.11 mM kanamycin, and 1 ml of trace element solution (19), however, without $Na_2MoO_4 \cdot 2H_2O$. The cells were grown to an A_{600} of 1–2, and 450 ml of culture medium was used to inoculate a fermenter (Chemap, Switzerland) to a final volume of 5 liters. The fermenter medium contained (per liter) 2.5 g of $(NH_4)_2SO_4$, 9 g of KH_2PO_4, 6 g of K_2HPO_4, 0.5 g of sodium citrate, 22 g of glucose monohydrate, 1 g of $MgSO_4 \cdot 7H_2O$, 0.11 mM kanamycin, 1 ml of a decanol (Asahi Denka Kogyo K.K., Japan), and 1 ml of trace element solution. The pH was kept at 7.0 by titration with 25% ammonia; the temperature was 25 °C and aeration was 5 liters/min. The partial pressure of dissolved O_2 was controlled to 30% by increasing agitation from 300 to 1000 rpm during batch phase and regulating the feed of 60% (w/v) glucose during fed batch phase. Product formation was induced at an A_{600} of 50 by adding 0.1 mM isopropyl-β-D-thiogalactopyranoside (IPTG). After fermentation the cells were removed by centrifugation at 8000 × *g* for 40 min at 4 °C. The clarified medium was either analyzed and purified directly or stored at −70 °C.

Purification Procedures—DNA present in the clarified medium was removed using precipitation with 0.19% polyethylenimine and 0.2 M NaCl for 30 min (20). After centrifugation as above, the supernatant was collected, and the NaCl concentration was adjusted to 0.5 M. This medium was applied to a protein G-Sepharose column (Pharmacia Biotech Inc.) equilibrated with 0.1 M sodium citrate, pH 6.0, containing 0.05% Tween 80. The column was washed with 1.5–2 column volumes of 0.1 M sodium citrate, pH 6.0, 0.05% Tween 80, 7.5 column volumes of 20 mM citric acid, 1 mM EDTA, 200 mM NaCl, 0.05% Tween 80, pH 4.7, and bound protein was eluted with 0.1 M acetic acid and 0.05% Tween 80. The pH of the sample was adjusted to 5.0 using 0.5 M sodium citrate, pH 7.5, diluted to a conductivity of 4.7 millisiemens/cm, applied to an SP-Sepharose HP column (Pharmacia), and equilibrated with 60 mM sodium acetate, pH 5.0, and 0.02% Tween 80. The column was then washed with 7.5 column volumes of equilibration buffer, and the fusion protein was eluted using a linear gradient from 60 to 350 mM sodium acetate over 13 column volumes.

Analytical Procedures—Cell extracts were prepared from 10 ml of freeze-thawed cell suspension containing both growth medium and cells. The samples were sonicated on an ice bed at an amplitude control of 35% for 3 min using a 3-mm probe, pulsing 70% of the time (VCX .600, Sonics & Materials Inc., Danbury, CT). After sonication, the samples were centrifuged at 8000 × *g* for 40 min, and the supernatants were analyzed. Product levels were measured in a sandwich enzyme-linked immunosorbent assay detecting assembled heterodimeric fusion protein. The wells were coated with antibodies directed against murine light chains, and full-length fusion protein was detected using horseradish peroxidase-conjugated antibodies against SEA. Standard curves were obtained for respective variant fusion proteins. After cell separation, DNA levels in the culture broth were measured using a DynaQuant 200 minifluorometer (Hoefer Scientific, San Francisco, CA) as recommended by the supplier.

Reverse phase HPLC was carried out on an AsahiPak ODP-50 column (4 × 250 mm) (Hewlett-Packard, Palo Alto, CA) using a linear gradient from 30 to 40% acetonitrile in 0.1% trifluoroacetic acid for 40 min and a flow rate of 1 ml/min at 60 °C. Absorbance was measured at 215 nm using a diode array detector (Hewlett-Packard). SDS-polyacrylamide gel electrophoresis was performed on precast Tris/glycine gels (NOVEX, San Diego, CA) containing 12% polyacrylamide. The products were analyzed as both reduced and non-reduced samples using the methods recommended by the supplier. Isoelectric focusing was performed on precast gels (Servalyt® Precotes®, Serva, Heidelberg, Federal Republic of Germany) with a pH working range from 3 to 10 using the methods recommended by the supplier. Mass spectrometry was carried out on a MALDI-TOF MS (Hewlett-Packard), and amino acid analysis was performed using a Beckman 6300 essentially as described (19).

Cytotoxicity Assay—Cytotoxicity was measured in a ^{51}Cr release assay after 4 h using the 5T4 antigen-positive Colo205 cultured in complete tissue culture medium (21) as target cells and human SEA-reactive T cell lines (12) at an effector to target ratio of 30:1. ^{51}Cr-labeled target cells were used in the assay at 2500 cells/200 μl of tissue culture medium in V-bottomed microtiter wells. 5T4Fab-SEch fusion proteins were added at various concentrations, and ^{51}Cr release was measured in a γ-counter. Specific cytotoxicity was calculated as 100 × [(cpm experimental release − cpm background release)/(cpm maximal release − cpm background release)].

Determination of Antigen Binding Characteristics—The human cancer cell lines Calu-1 (ATCC HTB 54) and ME-180 (ATCC HTB 33), both expressing high levels of 5T4 antigen as demonstrated by fluorescence-activated cell sorter staining, were cultivated in tissue culture medium as above. Adhered cells were detached from the flasks using non-enzymatic cell dissociation solution (Sigma), washed twice in a CO_2 independent medium without L-glutamine (Life Technologies, Inc.) containing 10% fetal calf serum, and finally suspended in that medium at a density of 6 × 10^5 cells/ml.

The 5T4Fab-SEch was radiolabeled with the lactoperoxidase technique using Enzymobeads (DuPont NEN). The reaction was stopped with 0.05% NaN_3, and the labeled protein was desalted by gel filtration (PD-10, Pharmacia) using culture medium as elution buffer. Conditions were chosen to obtain a ratio of iodine to protein of ≤2:1.

In a direct binding assay, 3 × 10^4 cells in 50 μl of solution were mixed with 50 μl of serially diluted radioiodinated fusion protein in a conical polypropylene tube in triplicate and incubated for 2 h at room temperature with intermittent mixing. Each tube was washed three times using 3 ml of phosphate-buffered saline containing 1% fetal calf serum, which was removed by centrifugation for 5 min at 600 × *g*. After the final wash, cell-bound radioactivity was determined in a γ-counter. The apparent dissociation constant and number of binding sites at saturation were calculated (22) after subtraction of nonspecific binding (*i.e.* binding after incubation in the absence of cells). This method was modified to an inhibition assay. Here serially diluted fusion proteins competed with wild-type ^{125}I-5T4Fab-SEch at a concentration corresponding to the K_d value determined in the direct assay. The concentration yielding half-maximum inhibition, IC_{50}, was determined after linear regression of log-logit transformed binding data, and the relative affinity index was determined as the ratio between the IC_{50} values of competitor and wild-type 5T4Fab-SEch.

Computer Modeling of the 5T4Fab Variable Region—The individual 5T4 V_H and V_L domains were built by homology modeling to known structures using the COMPOSER module in SYBYL 6.22 (Molecular modeling program SYBYL 6.22, Tripos Associates, St Louis, MO). A family of structurally homologous molecules with sequence identities of at least 60% to the modeled chains were used as templates. For the heavy chain, 7 immunoglobulin fragments were selected, while for the light chain, 22 fragments were used. The structurally conserved regions were built by averaging the template structures according to the COMPOSER algorithm. The remaining LOOP regions were built using template loop fragments found among Fab fragments in the protein structure data base of COMPOSER. The individual V_H and V_L domains were docked to each other to form the Fv fragments. A structural alignment between the individual V_H and V_L chains and the crystallographic structure of a murine Fab, entry 1MCP in the Protein Data Bank (23), was made using the ALIGN procedure of the ICM program (24). Finally, hydrogen atoms were added, and the structure was refined by a regularization procedure in the ICM algorithm (24).

RESULTS

Cloning and Expression of Recombinant 5T4Fab-SEch Constructs—The variable regions of the antibody 5T4 were cloned using PCR and introduced into an expression vector (12) coding for a Fab product with a superantigen linked to the C terminus of the heavy chain. The plasmid was transformed into an *ompT* strain of *E. coli*, UL635, and expression of the recombinant product was induced with IPTG. The product was secreted as

TABLE I

Biochemical and immunological characterization of the different fusion proteins studied

Using an enzyme-linked immunosorbent assay method the level in the growth medium and total yield in a sonicated mixture of growth medium and bacteria were determined. The IC_{50} values were obtained from affinity measurements to 5T4 antigen-positive cells, and the biological activity was determined using a cytotoxicity assay. The variants of the 5T4 heavy chain contain the following substitutions: H41P, S44G, I69T, and V113G (mutant 1 (m1)) and H41P, S44G, and V113G (mutant 2 (m2)).

Variant	Light chain replacements								Heavy chain	Yield		IC_{50}	Activity
	F10S	T45K	I63S	Y67S	F73L	T77S	L78V	L83A		Medium	Total		
										mg/liter		*nM*	%
wt									5T4	39	48	1.5	100
V1									C215	39	59	ND[a]	0
V2	C215-κ								5T4	224	297	1000	0
V3	X[b]								5T4	92	126	1.2	100
V4			X	X					5T4	39	52		
V5	X		X	X					5T4	93	136	2.9	100
V6					X				5T4	39	44		
V7						X			5T4	57	86		
V8							X		5T4	53	77		
V9								X	5T4	53	86	1.6	100
V10	X	X	X	X					5T4	214	250	2.6	100
V11	X	X			X	X	X		5T4	586	701		
V12	X		X	X	X	X	X		5T4	512	470	2.0	100
V13	X	X	X	X	X	X	X		5T4	578	560	1.4	100
V14	X	X	X	X	X	X			5T4 (m1)	288	730	1.9	100
V15	C215κ								5T4 (m2)	250	560		
V16			X	X	C215-(1–23)-5T4				5T4	110	124	5.4	100

[a] ND, not detected.

[b] X, substitution introduced in the respective variant.

two separate polypeptide chains that assembled to a heterodimeric product in the *E. coli* periplasm. During fermentation, a significant amount of the two-chain product is excreted to the growth medium and usually connected by a significant cell lysis. Normally the levels of Fab superantigen products range from 100 to 400 mg/liter in the growth medium (data not shown). However, for 5T4Fab-SEch the production level was around 40 mg/liter in the growth medium and less than 10 mg/liter in the periplasm, as determined with enzyme-linked immunosorbent assay (Table I). To increase the yield, several parameters in the fermentation procedure were varied such as time point and level of induction, temperature, and medium composition, but no further improvement in production level was achieved.

Construction and Investigation of Hybrid Molecules between 5T4-SEch and C215Fab-SEch—To determine whether one of the two polypeptide chains dominated the production problem, hybrid molecules of 5T4Fab-SEch and C215Fab-SEch were made. C215 is a murine antibody recognizing a colon cancer epitope (25), and fusion proteins between C215Fab and SEA-based superantigens are normally secreted at levels up to 400 mg/liter in *E. coli*. Fermentation of variant V1 with the 5T4 light and C215 heavy chain yielded 39 mg/liter product in the growth medium, while variant V2 with C215 light and 5T4 heavy chain yielded 224 mg/liter (Table I). For V1 and V2, most of the product was found in the growth medium instead of the periplasm (Table I). Hence, replacing the heavy chain of 5T4 did not affect the low production level, while replacement of the light chain resulted in a more than 5-fold increase.

One further observation was made during fermentation. For the 5T4 wild-type construct, as well as variant V2 that contained the C215 light chain, the A_{600} started to decline and the cell viability decreased more than 10-fold within a few hours after induction (Fig. 3), followed by an increased DNA level in the growth medium. The variant V1 that contained the C215 heavy chain behaved differently. The amount of viable *E. coli* cells was more than 10-fold higher for V1 than for V2 with 5T4 heavy chain when fermentation was terminated. In addition, the final cell density was much higher (Fig. 3).

The fusion proteins were purified using protein G affinity and then ion exchange chromatography to remove degraded forms. The purified products were analyzed with SDS-polyacrylamide gel electrophoresis, reverse phase HPLC, mass spectrometry, isoelectric focusing, and amino acid analysis. The latter technique was also used to determine protein concentrations. All of these assays indicated that the main product contained and constituted 85–95% of the expected characteristics. However, both products showed a strongly reduced affinity for the 5T4 antigen (16), and only variant V2 with the 5T4 heavy chain had measurable affinity. The IC_{50} value was lowered approximately 1000-fold, and the products were at least 1000-fold less potent in cytotoxic activity (Table I).

Three important conclusions could be made from these data. The low yield of product was mainly associated with the 5T4 light chain; the high cell lysis during fermentation was primarily associated with the 5T4 heavy chain, and both chains contain residues important for binding to the 5T4 antigen.

Molecular Modeling of 5T4 Fv—To explain the low production level of 5T4, a model was built. Here information regarding exposed hydrophobic residues, structural identification of the complementarity-determining regions, CDRs, and insights into the structural environment of the residues described below was obtained. The high sequence identity of more than 60% to a relatively large number of template structures ensured that the overall accuracy of the model was good. The most uncertain regions are those modeled as LOOP regions, *e.g.* either not structurally conserved within the family of template structures or not highly homologous to them. However, for these LOOP regions such templates, which fitted well to the structurally conserved regions, were found among other immunoglobulin structures. Of the residues investigated only Tyr-67 in the light chain and Val-113 in the heavy chain were situated in the LOOP regions. Therefore, the model most likely correctly predicts whether the residues studied were exposed or buried and whether a certain residue is needed to support the CDR loop structure.

Engineering of the 5T4Fab-SEch Construct—Based on the finding that V_L replacement in 5T4Fab efficiently increased the production level but affected the binding properties, the molecule was modified to identify residues that hampered high level production. Hydrophobic residues, suggested to be on the Fab surface by computer modeling (Fig. 2), were replaced by serine

COMPARISON OF THE LIGHT CHAIN VARIABLE DOMAINS

```
          1              XXXX           XXXXX XXXXXXXX        XXXXX       XXXXX
C215      DIVMTQSPSS LTVTAGEKVT MNCKSSQSLL NSRTQKNYLT WYQQKPGQPP KLLIYWASTR
5T4       SIVMTQTPTF LLVSAGDRVT ITCKASQSVS ND......VA WYQQKPGQSP TLLISYTSSR
          1         *                                             *
                    S                                             K

          XX  XXX        XXX          XXXXX       XXXXXX XXX         XXX
C215      RSGVPDRFTG SGSGTDFTLT ISSVQAEDLA VYYCQNDYVY PLTFGAGTKL ELK
5T4       YAGVPDRFIG SGYGTDFTFT ISTLQAEDLA VYFCQQDYNS PPTFGGGTKL EIK
        55        *    *    *    **    *
                  S    S    L    SV    A
```

COMPARISON OF THE HEAVY CHAIN VARIABLE DOMAINS

```
          XX        X XXXXX           XXXXX XX          XXX           XXXX   X
C215      QVQLQQPGAE LVRPGASVKL SCKASGYTFT NYWINWVKQR PGQGLEWIGN IYPSYIYTNY
5T4       EVQLQQSGPD LVKPGASVKI SCKASGYSFT GYYMHWVKQS HGKSLEWIGR INPSNGVTLY
          1                                          *  *
                                                     P  G

 XXXXX        XXX        XXXXXXXX X        X XXXXXXXXXX XXX         xxXX
 NQEFKDKVTL TVDESSSTAY MQLSSPTSED SAVYYCTRSP YGYDS...YG LDYWGQGTSV TVSS
 NQKFKDKAIL TVDKSSTTAY MELRSLTSED SAVYYCARST MITN....YV MDYWGQVTSV TVSS
61        *
          T                                                 *
                                                            G
```

FIG. 1. **Amino acid sequence of the Fv part of the antibodies 5T4 and C215 showing the substitutions examined.** The one-letter abbreviations are used for the amino acid residues. The CDRs (15) are indicated in *bold*, and the approximate positions of the loops are indicated by the letter *X*.

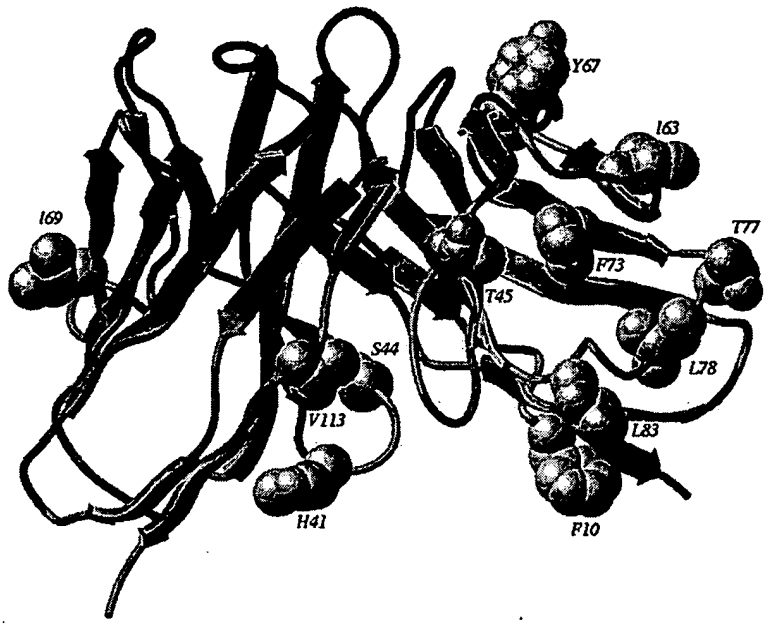

FIG. 2. **Ribbon representation of the 5T4 Fv model.** Substituted amino acid residues are indicated as space-filling models, and the CDRs are indicated by *black ribbons*.

residues. Selected residues differing from the equivalents in more readily produced Fab fragments such as C215 were exchanged for the latter (Fig. 1). To minimize putative effects in affinity and specificity, residues in the CDRs were not altered. The C_H1 and C_L regions were identical in all antibodies studied. The chosen substitutions were Phe-10 → Ser, Thr-45 → Lys, Ile-63 → Ser, Tyr-67 → Ser, Phe-73 → Leu, Thr-77 → Ser, Leu-78 → Val, and Leu-83 → Ala in the light chain. In addition, to identify heavy chain residues that could affect the yield or cell lysis as suggested by the hybrid studies, the substitutions His-41 → Pro, Ser-44 → Gly, Ile-69 → Thr, and Val-113 → Gly were investigated. The positions of these residues and a sequence alignment between the Fv regions of 5T4 and C215 are shown in Figs. 1 and 2. In the model, Phe-10, Thr-45, Ile-63, and Thr-77 in the light chain are exposed side-chain residues. Consequently, the replacements Phe-10 → Ser, Ile-63 → Ser, and to a lower degree Thr-77 → Ser should make the product less hydrophobic. The substitutions Phe-73 → Leu and Leu-78 → Val were made in the completely buried hydrophobic core of the light chain. The light chain residue Tyr-67 is in a loop close to the CDRs. Replacing this residue may therefore change the binding properties of the molecules. The heavy chain substitutions His-41 → Pro and Ser-44 → Gly involved exposed side chains positioned at the N and C terminus, respectively, of a sharp turn connecting two framework β strands. Both proline and glycine residues are important in stabilizing sharp turns in proteins. The substitutions Leu-83 → Ala in the light chain and especially Val-113 → Gly in the heavy chain may affect the interactions with the constant domains. Although not modeled, these residues are in the domain-domain interface of structural homologues. Finally, to find out if other residues in framework 1 affected the yields, a variant of 5T4 containing the 23 N-terminal residues of the C215 light chain instead of the wild-type ones, was constructed. The effects of the different substitutions were investigated as single or combined amino acid replacements. In a reverse phase HPLC system (Fig. 4), the variant chains of 5T4 are much more hydrophilic than the wild-type chains.

Impact of Engineering on Production Levels—The hybrid variants of 5T4 and C215 suggest a replacement of critical light chain residues in 5T4 to obtain a higher production level. Indeed, enzyme-linked immunosorbent assay measurements

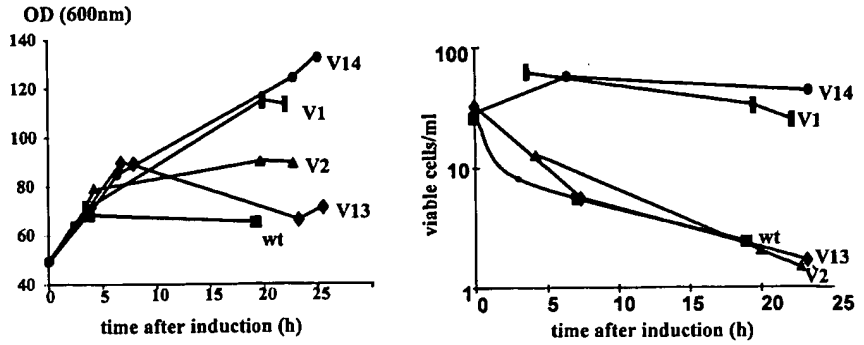

FIG. 3. **Growth curves and cell viability measured during fermentation of the wild-type and variant 5T4Fab-SEch constructs.** The variants shown are V1, V2, V13, and V14 (Table I). Variants V1 and V14, containing the C215 or a mutant heavy chain, differ markedly from the wild-type construct since the A_{600} (*OD*) reaches a much higher level, and the number of viable cells ($\times 10^9$) is not markedly decreased.

after fermentation showed that individual substitutions had substantial impact on the yields. Notably, a single substitution Phe-10 → Ser, variant V3, increased the level from 39 to 92 mg/liter in the growth medium (Table I). Further substitutions increased the production levels continuously and by introducing five or seven point mutations in the light chain, variants V11–V13, the growth medium levels exceeded 500 mg/liter. For these variants, the V_L moiety may no longer be the limiting component. Phe-10 → Ser was the most important replacement, followed by similar and almost additive effects from Thr-45 → Lys, Thr-77 → Ser, and Leu-78 → Val. Furthermore, Leu-83 → Ala also enhanced the yield but was not studied in combination with the others. Except for Phe-10 → Ser, replacing the complete framework 1 did not drastically alter the level as seen in variants V5 and V16.

Significant cell lysis was observed during cultivation of wild-type 5T4Fab-SEch and the most product was found in the growth medium. A few hours after induction with IPTG, the cell growth was markedly affected, and the cell mass in the fermenter started to decline, as determined by A_{600} (Fig. 3). In addition, the number of viable cells decreased more than 10-fold within 10–15 h (Fig. 3). These characteristics were not fundamentally changed by any of the light chain alterations in variants V3 to V13. However, substitutions in the heavy chain altered the properties markedly. The cell mass continued to increase throughout the fermentation to an A_{600} of almost 150 (Fig. 3) with repressed cell lysis. As a consequence, the most product was found in the periplasm. In variant V14 with seven light chain and four heavy chain substitutions, the level was 288 mg/liter in the growth medium and almost 450 mg/liter in the periplasm (Table I). Subsequently, combined with a suitable light chain, the heavy chain replacements increased the total level of fusion protein to 30%. The DNA levels in the growth medium, reflecting the cell lysis, showed that variant V13 contained more than 1 g of DNA/liter, while V14 contained less than 0.2 g. A hybrid molecule, V15, with C215 light chain and 5T4 heavy chain with the replacements His-41 → Pro, Ser-44 → Gly, and Val-113 → Gly, was also investigated. This molecule gave approximately the same yield of product in the growth medium, 250 mg/liter, as hybrid V2. However, similarly to variant V14, cell lysis was less pronounced with this heavy chain, indicating that the substitution Ile-69 → Thr was less important for increased cell viability.

Thus, replacing a few residues in the 5T4 light chain increased the yield almost 15-fold and was further augmented by heavy chain substitutions. The heavy chain replacements altered the phenotype of the *E. coli* cells during fermentation, and less lysis was observed. Subsequently, most of the product was found in the periplasm instead of the growth medium.

Analysis of the Mutated Forms of 5T4—Similar to the 5T4 and C215 hybrids, the variants of 5T4Fab-SEch were purified, and biochemical analyses showed approximately 85–95% of the main component (Fig. 4) with expected characteristics. The minor products seen on reverse phase HPLC are isomers of the light or heavy chains that are not separated from the wild-type chains on SDS-polyacrylamide gel electrophoresis.

To investigate whether the replacements affected biological properties, the different products were analyzed for binding to the 5T4 antigen, and since the constructs were aimed for immunotherapy, a functional *in vitro* assay was also performed. None of the substitutions seemed to have a significant effect on cytotoxic activity (Table I), but replacement of Ile-63 and Tyr-67 with serine residues as in variants V4, V5, and V10 resulted in a reduced affinity for the antigen by approximately 50% (Fig. 5 and Table I). Surprisingly, this effect was reversed by the light chain substitutions Phe-73 → Leu, Thr-77 → Ser, and Leu-78 → Val in variants V12 and V13. The variant V16 containing the 23 N-terminal residues from C215 combined with the substitutions Ile-63 → Ser and Tyr-67 → Ser had an affinity of approximately 30% compared with the wild-type 5T4Fab-SEch (Fig. 5 and Table I). This indicated that unknown residues in framework 1 of 5T4 stabilized the antigen binding site, and if replaced by the equivalents from C215, the binding properties were affected. These effects were not studied further.

In conclusion, none of the replacements resulted in a dramatic alteration in either affinity or cytotoxic activity of the 5T4Fab-SEch molecule. However, some of the substitutions slightly changed the binding properties.

DISCUSSION

It was recently demonstrated that particular amino acid residues in the CDRs of recombinant antibodies can influence the level of secreted product in *E. coli* (26, 27). Here that finding was extended showing that Fv framework substitutions significantly enhanced the yield of a secreted Fab-fusion protein in *E. coli*. Two approaches were used to design variants of the antibody 5T4. Hydrophobic residues, likely to be on the framework surface according to molecular modeling, were replaced with Ser or Ala, and a few less frequent residues were replaced by those of an antibody that can be produced at relatively high yields in *E. coli* (Fig. 1). To minimize the risk of changing the binding properties, CDR engineering was not performed. Using only five light chain substitutions, the product level in the growth medium increased approximately 15 times without significantly modifying the affinity for the antigen. This level was higher than for the model antibody C215. The high producing variants V11–V13 all reach a level above 500 mg/liter, and here the V_L part may not be the limiting component. The hydrophobic light chain residue Phe-10, which is totally exposed in the model (Fig. 2), was very limiting for high level production. In variant V3, Phe-10 was replaced with Ser, which resulted in a 2.5-fold increase in the production level. In addition, the substitutions Thr-45 → Lys, Thr-77 →

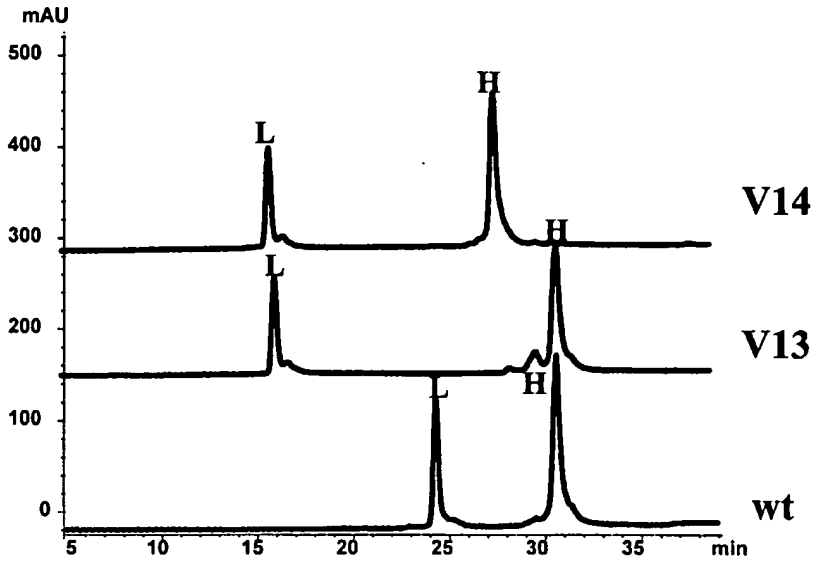

FIG. 4. **Reverse phase HPLC analysis of purified wild-type 5T4Fab-SEch, variant V13 with seven substitutions in the light chain, and V14 with seven substitutions in the light chain and four in the heavy chain.** The analytical conditions are described under "Experimental Procedures." Since the polypeptide chains are not covalently attached to each other, they are detected individually, and it is estimated that each product has a homogeneity of 85–95%. *L*, light chains; *H*, heavy chains; and *wt*, wild-type. In this assay, the variant chains are significantly less hydrophobic than wild type.

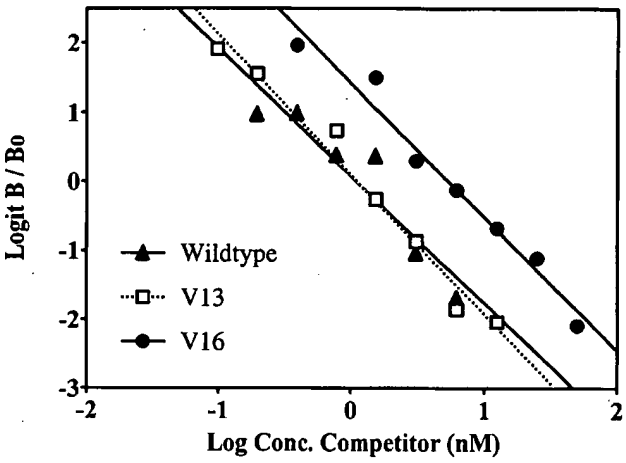

FIG. 5. **Determination of the affinities for the 5T4 antigen in one representative experiment for wild-type 5T4Fab-SEch and its variants V13 and V16.** The affinities were determined on Calu-1 cells as described under "Experimental Procedures." Variant V16 has a relative affinity of approximately 20% compared with wild-type and variant V13 (Table I).

Ser, Leu-78 → Val, and Leu-83 → Ala increased the yield especially when Phe-10 was replaced as observed with the variants V5 and V7–V13 (Table I).

While the light chain substitutions had a tremendous impact on the final yield, the heavy chain replacements primarily affected product localization (Fig. 3, Table I). Thereby, a tool that enables targeting of recombinant antibody fragments to either the periplasm or the growth medium might have been identified. Whether it is optimal to obtain a recombinant product in the periplasm or growth medium can be questioned, but for downstream processing there are definite advantages to recovering a product from the growth medium. In accordance with this study, a recent investigation of heavy chain loop substitutions show that residues controlling production level and periplasmic leakiness may differ (26). A Pro as residue 40 led to a higher leakiness compared with Ala, while the substitutions Ser-61 → Ala and Ala-62 → Asp (using the 5T4 positions) lead to higher production levels. Notably, Pro-40 resided in the corresponding turn that appeared to be important for periplasmic leakiness in this study. By comparing previously reported yields with our results, it seems possible that the residues studied here generally determine the production level for secreted antibody fragments. For instance, one antibody reported to be produced very poorly in *E. coli* contains a Phe at position 10 (27). Also, the humanized Fab secreted in approximately 1 g/liter (7) contains most of the optimal residues like Ser-10, Lys-45, and Ser-77 as well as those found important by Knappik and Plückthun (26). The heavy chain substitution Ile-69 → Thr seems to have less impact on product levels and localization (Table I) (26).

There are several possible explanations for the drastic differences observed. For instance, compared with the engineered variants, wild-type 5T4Fab may have poor folding properties, lower solubility of the unpaired chains, a higher tendency for aggregation, a higher formation rate of unproductive light chain dimers (28), or a lower stability toward proteolysis (29). Also the wild-type mRNA could have a low stability, or less likely there may be problems with the translocation initiation process (30). The periplasmic folding process has been suggested to be the major limitation for secretion of recombinant antibodies in *E. coli* (31, 32). Furthermore, replacing residues identified as limiting indeed improved *in vitro* refolding of reduced and denatured Fv molecules (26), and proline isomerization was rate-limiting for that folding process (33). It is therefore likely that at least some of the substitutions in 5T4 caused an effect that facilitated proper folding. Replacing hydrophobic residues on protein surfaces with more hydrophilic ones has yielded products with suppressed tendencies for aggregation or dimer formation during production (34). Therefore, the variant light chains of 5T4, which are more hydrophilic than the wild-type chain, are probably less prone to aggregate. Preliminary analyses on the amount of light chain dimers indicate that in no case does the level exceed that of Fab (data not shown). Recently, a folding model for recombinant antibodies in *E. coli* was suggested (33). Here, the light chain acts as a folding template for the heavy chain that would otherwise aggregate. Our data do not contrast that model. Thus, the final yield was probably determined by the folding and aggregate-forming properties of the light chain and the time needed for the heavy chain to find its partner chain before precipitation, which may induce stress to the host cell.

None of the substitutions in 5T4 resulted in a drastic change in affinity for the antigen. According to the model (Fig. 2) only Tyr-67 is positioned close to the CDRs. Combining the substitutions Ile-63 → Ser and Tyr-67 → Ser or replacing the light

chain framework 1 resulted in a decrease in affinity by approximately 50%, but additional substitutions reversed this effect (Fig. 5 and Table I). Similar to previous experiences (35, 36), this shows that particular residues in individual framework regions stabilize the unique conformation of an antibody's antigen binding site. For tumor therapy it is unclear what affinities are optimal, but the repertoire of antibodies generated here, perhaps differing in the k_{on} and k_{off}, may be used to investigate these issues.

The mechanisms inducing leakage of proteins from periplasm to growth medium are not well known (37, 38). The data presented here and elsewhere (26, 39) show that small variations in the composition of a secreted product can induce a large difference in stress for the host cell, which leads to lysis during fermentation. Cell lysis was certainly one important reason for the high amounts of product found in the growth medium in this study, but apparently leakiness that was not directly coupled to lysis was observed in two different ways. First, despite great similarities between variants V1, V14, and V15 regarding viable cells, etc. during fermentation (Fig. 3), the ratios of product found in the growth medium and periplasm differ (Table I). Second, even though replacing heavy chain residues resulted in a higher viability of the *E. coli* cells and subsequently less lysis, at least 40% of the product was still found in the growth medium. It is less likely that all of this product was released by cell lysis since after fermentation of variant V14 the DNA level in the growth medium was less than 20% compared with V13. Also, a few other recombinant products tend to be found primarily in the growth medium after secretion without any connected cell lysis (40, 41). Consequently, there must be a complex relationship between how individual residues affect cell lysis and periplasmic leakage. Further studies with this system may explain some of the molecular mechanisms behind these events for antibody fragments.

In conclusion, this paper has shown that problems with low production of a secreted antibody fragment may be circumvented by molecular engineering. It may also be feasible to modify the framework so the product can be recovered from either the growth medium or the periplasm. More speculatively, the substitutions identified here in combination with those found by others could constitute a platform for the design of frameworks that are generally suitable for *E. coli* production of recombinant antibodies.

Acknowledgments—We are grateful for the help of Åsa Gahne, Andrea Varadi, Sven-Åke Franzén, Marianne Israelsson, Birger Jansson, Andreas Castan, Erene Strandberg, Christina Kalderén, Elinor Robertson, Christina Nyhlén, Gunilla Fant, Staffan Lindqvist, Elin Arvesen, Anders Forsman, Anna Rosén, Johan Hansson, Peter Lando, Ulrika Pettersson, and Christine Valfridsson. We also thank Lars Abrahmsén, Ebba Florin Robertsson, and Mikael Dohlsten for stimulating discussions and Per Wikström for suggesting the use of polyethylenimine.

REFERENCES

1. Riethmüller, G., Scneider-Gaedicke, E., and Johnson, J. P. (1993) *Curr. Opin. Immunol.* **5**, 732–739
2. Huse, W. D., Sastry, L., Iverson, S., Kang, A. S., Alting-Mees, M., Burton, D. R., Benkovic, S. J., and Lerner, R. A. (1989) *Science* **246**, 1275–1281
3. Plückthun, A. (1991) *Methods Companion Methods Enzymol.* **2**, 88–96
4. Marks, J. D., Hoogenboom, H. R., Bonnet, T. P., McCafferty, J., Griffiths, A. D., and Winter, G. (1991) *J. Mol. Biol.* **222**, 581–597
5. Barbas, C. F., Bain, J. D., Hoekstra, D. M., and Lerner, R. A. (1992) *Proc. Natl. Acad. Sci. U. S. A.* **89**, 4457–4461
6. Ward, E. S. (1992) *FASEB J.* **6**, 2422–2427
7. Carter, P., Kelley, R. F., Rodrigues, M. L., Snedecor, B., Covarrubias, M., Velligan, M. D., Wong, W. L. T., Rowland, A. M., Kotts, C. E., Carver, M. E., Yang, M., Bourell, J. H., Shepard, H. M., and Henner, D. (1992) *Bio/Technology* **10**, 163–167
8. Pack, P., Kujau, M., Schroeckh, V., Knüpfer, U., Wenderoth, R., Riesenberg, D., and Plückthun, A. (1993) *Bio/Technology* **11**, 1271–1277
9. Buchner, J., and Rudolph, R. (1991) *Bio/Technology* **9**, 157–162
10. Shibui, T., Munakata, K., Matsumoto, R., Ohta, K., Matsuhima, R., Morimoto, Y., and Nagahari, K. (1993) *Appl. Microbiol. Biotechnol.* **38**, 770–775
11. Kalland, T., Dohlsten, M., Lind, P., Sundstedt, A., Abrahmsén, L., Hedlund, G., Björk, P., Lando, P. A., and Björklund, M. (1993) *Med. Oncol. Tumor Pharmacother.* **10**, 37–47
12. Dohlsten, M., Abrahmsén, L., Björk, P., Lando, P. A., Hedlund, G., Forsberg, G., Brodin, T., Gascoigne, N. R. J., Förberg, C., Lind, P., and Kalland, T. (1994) *Proc. Natl. Acad. Sci. U. S. A.* **91**, 8945–8949
13. Dohlsten, M., Hansson, J., Ohlsson, L., Litton, M., and Kalland, T. (1995) *Proc. Natl. Acad. Sci. U. S. A.* **92**, 9791–9795
14. Abrahmsén, L., Dohlsten, M., Segrén, S., Björk, P., Jonsson, E., and Kalland, T. (1995) *EMBO J.* **14**, 2978–2986
15. Kabat, E. A., Wu, T. T., Perry, H. M., Gottesman, K. S., and Foeller, C. (1991) *Sequences of Proteins of Immunological Interest*, 5th Ed., National Institutes of Health, Bethesda, MD
16. Southall, P. J., Boxer, G. M., Bagshawe, K. D., Hole, N., Bromley, M., and Stern, P. L. (1990) *Br. J. Cancer* **61**, 89–95
17. Myers, K. A., Rahi-Saund, V., Davison, M., Young, J., Cheater, A. J., and Stern, P. L. (1994) *J. Biol. Chem.* **269**, 9319–9324
18. Sambrook, J., Fritsch, E. F., and Maniatis, T. (1989) *Molecular Cloning: A Laboratory Manual*, 2nd Ed., Cold Spring Harbor Laboratory, Cold Spring Harbor, NY
19. Forsberg, G., Baastrup, B., Brobjer, M., Lake, M., Jörnvall, H., and Hartmanis, M. (1989) *Biofactors* **2**, 105–112
20. Atkinson, A., and Jack, G. W. (1973) *Biochim. Biophys. Acta* **308**, 41–52
21. Dohlsten, M., Hedlund, G., Åkerblom, E., Lando, P. A., and Kalland, T. (1991) *Proc. Natl. Acad. Sci. U. S. A.* **88**, 9287–9291
22. Scatchard, G. (1949) *Ann. N. Y. Acad. Sci.* **51**, 660–672
23. Bernstein, F. C., Koetzle, T. F., Williams, G. J. B., Meyer, E. F., Jr., Brice, M. D. J., Rodgers, J. R., Kennard, O., Shimanouchi, T., and Tasumi, M. (1977) *J. Mol. Biol.* **112**, 535–542
24. Abagyan, R. M., Totrov, M., and Kuznetsov, D. A. (1994) *J. Comput. Chem.* **15**, 488–506
25. Björk, P., Jönsson, U., Svedberg, H., Larsson, K., Lind, P., Dillner, J., Hedlund, G., Dohlsten, M., and Kalland, T. (1993) *J. Biol. Chem.* **268**, 24232–24241
26. Knappik, A., and Plückthun, A. (1995) *Protein Eng.* **8**, 81–89
27. Ulrich, H. D., Patten, P. A., Yang, P. L., Romesberg, F. E., and Schultz, P. G. (1995) *Proc. Natl. Acad. Sci. U. S. A.* **92**, 11907–11911
28. Brinkmann, U., Lee, B. K., and Pastan, I. (1993) *J. Immunol.* **150**, 2774–2782
29. Alfthan, K., Takkinen, K., Sizmann, D., Seppälä, I., Immonen, T., Vanne, L., Keränen, S., Kaartinen, M., Knowles, J. K. C., and Teeri, T. T. (1993) *Gene (Amst.)* **128**, 203–209
30. Ayala, M., Balint, R. F., Fernández-de-Cossio, M. E., Canaán-Haden, Larrick, J. W., and Gavilondo, J. V. (1995) *BioTechniques* **18**, 832–842
31. Knappik, A., Krebber, C., and Plückthun, A. (1993) *Bio/Technology* **11**, 77–83
32. Skerra, A., and Plückthun, A. (1991) *Protein Eng.* **4**, 971–979
33. Freund, C., Honegger, A., Hunziker, P., Holak, T. A., and Plückthun, A. (1996) *Biochemistry* **35**, 8457–8464
34. Leistler, B., and Perham, R. N. (1994) *Biochemistry* **33**, 2773–2781
35. Bendig, M. M. (1995) *Methods Companion Methods Enzymol.* **8**, 83–93
36. Ge, L., Lupas, A., Peraldi-Roux, S., Spada, S., and Plückthun, A. (1995) *J. Biol. Chem.* **270**, 12446–12451
37. Hockney, R. C. (1994) *Trends Biotechnol.* **12**, 456–463
38. Blight, M. A., Chervaux, C., and Holland, I. B. (1994) *Curr. Opin. Biotechnol.* **5**, 468–474
39. Somerville, J. E., Goshorn, S. C., Fell, H. P., and Darveau, R. P. (1994) *Appl. Microbiol. Biotechnol.* **42**, 595–603
40. Abrahmsén, L., Moks, T., Nilsson, B., and Uhlén, M. (1986) *Nucleic Acids Res.* **14**, 7487–7500
41. Hewinson, R. G., and Russell, W. P. (1993) *J. Gen. Microbiol.* **139**, 1253–1259

Protein Engineering vol.12 no.5 pp.417–421, 1999

Light-chain framework region residue Tyr71 of chimeric B72.3 antibody plays an important role in influencing the TAG72 antigen binding

Jim Xiang[1], Lata Prasad[2], Louis T.J.Delbaere[2] and Zongchao Jia[3]

Saskatoon Cancer Center, Departments of Oncology and [2]Biochemistry, University of Saskatchewan, Saskatoon, Saskatchewan S7N 4H4 and [3]Department of Biochemistry, Queen's University, Kingston, Ontario K7L 3N6, Canada

[1]To whom correspondence should be addressed

The crystallographic study of chimeric B72.3 antibody illustrated that there are three FR side-chain interactions with either CDR residue's side chain or main chain. For example, hydrogen bonds are formed between the hydroxyl group of threonine at L5 in FR1 and the guanidinal nitrogen group of arginine at L24 in CDR1, between the hydroxyl group of tyrosine at L36 in FR2 and the amide nitrogen group of glutamine at L89 in CDR3 and between the hydroxyl group of tyrosine at L71 in FR3 and the carbonyl group of isoleucine at L29 as well as the amide nitrogen group of serine at L31 in CDR1. Elimination of these hydrogen bonds at these FR positions may affect CDR loop conformations. To confirm these assumptions, we altered these FR residues by site-directed mutagenesis and determined binding affinities of these mutant chimeric antibodies for the TAG72 antigen. We found that the substitution of tyrosine by phenylalanine at L71, altering main-chain hydrogen bonds, significantly reduced the binding affinity for the TAG72 antigen by 23-fold, whereas the substitution of threonine and tyrosine by alanine and phenylalanine at L5 and L36, eliminating hydrogen bonds to side-chain atoms, did not affect the binding affinity for the TAG72 antigen. Our results indicate that the light-chain FR residue tyrosine at L71 of chimeric B72.3 antibody plays an important role in influencing the TAG72 antigen binding. Our results will thus be of importance when the humanized B72.3 antibody is constructed, since this important mouse FR residue tyrosine at L71 must be maintained.

Keywords: binding affinity/FR residues/site-directed mutagenesis/TAG72 antigen

Introduction

The determination of the three-dimensional structures of antibody fragments by X-ray crystallography has led to the realization that the polypeptide chains of the immunoglobulin G (IgG) molecules are folded into globular domains, four in the heavy (H) and two in the light (L) chain, which are connected by extended peptide segments like pearls on a string (Amzel and Poljak, 1979). All domains exhibit a similar polypeptide folding pattern characterized by two β-sheets. Sequence comparisons among heavy- and light-chain variable (V) domains reveal that each domain has three complementary-determining regions (CDR) flanked by four framework regions (FR) of less variable sequences (Kabat *et al.*, 1991). The antibody-combining site is formed by the juxtaposition of six CDRs appearing as loops at one end of the β-sheet, three from V_H and another three from V_L. These CDR loops present a surface that interacts with the antigen and determine the antibody specificity and the antigen binding affinity. Although the FRs comprise the conserved β-sheet framework and are involved in the interchain interactions that bring domains together (Chothia *et al.*, 1985), some of them may also directly or indirectly contribute to the antigen binding. For example, some FR residues, especially those in conjunction with CDR, have been found on occasion to be involved in the direct interaction with the antigen (Fischmann *et al.*, 1991; Tulip *et al.*, 1992). Sometimes, FR residues having the atomic interaction with CDR residues were found to influence indirectly the antibody binding affinity by altering the conformation of CDR loops (Kettleborough *et al.*, 1991; Foote and Winter, 1992; Lavoie *et al.*, 1992; Kao and Sharon, 1993; Xiang *et al.*, 1995).

B72.3 is a mouse antibody with specificity for the tumor-associated TAG72 antigen (Thor *et al.*, 1986). The TAG72 epitope defined by the B72.3 antibody is NeuAc2–6αGalNAcα1-*O*-Ser/Thr (sTn) (Kjeldsen *et al.*, 1988). Recently, the data showed that the minimal epitope for the B72.3 antibody is the dimeric sTn–serine cluster (sTn^2) (Reddish *et al.*, 1997). The crystallization of the chimeric B72.3 Fab′ fragment was reported previously (Brady *et al.*, 1991). A model for the Fab′ has been determined by molecular replacement and refined to a resolution of 3.1 Å with an *R*-factor of 17.6%. The crystallographic analysis of the chimeric B72.3 Fab′ illustrated that some H-chain FR residues (H71, H73 and H93) form hydrogen bonds to CDR residues (Brady *et al.*, 1992). These H-chain FR residues may affect the conformation of H-chain CDR loops. Our site-directed mutagenesis study (Xiang *et al.*, 1995) has confirmed that H-chain FR residues 71 and 93 are the major determinants for H-chain CDR loop conformations. A single amino acid substitution at these FR residues significantly reduced the binding affinity for the TAG72 antigen by 12- and 20-fold, respectively. In addition to atomic interactions between H-chain FR and CDR residues, the crystallographic study has also illustrated that there are three FR side-chain interactions with either CDR residue's side chain or main chain, although there are many main-chain atoms of FR residues that make hydrogen bonds to CDR residues. For example, hydrogen bonds are formed between the hydroxyl group of threonine at L5 in FR1 and the guanidinal nitrogen group of arginine at L24 in CDR1, between the hydroxyl group of tyrosine at L36 in FR2 and the carbonyl group of glutamine at L89 in CDR3 and between the hydroxyl group of tyrosine at L71 in FR3 and the carbonyl group of isoleucine at L29 as well as the amide nitrogen group of serine at L31 in CDR1. Elimination of hydrogen bonds at these FR residues may affect L-chain CDR loop conformations. To confirm these assumptions, we conducted site-directed mutagenesis at these mouse FR residues. The binding affinities of these mutant antibodies

```
|FR1                              |CDR1          |FR2
DIQMTQSPAS LSVSVGELVT ITCRASENIY SNLAWYQQKQ
          10                  20          30          40

          |CDR2      |FR3
GKSPGLLVYA ATNLADGVPS RFSGSGSGTQ YSLKINSLQS
          50                  60          70          80

          |CDR3          |J2
EDFGSYYCQH FWGTPYTFGQ GTKLEIKP
          90          100
```

Fig. 1. Amino acid sequence of the cB72.3 V_κ region. The one-letter amino acid code is used. Amino acids are numbered sequentially according to Kabat's method. Demarcated are respective framework regions (FR), complementary-determining regions (CDR) and joining segment (J).

were measured in a solid-phase radioimmunoassay (RIA) and compared with the original chimeric antibody cB72.3-1-3 (Xiang *et al.*, 1990).

Materials and methods

Expression vector, antigen and cell line

The expression vectors mpSV2neo-EP-V_H-$C_{\gamma 1}$ and mpSV2gpt-EP-C_κ were previously constructed for expression of the cB72.3-1-3 H- and L-chains, respectively (Xiang *et al.*, 1990, 1992). Bovine mucin from submaxillary glands (Sigma Chemical, St Louis, MO) containing the TAG72 epitope (Xiang *et al.*, 1990) was used as the antigen source. The SP2/0Ag14 myeloma cell line lacking the expression of its own internal H- and L-chains was obtained from the American Type Culture Collection (ATCC, Rockville, MD). This cell line was maintained in Dulbecco's modified Eagle's medium (DMEM) containing 10% fetal calf serum (FCS).

Site-directed mutagenesis

Amino acids of the cB72.3-1-3 V_κ region are numbered according to Kabat's method (Kabat *et al.*, 1991) and shown in Figure 1. The major atomic interactions between L-chain FR-CDR residues are illustrated in Figure 2. To eliminate the hydrogen bond (4.7 Å) between the hydroxyl group of threonine at L5 in FR1 and the guanidinal nitrogen group of arginine at L24 in CDR1 (Figure 2A), oligo 29 (5′ gacat ccaga tggct cagtc tccag 3′) was synthesized for site-directed mutagenesis. It is complementary to L-chain FR1 with substitution of threonine by alanine at L5. To eliminate the hydrogen bond (2.61 Å) between the hydroxyl group of tyrosine at L36 in FR2 and the amide nitrogen group of glutamine at L89 in CDR3 (Figure 2B), oligo 30 (5′ aattt agcat ggttt caaca gaaac 3′) was synthesized for site-directed mutagenesis. It is complementary to the L-chain FR2 with substitution of tyrosine by phenylalanine at L36. To eliminate the hydrogen bonds (2.65 and 3.02 Å) between the hydroxyl group of tyrosine at L71 in FR3 and the carbonyl group of isoleucine at L29 and also the amide nitrogen group of serine at L31 in CDR1 (Figure 2C), oligo 31 (5′ cggca cacag ttttc cctca agatc 3′) complementary to the L-chain FR3 was synthesized for site-directed mutagenesis. Mutations were introduced into M13mp18-V_κ by these three primers in site-directed mutagenesis to form three plasmids M13mp18-$V_{\kappa M29-31}$. Sequences of these mutant $V_{\kappa M29-31}$ regions were verified by the dideoxy nucleotide sequencing method (Sanger *et al.*, 1977).

Construction of expression vectors

The expression vectors mpSV2gpt-EP-$V_{\kappa M29-31}$-C_κ were constructed for production of mutant chimeric L-chains. The mutant $V_{\kappa M29-31}$ region cDNA fragments (*Kpn*I) was purified from M13-mp18-$V_{\kappa M29-31}$ by *Kpn*I digestion and introduced into the *Kpn*I site in the multiple cloning region of mpSV2gpt-EP-C_κ (Xiang *et al.*, 1992) to form the mutant L-chain expression vectors mpSV2gpt-EP-$V_{\kappa M29-31}$-C_κ. These expression vectors contain the *gpt* gene for mycophenolic acid selection and a complete transcription unit including enhancer (E), immunoglobulin promoter (P), mutant $V_{\kappa M29-31}$ region cDNA fragments and human genomic DNA fragment of κ constant region (C_κ).

Expression and purification of mutant chimeric antibodies

The mutant L-chain expression vector DNA mpSV2gpt-EP-$V_{\kappa M29-31}$-C_κ was first transfected into SP2/0Ag14 cells by electroporation as described (Xiang *et al.*, 1990). Cells were selected for growth in media containing mycophenolic acid at 0.8 μg/ml. After 14 days, growth supernatants were screened in a human L-chain capture ELISA for examining the expression of mutant chimeric L-chains (Xiang *et al.*, 1996). The positive clones derived from SP2/0Ag14 cell line secreting mutant chimeric L-chains were further transfected with the chimeric H-chain expression vector DNA mpSV2neo-EP-V_H-$C_{\gamma 1}$ (Xiang *et al.*, 1990) and selected for growth in media containing both G418 at 2 mg/ml and mycophenolic acid at 0.8 μg/ml. The growth supernatants were then screened by a TAG72-binding ELISA for examining the expression of three mutant chimeric antibodies cB72.3m29–31 (Xiang *et al.*, 1990). These mutant chimeric antibodies were further purified from supernatants by protein A-Sepharose chromatography (Xiang *et al.*, 1990). Protein concentrations were determined using a Bio-Rad (Richmond, CA) protein assay kit according to the method described in the manual.

Affinity constants

The affinity constants (K_a) of mutant chimeric antibodies cB72.3m29–31 were determined in a solid-phase RIA using the bovine mucin as a source of the TAG72 antigen as described previously (Xiang *et al.*, 1993). Briefly, serial dilutions of mutant antibodies were added to each mucin-coated well (in triplicate) of the first microtiter plate for incubation overnight at 4°C. The supernatants of each well, which contained the free mutant antibody, were transferred to each well of the second microtiter plate, which had previously been coated with goat anti-human IgG antibody. The amount of bound and free antibodies on the first and second plates was measured using the ^{125}I-labeled goat anti-human IgG antibody. To calculate K_a, the method of Scatchard (1949) was used. The ratios of the concentrations of bound to free antibody were plotted against the concentration of bound antibody. The slope represents K_a of each mutant antibody (Xiang *et al.*, 1993).

Results and discussion

The FRs of antibodies fold into a conserved β-sheet structure that acts as scaffolding for the antigen-contacting CDR. Some FR residues may also directly affect the conformation of CDR loops by atomic interactions between FR and CDR residues (Kettleborough *et al.*, 1991; Foote and Winter, 1992; Lavoie *et al.*, 1992; Xiang *et al.*, 1995). According to the crystallographic study of chimeric B72.3 Fab′, there are hydrogen bonds formed between side-chains of three L-chain FR residues (L5, L36 and L71) and CDR residues (Figure 2A–C). These three FR residues may thus affect the conformation of L-chain CDR loops. To confirm these assumptions, we performed site-directed mutagenesis at these three FR positions (L5, L36 and

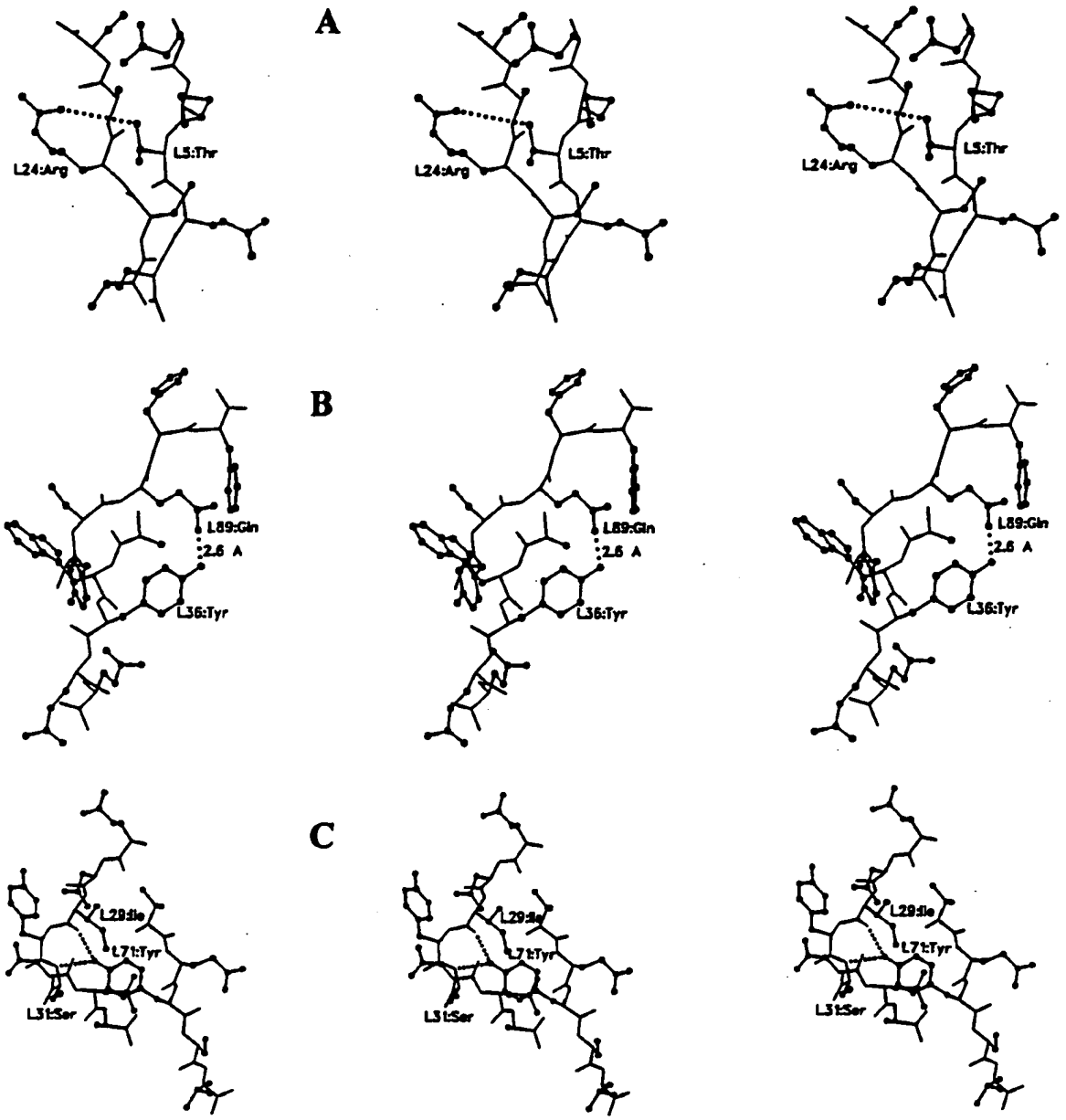

Fig. 2. Stereo diagrams of some L-chain FR residues with atomic interaction with L-chain CDR residues from the coordinates of crystallographic analysis of chimeric B72.3 Fab' deposited in the Brookhaven Data Bank. (A) The hydrogen bond formed between the hydroxyl group of threonine at L5 in FR1 and the guanidinal nitrogen group of arginine at L24 in CDR1. (B) The hydrogen bond formed between the hydroxyl group of tyrosine at L36 and the amide nitrogen group of glutamine at L89 in CDR3. (C) The hydrogen bond formed between the hydroxyl group of tyrosine at L71 in FR3 and the carbonyl group of isoleucine at L29 as well as the amide nitrogen group of serine at L31 in CDR1 The α-carbon trace and the amino acid side-chain conformation are marked. Putative hydrogen bonds are shown as broken lines.

L71) with three oligonucleotides (oligos 29–31) resulting in three mutant chimeric antibodies cB72.3m29–31. The affinity constants of these three mutant antibodies for the TAG72 antigen were determined in a solid-phase RIA compared with that of the original cB72.3-1-3 antibody.

The hydrogen bond formed between the hydroxyl group of threonine at L5 in FR1 and the guanidinal nitrogen group of arginine at L24 in CDR1 is a borderline one because of the long distance of 4.17 Å. It would be a very weak interaction, if it could indeed be considered as a hydrogen bond at all. To clarify the ambiguity and determine whether it is an important interaction, we performed a single amino acid substitution of threonine by alanine at L5 to eliminate this hydrogen bond. Our results showed that the affinity constant (K_a) of cB72.3m29 with substitution of threonine by alanine at L5 is 6.5×10^8 M^{-1}, which is similar to that of the original cB72.3-1-3 antibody (6.8×10^8 M^{-1}) (Table I), indicating that this weak interaction is not important. This is not surprising in the light of the long interaction distance of 4.17 Å. The influence of threonine at L5 on the CDR loop conformation would be minimal. Arginine at L24 of CDR1, being surface exposed, is very flexible and one would not expect that a weak interaction with its guanidinal group could exert much effect on the main-chain conformation. This notion is evidently supported by our

Table I. Affinity constants of mutant cB72.3m antibodies

Antibody	Amino acid substitution	Affinity constant (K_a)
cB72.3-1-3	–	6.8
cB72.3m29	Threonine by alanine (L5)	6.5
cB72.3m30	Tyrosine by phenylalanine (L36)	7.0
cB72.3m31	Tyrosine by phenylalanine (L71)	0.3

Affinity constants (K_a, $\times 10^8$ M^{-1}) were determined from Scatchard plots of the binding of different L-chain mutant chimeric antibodies of cB72.3m29–31 to the TAG72 antigen.

mutagenesis result. Alternatively, it could be that residues and solvents rearranged to compensate for the missing hydrogen bond caused by the site-directed mutagenesis. Therefore, it does not play any role in the L-chain CDR1 loop conformation. In addition, a strong hydrogen bond is formed between the main-chain carbonyl groups of isoleucine at L2 in FR1 and serine at L26 in CDR1 (Brady *et al.*, 1992), which may play some role in keeping the L-chain CDR1 loop conformation.

A single amino acid substitution of tyrosine by phenylalanine at L36 and L71 eliminated the hydrogen bonds formed between the hydroxyl group of tyrosine at L36 in FR2 and the amide nitrogen group of glutamine at L89 in CDR3, and between the hydroxyl group of tyrosine at L71 in FR3 and the carbonyl group of isoleucine at L29 as well as the amide nitrogen group of serine at L31 in CDR1. Our results showed that the affinity constant (K_a) of cB72.3m30 with substitution of tyrosine by phenylalanine at L36 is 7.0×10^8 M^{-1}, which is similar to that of the original cB72.3-1-3 antibody (6.8×10^8 M^{-1}), while the K_a of cB72.3m31 (0.3×10^8 M^{-1}), with substitution of tyrosine by phenylalanine at L71, was significantly reduced by 23-fold (Table I), indicating that L71 in FR3 plays an important role in influencing the TAG72 antigen binding. Interestingly, the importance of the L71 residue in the CDR loop conformation has also been reported previously in an anti-lysozyme D1.3 antibody (Foote and Winter, 1992). Substitution of phenylalanine by tyrosine at L71 of D1.3 antibody resulted in an additional contribution of 0.8 kcal/mol in binding affinity for the lysozyme.

It is not totally surprising to see that the mutation of tyrosine to phenylalanine at L36 did not affect antigen binding. Generally, side-chain interactions would not necessarily affect the main-chain conformation. Even if they do, they would be less effective than interactions that directly involve main-chain atoms. Akin to arginine at L24, glutamine at L89 has a relatively long side-chain, and loss of a hydrogen bond may just increase its side-chain flexibility which does not have much impact on the main-chain conformation. As far as tyrosine at L71 is concerned, the interactions are much more significant. First, there are two hydrogen bonds with distances of 2.65 and 3.02 Å. More importantly, these two hydrogen bonds involve main-chain atoms of isoleucine at L29 and serine at L31. The hydroxyl group of tyrosine at L71 does not make any hydrogen bond to side-chain atoms. Loss of these two hydrogen bonds decreased its antigen binding by 23-fold, strongly suggesting the critical role that tyrosine at L71 plays. In this case, it is plausible that the main-chain interactions have an important structural role and loss of these two critical main-chain hydrogen bonds could translate into a conformational change in and around the isoleucine (L29)–serine (L31) segment of CDR. Alternatively, it could be due to an entropic effect residing in the overall tightening upon the antigen binding of a structure that was rendered more mobile by the amino acid replacement at L71, without really affecting the CDR loop conformation. Without structural data, it is indeed very difficult to ascertain whether these hydrogen bonds could influence the CDR loop conformation. However, based on the mutagenesis, binding affinities and structural comparison involving L5, L36 and L71, in which only main-chain interactions seem to have a significant impact, we suggest that tyrosine at L71 is an important residue that is involved in the stabilization of the CDR loop conformation. It is evident that CDR main-chain hydrogen bonds are important and may have a general implication when humanization of B72.3 antibody is considered.

A number of mouse/human chimeric B72.3 antibodies have been constructed by recombinant DNA technology in order to reduce the human anti-mouse antibody response (Whittle *et al.*, 1987; Xiang *et al.*, 1992). However, clinical studies suggested that an anti-idiotypic immune response to the V region was still present (Khazaeli *et al.*, 1991). To minimize the anti-idiotype response, the approach of genetic engineering of a humanized antibody has been taken, in which mouse CDR loops will be directly grafted on to a human framework (Jones *et al.*, 1986). To retain the binding specificity and affinity of its mouse counterpart, some important mouse FR residues were maintained in humanized antibodies (Graziano *et al.*, 1995; Presta *et al.*, 1997). For construction of a humanized B72.3 antibody, a proper human framework with the highest homology to the B72.3 antibody should be chosen for maintenance of B72.3 CDR loop conformations. Based on the sequence homology search using the MicroGenie sequence analysis software of Beckmann, the human myeloma protein Eu showed the highest homology to both the B72.3 V_H (59%) and V_K (63%) regions simultaneously (Glaser *et al.*, 1992). In this paper we have reported our experimental proof of the importance of the L-chain FR residue (L71) in influencing the TAG72 antigen binding. However, the L-chain FR residue of Eu at L71 is phenylalanine. Therefore, our results will be of importance when the humanized B72.3 antibody is constructed by grafting the B72.3 CDRs on to the Eu FRs, since this important mouse FR residue tyrosine at L71 must be maintained in the final humanized B72.3 antibody.

Acknowledgement

This study was supported by a research grant funded by the Saskatchewan Cancer Agency.

References

Amzel,L. and Poljak,R. (1979) *Annu. Rev. Biochem.*, **48**, 961–994.
Brady,R., Hubbard,R., King,D., Low,D., Roberts,S. and Todd,R. (1991) *J. Mol. Biol.*, **219**, 603–604.
Brady,R., Edwards,D., Hubbard,R., Jiang,J., Lange,G., Roberts,S. and Todd,R. (1992) *J. Mol. Biol.*, **227**, 253–264.
Chothia,C., Novotny,J., Bruccoleri,R. and Karplus,M. (1985) *J. Mol. Biol.*, **186**, 651–663.
Fischmann,T., Bentley,G., Bhat,T., Boulet,G., Marivzza,R., Phillips,S., Tello,D. and Poljak,R. (1991) *J. Biol. Chem.*, **266**, 12915–12920.
Foote,J. and Winter,G. (1992) *J. Mol. Biol.*, **224**, 487–499.
Glaser,S., Vasquez,M., Payne,P. and Schneider,W. (1992) *J. Immunol.*, **149**, 2607–2613.
Graziano,R. *et al.* (1995) *J. Immunol.*, **155**, 4996–5002.
Jones,P., Dear,P., Foote,J., Neuberger,M. and Winter,G. (1986) *Nature*, **321**, 522–525.
Kabat,E., Wu,T. and Perry,H. (1991) *Sequences of Proteins of Immunological Interest*. US Department of Health and Human Services, National Institutes of Health publication, Bethesda, MD.
Kao,C. and Sharon,J. (1993) *J. Immunol.*, **151**, 1968–1979.

Kettleborough,C., Saldanha,J., Heath,V., Morrison,C. and Bendig,M. (1991) *Protein Engng*, **4**, 773–783.
Khazaeli,M. *et al.* (1991) *Cancer Res.*, **51**, 5461–5466.
Kjeldsen,T., Clausen,H., Hirohashi,S., Ogawa,T. and Hakomori,S. (1988) *Cancer Res.*, **48**, 2214–2220.
Lavoie,T., Drohan,W. and Smith-Gill,S. (1992) *J. Immunol.*, **148**, 503–513.
Presta,L., Chen,H., O'Connor,S., Chisholm,V., Meng,G., Krummen,L., Winkler,M. and Ferrara,N. (1997) *Cancer Res.*, **57**, 4593–4599.
Reddish,M., Jackson,L., Koganty,R., Qiu,D., Hong,W. and Longenecker,M. (1997) *Glycoconj. J.*, **14**, 549–560.
Sanger,F., Nicklen,S. and Coulson,A. (1977) *Proc. Natl Acad. Sci. USA*, **74**, 5463–5467.
Scatchard,G. (1949) *Ann. N.Y. Acad. Sci.*, **51**, 660–672.
Thor,A., Ohuchi,N., Szpak,C., Johnston,W. and Schlom,J. (1986) *Cancer Res.*, **46**, 3118–3124.
Tulip,W., Varghese,J., Laver,W., Webster,R. and Colman,P. (1992) *J. Mol. Biol.*, **227**, 122–148.
Whittle,N., Adair,J., Lloyd,C., Jenkins,L., Devine,J., Schlom,J., Raubitschek,A., Colcher,D. and Bodmer,M. (1987) *Protein Engng*, **1**, 499–505.
Xiang,J., Roder,J. and Hozumi,N. (1990) *Mol. Immunol.*, **27**, 809–817.
Xiang,J., Moyana,T., Kalra,J., Hamilton,T. and Qi,Y. (1992) *Mol. Biother.*, **4**, 174–183.
Xiang,J., Delbaere,L. and Liu,E. (1993) *Immunol. Cell Biol.*, **71**, 239–246.
Xiang,J., Sha,Y., Jia,Z., Prasad,L. and Delbaere,L. (1995) *J. Mol. Biol.*, **253**, 385–390.
Xiang,J., Sha,Y., Prazad,L. and Delbaere,L. (1996) *Protein Engng*, **9**, 539–543.

Received August 7, 1998; revised November 18, 1998; accepted February 10, 1999

[CANCER RESEARCH 57, 4593–4599, October 15, 1997]

Humanization of an Anti-Vascular Endothelial Growth Factor Monoclonal Antibody for the Therapy of Solid Tumors and Other Disorders

Leonard G. Presta, Helen Chen, Shane J. O'Connor, Vanessa Chisholm, Y. Gloria Meng, Lynne Krummen, Marjorie Winkler, and Napoleone Ferrara[1]

Departments of Immunology, Process Sciences, Molecular Biology, Bioanalytical Technology and Cardiovascular Research, Genentech, Inc., South San Francisco, California 94080

ABSTRACT

Vascular endothelial growth factor (VEGF) is a major mediator of angiogenesis associated with tumors and other pathological conditions, including proliferative diabetic retinopathy and age-related macular degeneration. The murine anti-human VEGF monoclonal antibody (muMAb VEGF) A.4.6.1 has been shown to potently suppress angiogenesis and growth in a variety of human tumor cells lines transplanted in nude mice and also to inhibit neovascularization in a primate model of ischemic retinal disease. In this report, we describe the humanization of muMAb VEGF A.4.6.1. by site-directed mutagenesis of a human framework. Not only the residues involved in the six complementarity-determining regions but also several framework residues were changed from human to murine. Humanized anti-VEGF F(ab) and IgG1 variants bind VEGF with affinity very similar to that of the original murine antibody. Furthermore, recombinant humanized MAb VEGF inhibits VEGF-induced proliferation of endothelial cells *in vitro* and tumor growth *in vivo* with potency and efficacy very similar to those of muMAb VEGF A.4.6.1. Therefore, recombinant humanized MAb VEGF is suitable to test the hypothesis that inhibition of VEGF-induced angiogenesis is a valid strategy for the treatment of solid tumors and other disorders in humans.

INTRODUCTION

It is now well established that angiogenesis is implicated in the pathogenesis of a variety of disorders. These include solid tumors, intraocular neovascular syndromes such as proliferative retinopathies or AMD,[2] rheumatoid arthritis, and psoriasis (1, 2, 3). In the case of solid tumors, the neovascularization allows the tumor cells to acquire a growth advantage and proliferative autonomy compared to the normal cells. Accordingly, a correlation has been observed between density of microvessels in tumor sections and patient survival in breast cancer as well as in several other tumors (4–6).

The search for positive regulators of angiogenesis has yielded several candidates, including acidic fibroblast growth factor (FGF), bFGF, transforming growth factor α, transforming growth factor β, hepatocyte growth factor, tumor necrosis factor-α, angiogenin, interleukin 8, and others (1, 2). However, in spite of extensive research, there is still uncertainty as to their role as endogenous mediators of angiogenesis. The negative regulators thus far identified include thrombospondin (7), the M_r 16,000 NH_2-terminal fragment of prolactin (8), angiostatin (9), and endostatin (10).

Work done over the last several years has established the key role of VEGF in the regulation of normal and abnormal angiogenesis (11). The finding that the loss of even a single VEGF allele results in embryonic lethality points to an irreplaceable role played by this factor in the development and differentiation of the vascular system (11). Also, VEGF has been shown to be a key mediator of neovascularization associated with tumors and intraocular disorders (11). The VEGF mRNA is overexpressed by the majority of human tumors examined (12–16). In addition, the concentration of VEGF in eye fluids is highly correlated to the presence of active proliferation of blood vessels in patients with diabetic and other ischemia-related retinopathies (17). Furthermore, recent studies have demonstrated the localization of VEGF in choroidal neovascular membranes in patients affected by AMD (18).

The muMAb VEGF A.4.6.1 (19) has been used extensively to test the hypothesis that VEGF is a mediator of pathological angiogenesis *in vivo*. This high affinity MAb is able to recognize all VEGF isoforms (19) and has been shown to inhibit potently and reproducibly the growth of a variety of human tumor cell lines in nude mice (11, 20–23). Moreover, intraocular administration of muMAb VEGF A.4.6.1 resulted in virtually complete inhibition of iris neovascularization secondary to retinal ischemia in a primate model (24).

A major limitation in the use of murine antibodies in human therapy is the anti-globulin response (25, 26). Even chimeric molecules, where the variable (V) domains of rodent antibodies are fused to human constant (C) regions, are still capable of eliciting a significant immune response (27). A powerful approach to overcome these limitations in the clinical use of monoclonal antibodies is "humanization" of the murine antibody. This approach was pioneered by Jones *et al.* (28) and Riechman *et al.* (29), who first transplanted the CDRs of a murine antibody into human V domains antibody.

In the present article, we report on the humanization of muMAb VEGF A.4.6.1. Our strategy was to transfer the six CDRs, as defined by Kabat *et al.* (30), from muMAb VEGF A.4.6.1 to a consensus human framework used in previous humanizations (31–33). Seven framework residues in the humanized variable heavy (VH) domain and one framework residue in the humanized variable light (VL) domain were changed from human to murine to achieve binding equivalent to muMAb VEGF A.4.6.1. This humanized MAb is suitable for clinical trials to test the hypothesis that inhibition of VEGF action is an effective strategy for the treatment of cancer and other disorders in humans.

MATERIALS AND METHODS

Cloning of Murine Mab A.4.6.1 and Construction of Mouse-Human Chimeric Fab. Total RNA was isolated from hybridoma cells producing the anti-VEGF MAb A.4.6.1 using RNAsol (Tel-Test) and reverse-transcribed to cDNA using Oligo-dT primer and the SuperScript II system (Life Technologies, Inc., Gaithersburg, MD). Degenerate oligonucleotide primer pools, based of the NH_2-terminal amino acid sequences of the light and heavy chains of the antibody, were synthesized and used as forward primers. Reverse primers were based on framework 4 sequences obtained from murine light chain subgroup κV and heavy chain subgroup II (30). After PCR amplification, DNA fragments were ligated to a TA cloning vector (Invitrogen, San Diego, CA). Eight clones each of the light and

Received 5/27/97; accepted 8/16/97.

The costs of publication of this article were defrayed in part by the payment of page charges. This article must therefore be hereby marked *advertisement* in accordance with 18 U.S.C. Section 1734 solely to indicate this fact.

[1] To whom requests for reprints should be addressed, at Department of Cardiovascular Research, Genentech, Inc., 460 Point San Bruno Boulevard, South San Francisco, CA 94080. Phone: (415) 225-2968; Fax: (415) 225-6327; E-mail: Ferrara.Napoleone@gene.com.

[2] The abbreviations used are: AMD, age-related macular degeneration; bFGF, basic fibroblast growth factor; VEGF, vascular endothelial growth factor; MAb, monoclonal antibody; muMAb, murine MAb; rhuMAb, recombinant humanized MAb; CDR, complementarity-determining region.

heavy chains were sequenced. One clone with a consensus sequence for the light chain VL domain and one with a consensus sequence for the heavy chain VH domain were subcloned, respectively, into the pEMX1 vector containing the human CL and CH1 domains (31), thus generating a mouse-human chimeric F(ab). This chimeric F(ab) consisted of the entire murine A.4.6.1 VH domain fused to a human CH1 domain at amino acid SerH113, and the entire murine A.4.6.1 VL domain fused to a human CL domain at amino acid LysL107. Expression and purification of the chimeric F(ab) were identical to those of the humanized F(ab)s. The chimeric F(ab) was used as the standard in the binding assays.

Computer Graphics Models of Murine and Humanized F(ab)s. Sequences of the VL and VH domains (Fig. 1) were used to construct a computer graphics model of the murine A.4.6.1 VL-VH domains. This model was used to determine which framework residues should be incorporated into the humanized antibody. A model of the humanized F(ab) was also constructed to verify correct selection of murine framework residues. Construction of models was performed as described previously (32, 33).

Construction of Humanized F(ab)s. The plasmid pEMX1 used for mutagenesis and expression of F(ab)s in *Escherichia coli* has been described previously (31). Briefly, the plasmid contains a DNA fragment encoding a consensus human κ subgroup I light chain (VLκI-CL) and a consensus human subgroup III heavy chain (VHIII-CH1) and an alkaline phosphatase promoter. The use of the consensus sequences for VL and VH has been described previously (32).

To construct the first F(ab) variant of humanized A.4.6.1, F(ab)-1, site-directed mutagenesis (34) was performed on a deoxyuridine-containing template of pEMX1. The six CDRs were changed to the murine A.4.6.1 sequence; the residues included in each CDR were from the sequence-based CDR definitions (30). F(ab)-1, therefore, consisted of a complete human framework (VLκ subgroup I and VH subgroup III) with the six complete murine CDR sequences. Plasmids for all other F(ab) variants were constructed from the plasmid template of F(ab)-1. Plasmids were transformed into *E. coli* strain XL-1 Blue (Stratagene, San Diego, CA) for preparation of double- and single-stranded DNA. For each variant, DNA coding for light and heavy chains was completely sequenced using the dideoxynucleotide method (Sequenase; U.S. Biochemical Corp., Cleveland, OH). Plasmids were transformed into *E. coli* strain 16C9, a derivative of MM294, plated onto Luria broth plates containing 50 μg/ml carbenicillin, and a single colony selected for protein expression. The single colony was grown in 5 ml of Luria broth-100 μg/ml carbenicillin for 5–8 h at 37°C. The 5-ml culture was added to 500 ml of AP5–50 μg/ml carbenicillin and allowed to grow for 20 h in a 4-liter baffled shake flask at 30°C. AP5 media consists of 1.5 g of glucose, 11.0 g of Hycase SF, 0.6 g of yeast extract (certified), 0.19 g of $MgSO_4$ (anhydrous), 1.07 g of NH_4Cl, 3.73 g of KCl, 1.2 g of NaCl, 120 ml of 1 M triethanolamine, pH 7.4, to 1 liter of water and then sterile filtered through a 0.1-mm Sealkeen filter. Cells were harvested by centrifugation in a 1-liter centrifuge bottle at 3000 × *g*, and the supernatant was removed. After freezing for 1 h, the pellet was resuspended in 25 ml of cold 10 mM Tris, 1 mM EDTA, and 20% sucrose, pH 8.0. Two hundred fifty ml of 0.1 M benzamidine (Sigma Chemical Co., St. Louis, MO) was added to inhibit proteolysis. After gentle stirring on ice for 3 h, the sample was centrifuged at 40,000 × *g* for 15 min. The supernatant was then applied to a protein G-Sepharose CL-4B (Pharmacia Biotech, Inc., Uppsala, Sweden) column (0.5-ml bed volume) equilibrated with 10 mM Tris-1 mM EDTA, pH 7.5. The column was washed with 10 ml of 10 mM Tris-1 mM EDTA, pH 7.5, and eluted with 3 ml of 0.3 M glycine, pH 3.0, into 1.25 ml of 1 M Tris, pH 8.0. The F(ab) was then buffer exchanged into PBS using a Centricon-30 (Amicon, Beverly, MA) and concentrated to a final volume of 0.5 ml. SDS-PAGE gels of all F(ab)s were run to ascertain purity, and the molecular weight of each variant was verified by electrospray mass spectrometry.

Construction, Expression, and Purification of Chimeric and Humanized IgG Variants. For the generation of human IgG1 variants of chimeric (chIgG1) and humanized (rhuMAb VEGF) A.4.6.1, the appropriate murine or humanized VL and VH (F(ab)-12, Table 1) domains were subcloned into separate, previously described pRK vectors (35). The DNA coding for the entire light and the entire heavy chain of each variant was verified by dideoxynucleotide sequencing.

For transient expression of variants, heavy and light chain plasmids were cotransfected into human 293 cells (36) using a high efficiency procedure (37). Media were changed to serum free and harvested daily for up to 5 days. Antibodies were purified from the pooled supernatants using protein A-Sepharose CL-4B (Pharmacia). The eluted antibody was buffer exchanged into PBS using a Centricon-30 (Amicon), concentrated to 0.5 ml, sterile filtered using a Millex-GV (Millipore, Bedford, MA), and stored at 4°C.

For stable expression of the final humanized IgG1 variant (rhuMAb VEGF), Chinese hamster ovary (CHO) cells were transfected with dicistronic vectors designed to coexpress both heavy and light chains (38). Plasmids were introduced into DP-12 cells, a proprietary derivative of the CHO-K1 DUX B11 cell line developed by L. Chasin (Columbia University, New York, NY), via lipofection and selected for growth in glycine/hypoxanthine/thymidine (GHT)-free medium (39). Approximately 20 unamplified clones were randomly chosen and reseeded into 96-well plates. Relative specific productivity of each colony was monitored using an ELISA to quantitate the full-length human IgG accumulated in each well after 3 days and a fluorescent dye, Calcien AM, as a surrogate marker of viable cell number per well. Based on these data, several unamplified clones were chosen for further amplification in the presence of increasing concentrations of methotrexate. Individual clones surviving at 10, 50, and 100 nM methotrexate were chosen and transferred to 96-well plates for productivity screening. One clone, which reproducibly exhibited high specific productivity, was expanded in T-flasks and used to inoculate a spinner

Table 1 *Binding of humanized anti-VEGF F(ab) variants to VEGF*[a]

Variant	Template	Changes[b]	Purpose	EC50 F(ab)-X / EC_{50} chimeric F(ab)[c] Mean	SD	N
chim-F(ab)	Chimeric F(ab)		1.0			
F(ab)-1	Human FR		Straight CDR swap	>1350		2
F(ab)-2			Chimera light chain F(ab)-1 heavy chain	>145		3
F(ab)-3			F(ab)-1 light chain Chimera heavy chain	2.6	0.1	2
F(ab)-4	F(ab)-1	ArgH71Leu AspH73Asn	CDR-H2 conformation Framework	>295		3
F(ab)-5	F(ab)-4	LeuL46Val	VL-VH interface	80.9	6.5	2
F(ab)-6	F(ab)-5	LeuH78Ala	CDR-H1 conformation	36.4	4.2	2
F(ab)-7	F(ab)-5	IleH69Phe	CDR-H2 conformation	45.2	2.3	2
F(ab)-8	F(ab)-5	IleH69Phe LeuH78Ala	CDR-H2 conformation CDR-H1 conformation	9.6	0.9	4
F(ab)-9	F(ab)-8	GlyH49Ala	CDR-H2 conformation	>150		2
F(ab)-10	F(ab)-8	AsnH76Ser	Framework	6.4	1.2	4
F(ab)-11	F(ab)-10	LysH75Ala	Framework	3.3	0.4	2
F(ab)-12	F(ab)-10	ArgH94Lys	CDR-H3 conformation	1.6	0.6	

[a] Anti-VEGF F(ab) variants were incubated with biotinylated VEGF and then transferred to ELISA plates coated with KDR-IgG (40).
[b] Murine residues are underlined; residue numbers are according to Kabat *et al.* (30).
[c] Mean and SD are the average of the ratios calculated for each of the independent assays; the EC_{50} for chimeric F(ab) was 0.049 ± 0.013 mg/ml (1.0 nM).

culture. After several passages, the suspension-adapted cells were used to inoculate production cultures in GHT-containing, serum-free media supplemented with various hormones and protein hydrolysates. Harvested cell culture fluid containing rhuMAb VEGF was purified using protein A-Sepharose CL-4B. The purity after this step was ~99%. Subsequent purification to homogeneity was carried out using an ion exchange chromatography step. The endotoxin content of the final purified antibody was <0.10 eu/mg.

F(ab) and IgG Quantitation. For quantitating F(ab) molecules, ELISA plates were coated with 2 μg/ml of goat anti-human IgG Fab (Organon Teknika, Durham, NC) in 50 mM carbonate buffer, pH 9.6, at 4°C overnight and blocked with PBS-0.5% BSA (blocking buffer) at room temperature for 1 h. Standards [0.78–50 ng/ml human F(ab)] were purchased from Chemicon (Temecula, CA). Serial dilutions of samples in PBS-0.5% BSA-0.05% polysorbate 20 (assay buffer) were incubated on the plates for 2 h. Bound F(ab) was detected using horseradish peroxidase-labeled goat anti-human IgG F(ab) (Organon Teknika), followed by 3,3',5,5'-tetramethylbenzidine (Kirkegaard & Perry Laboratories, Gaithersburg, MD) as the substrate. Plates were washed between steps. Absorbance was read at 450 nm on a V_{max} plate reader (Molecular Devices, Menlo Park, CA). The standard curve was fit using a four-parameter nonlinear regression curve-fitting program developed at Genentech. Data points that fell in the range of the standard curve were used for calculating the F(ab) concentrations of samples.

The concentration of full-length antibody was determined using goat anti-human IgG Fc (Cappel, Westchester, PA) for capture and horseradish peroxidase-labeled goat anti-human Fc (Cappel) for detection. Human IgG1 (Chemicon) was used as standard.

VEGF Binding Assays. For measuring the VEGF binding activity of F(ab)s, ELISA plates were coated with 2 μg/ml rabbit $F(ab')_2$ to human IgG Fc (Jackson ImmunoResearch, West Grove, PA) and blocked with blocking buffer (described above). Diluted conditioned medium containing 3 ng/ml of KDR-IgG (40) in blocking buffer were incubated on the plate for 1 h. Standards [6.9–440 ng/ml chimeric F(ab)] and 2-fold serial dilutions of samples were incubated with 2 nM biotinylated VEGF for 1 h in tubes. The solutions from the tubes were then transferred to the ELISA plates and incubated for 1 h. After washing, biotinylated VEGF bound to KDR was detected using horseradish peroxidase-labeled streptavidin (Zymed, South San Francisco, CA or Sigma) followed by 3,3',5,5'-tetramethylbenzidine as the substrate. Titration curves were fit with a four-parameter nonlinear regression curve-fitting program (KaleidaGraph; Synergy Software, Reading, PA). Concentrations of F(ab) variants corresponding to the midpoint absorbance of the titration curve of the standard were calculated and then divided by the concentration of the standard corresponding to the midpoint absorbance of the standard titration curve. Assays for full-length IgG were the same as for the F(ab)s except that the assay buffer contained 10% human serum.

BIAcore Biosensor Assays. VEGF binding of the humanized and chimeric F(ab)s were compared using a BIAcore biosensor (41). Concentrations of F(ab)s were determined by quantitative amino acid analysis. VEGF was coupled to a CM-5 biosensor chip through primary amine groups according to manufacturer's instructions (Pharmacia). Off-rate kinetics were measured by saturating the chip with F(ab) [35 μl of 2 μM F(ab) at a flow rate of 20 μl/min] and then switching to buffer (PBS-0.05% polysorbate 20). Data points from 0–4500 s were used for off-rate kinetic analysis. The dissociation rate constant (k_{off}) was obtained from the slope of the plot of $\ln(R0/R)$ *versus* time, where $R0$ is the signal at $t = 0$ and R is the signal at each time point.

On-rate kinetics were measured using 2-fold serial dilutions of F(ab) (0.0625–2 mM). The slope, K_s, was obtained from the plot of $\ln(-dR/dt)$ *versus* time for each F(ab) concentration using the BIAcore kinetics evaluation software as described in the Pharmacia Biosensor manual. R is the signal at time t. Data between 80 and 168, 148, 128, 114, 102, and 92 s were used for 0.0625, 0.125, 0.25, 0.5, 1, and 2 mM F(ab), respectively. The association rate constant (k_{on}) was obtained from the slope of the plot of K_s *versus* F(ab) concentration. At the end of each cycle, bound F(ab) was removed by injecting 5 μl of 50 mM HCl at a flow rate of 20 μl/min to regenerate the chip.

Endothelial Cell Growth Assay. Bovine adrenal cortex-derived capillary endothelial cells were cultured in the presence of low glucose DMEM (Life Technologies, Inc.) supplemented with 10% calf serum, 2 mM glutamine, and antibiotics (growth medium), essentially as described previously (42). For mitogenic assays, endothelial cells were seeded at a density of 6×10^3 cells/well in 6-well plates in growth medium. Either muMAb VEGF A.4.6.1 or rhuMAb VEGF was then added at concentrations ranging between 1 and 5000 ng/ml. After 2–3 h, purified *E. coli*-expressed $rhVEGF_{165}$ was added to a final concentration of 3 ng/ml. For specificity control, each antibody was added to endothelial cells at the concentration of 5000 ng/ml, either alone or in the presence of 2 ng/ml bFGF. After 5 or 6 days, cells were dissociated by exposure to trypsin, and duplicate wells were counted in a Coulter counter (Coulter Electronics, Hialeah, FL). The variation from the mean did not exceed 10%. Data were analyzed by a four-parameter curve fitting program (KaleidaGraph).

***In Vivo* Tumor Studies.** Human A673 rhabdomyosarcoma cells (American Type Culture Collection; CRL 1598) were cultured as described previously in DMEM/F12 supplemented with 10% fetal bovine serum, 2 mM glutamine, and antibiotics (20, 22). Female BALB/c nude mice, 6–10 weeks old, were injected s.c. with 2×10^6 tumor cells in the dorsal area in a volume of 200 μl. Animals were then treated with muMAb VEGF A.4.6.1, rhuMAb VEGF, or a control murine MAb directed against the gp120 protein. Both anti-VEGF MAbs were administered at the doses of 0.5 and 5 mg/kg; the control MAb was given at the dose of 5 mg/kg. Each MAb was administered twice weekly i.p. in a volume of 100 μl, starting 24 h after tumor cell inoculation. Each group consisted of 10 mice. Tumor size was determined at weekly intervals. Four weeks after tumor cell inoculation, animals were euthanized, and the tumors were removed and weighed. Statistical analysis was performed by ANOVA.

RESULTS

Humanization. The consensus sequence for the human heavy chain subgroup III and the light chain subgroup κ I were used as the framework for the humanization (Ref. 30; Fig. 1). This framework has been successfully used in the humanization of other murine antibodies (31, 32, 43, 44). All humanized variants were initially made and screened for binding as F(ab)s expressed in *E. coli*. Typical yields from 500-ml shake flasks were 0.1–0.4 mg F(ab).

Two definitions of CDR residues have been proposed. One is based on sequence hypervariability (30) and the other on crystal structures of F(ab)-antigen complexes (45). The sequence-based CDRs are larger than the structure-based CDRs, and the two definitions are in agreement except for CDR-H1; CDR-H1 includes residues H31–H35 according to the sequence-based definition, and residues H26–H32 according to the structure-based definition (light chain residue numbers are prefixed with L; heavy chain residue numbers are prefixed with H). We, therefore, defined CDR-H1 as a combination of the two, *i.e.*, including residues H26–H35. The other CDRs were defined using the sequence-based definition (30).

The chimeric F(ab) was used as the standard in the binding assays. In the initial variant, F(ab)-1, the CDR residues were transferred from the murine antibody to the human framework and, based on the models of the murine and humanized F(ab)s, the residue at position H49 (Ala in humans) was changed to the murine Gly. In addition, F(ab)s that consisted of the chimeric heavy chain/F(ab)-1 light chain [F(ab)-2] and F(ab)-1 heavy chain/chimeric light chain [F(ab)-3] were generated and tested for binding. F(ab)-1 exhibited a binding affinity greater than 1000-fold reduced from the chimeric F(ab) (Table 1). Comparing the binding affinities of F(ab)-2 and F(ab)-3 suggested that framework residues in the F(ab)-1 VH domain needed to be altered to increase binding.

Previous humanizations (31, 32, 43, 44) as well as studies of F(ab)-antigen crystal structures (45, 47) have shown that residues H71 and H73 can have a profound effect on binding, possibly by influencing the conformations of CDR-H1 and CDR-H2. Changing the human residues to their murine counterparts in F(ab)-4 improved binding by 4-fold (Table 1). Inspection of the models of the murine

Variable Heavy

```
A.4.6.1    EIQLVQSGPELKQPGETVRISCKASGYTFTNYGMNWVKQAPGKGLKWMG
F(ab)-12   EVQLVESGGGLVQPGGSLRLSCAASGYTFTNYGMNWVRQAPGKGLEWVG
humIII     EVQLVESGGGLVQPGGSLRLSCAASGFTFSSYAMSWVRQAPGKGLEWVS
           1         10        20        30        40

A.4.6.1    MINTYTGEPTYAADFKRRFTFSLETSASTAYLQISNLKNDDTATYFCAK
F(ab)-12   MINTYTGEPTYAADFKRRFTFSLDTSKSTAYLQMNSLRAEDTAVYYCAK
humIII     VISGDGGSTYYADSVKGRFTISRDNSKNTLYLQMNSLRAEDTAVYYCAR
           50  a      60        70        80  abc   90

A.4.6.1    YPHYYGSSHWYFDVWGAGTTVTVSS
F(ab)-12   YPHYYGSSHWYFDVWGQGTLVTVSS
humIII     G----------FDYWGQGTLVTVSS
                      110
```

Variable Light

```
A.4.6.1    DIQMTQTTSSLSASLGDRVIISCSASQDISNYLNWYQQKPDGTVKVLIY
F(ab)-12   DIQMTQSPSSLSASVGDRVTITCSASQDISNYLNWYQQKPGKAPKVLIY
humKI      DIQMTQSPSSLSASVGDRVTITCRASQSISNYLAWYQQKPGKAPKLLIY
           1         10        20        30        40

A.4.6.1    ETSSLHSGVPSRFSGSGSGTDYSLTISNLEPEDIATYYCQQYSTVPWTF
F(ab)-12   ETSSLHSGVPSRFSGSGSGTDFTLTISSLQPEDFATYYCQQYSTVPWTF
humKI      AASSLESGVPSRFSGSGSGTDFTLTISSLQPEDFATYYCQQYNSLPWTF
           50        60        70        80        90

A.4.6.1    GGGTKLEIKR
F(ab)-12   GQGTKVEIKR
humKI      GQGTKVEIKR
           100
```

Fig. 1. Amino acid sequence of variable heavy and light domains of muMAbVEGF A.4.6.1 humanized F(ab) with optimal VEGF binding [F(ab)-12] and human consensus frameworks (*humIII*, heavy subgroup III; *humKI*, light κ subgroup I). *Asterisks*, differences between humanized F(ab)-12 and the murine MAb or between F(ab)-12 and the human framework. CDRs are *underlined*.

and humanized F(ab)s suggested that residue L46, buried at the VL-VH interface and interacting with CDR-H3 (Fig. 2), might also play a role either in determining the conformation of CDR-H3 and/or affecting the relationship of the VL and VH domains. When the murine Val was exchanged for the human Leu at L46 [F(ab)-5], the binding affinity increased by almost 4-fold (Table 1). Three other buried framework residues were evaluated based on the molecular models: H49, H69, and H78. Position H69 may affect the conformation of CDR-H2, whereas position H78 may affect the conformation of CDR-H1 (Fig. 2). When each was individually changed from the human to murine counterpart, the binding improved by 2-fold in each case [F(ab)-6 and F(ab)-7; Table 1]. When both were simultaneously changed, the improvement in binding was 8-fold [F(ab)-8; Table 1]. Residue H49 was originally included as the murine Gly; when changed to the human consensus counterpart Ala, the binding was reduced by 15-fold [F(ab)-9; Table 1].

We have found during previous humanizations that residues in a framework loop, FR-3 (30) adjacent to CDR-H1 and CDR-H2, can affect binding (44). In F(ab)-10 and F(ab)-11, two residues in this loop were changed to their murine counterparts: AsnH76 to murine Ser [F(ab)-10] and LysH75 to murine Ala [F(ab)-11]. Both effected a relatively small improvement in binding (Table 1). Finally, at position H94, human and murine sequences most often have an Arg (30). In F(ab)-12, this Arg was replaced by the rare Lys found in the murine antibody (Fig. 1), and this resulted in binding that was less than 2-fold from the chimeric F(ab) (Table 1). F(ab)-12 was also compared to the chimeric F(ab) using the BIAcore system (Pharmacia). Using this technique, the K_d of the humanized F(ab)-12 was 2-fold weaker than that of the chimeric F(ab) due to both a slower k_{on} and faster k_{off} (Table 2).

Full-length MAbs were constructed by fusing the VL and VH domains of the chimeric F(ab) and variant F(ab)-12 to the constant domains of human κ light chain and human IgG1 heavy chain. The full-length 12-IgG1 [F(ab)-12 fused to human IgG1] exhibited binding that was 1.7-fold weaker than the chimeric IgG1 (Table 3). Both 12-IgG1 and the chimeric IgG1 bound slightly less well than the original muMAb VEGF A.4.6.1 (Table 3).

Biological Studies. rhuMAb VEGF and muMAb VEGF A.4.6.1 were compared for their ability to inhibit bovine capillary endothelial cell proliferation in response to a near maximally effective concentration of $VEGF_{165}$ (3 ng/ml). In several experiments, the two MAbs were found to be essentially equivalent, both in potency and efficacy. The ED_{50}s were, respectively, 50 ± 5 and 48 ± 8 ng/ml (~0.3 nM). In both cases, 90% inhibition was achieved at the concentration of 500 ng/ml (~3 nM). Fig. 3 illustrates a representative experiment. Neither muMAb VEGF A.4.6.1 nor rhuMAb VEGF had any effect on basal or bFGF-stimulated proliferation of capillary endothelial cells (data not shown), confirming that the inhibition is specific for VEGF.

To determine whether similar findings could be obtained also in an *in vivo* system, we compared the two antibodies for their ability to suppress the growth of human A673 rhabdomyosarcoma cells in nude mice. Previous studies have shown that muMAb VEGF A.4.6.1 has a dramatic inhibitory effect in this tumor model (20, 22). As shown in Fig. 4, at both doses tested (0.5 and 5 mg/kg), the two antibodies markedly suppressed tumor growth as assessed by tumor weight measurements 4 weeks after cell inoculation. The decreases in tumor weight compared to the control group were, respectively, 85 and 93% at each dose in the animals treated with muMAb VEGF A.4.6.1 *versus* 90 and 95% in those treated with rhuMAb VEGF. Similar results were obtained with the breast carcinoma cell line MDA-MB 435 (data not shown).

DISCUSSION

The murine MAb A.4.6.1, directed against human VEGF (42), was humanized using the same consensus frameworks for the light and heavy chains used in previous humanizations (31, 32, 43, 44), *i.e.*, VκI and VHIII (30). Simply transferring the CDRs from the murine antibody to the human framework resulted in a F(ab) that exhibited binding to VEGF reduced by over 1000-fold compared to the parent murine antibody. Seven non-CDR, framework residues in the VH domain and one in the VL domain were altered from human to murine to achieve binding equivalent to the parent murine antibody.

In the VH domain, residues at positions H49, H69, H71, and H78 are buried or partially buried and probably effect binding by influencing the conformation of the CDR loops. Residues H73 and H76 should be solvent exposed (Fig. 2) and hence may interact directly with the VEGF; these two residues are in a non-CDR loop adjacent to CDRs H1 and H2 and have been shown to play a role in binding in previous humanizations (31, 32, 44). The requirement for lysine at position H94 was surprising given that this residue is arginine in the human framework (Fig. 1). In some crystal structures of F(ab)s, ArgH94 forms a hydrogen-bonded salt-bridge with

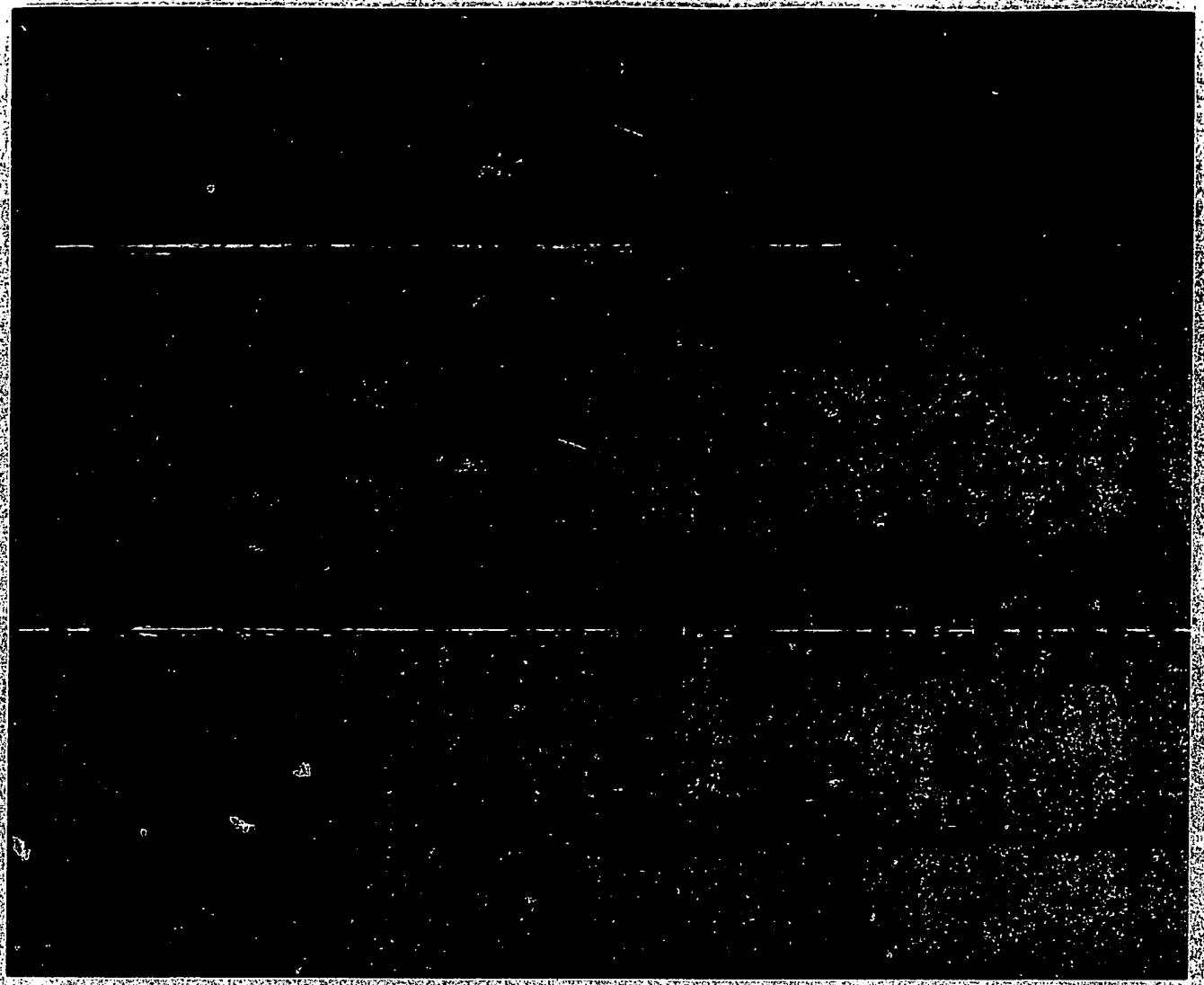

Fig. 2. Ribbon diagram of the model of humanized F(ab)-12 VL and VH domains. VL domain is shown in *brown* with CDRs in *tan*. The side chain of residue L46 is shown in *yellow*. VH domain is shown in *purple* with CDRs in *pink*. Side chains of VH residues changed from human to murine are shown in *yellow*.

Table 2 *Binding of anti-VEGF F(ab) variants to VEGF using the BIAcore system*[a]

Variant	Amount of (Fab) bound (RU)	k_{off} (s^{-1})	k_{on} ($M^{-1}s^{-1}$)	K_d (nM)
chim-F(ab)[b]	4250	5.9×10^{-5}	6.5×10^{4}	0.91
F(ab)-12	3740	6.3×10^{-5}	3.5×10^{4}	1.8

[a] The amount of F(ab) bound, in resonance units (RU), was measured using a BIAcore system when 2 μg F(ab) was injected onto a chip containing 2480 RU of immobilized VEGF. Off-rate kinetics (k_{off}) were measured by saturating the chip with F(ab) and then monitoring dissociation after switching to buffer. On-rate kinetics (k_{on}) were measured using 2-fold serial dilutions of F(ab). K_d, the equilibrium dissociation constant, was calculated as k_{off}/k_{on}.

[b] chim-F(ab) is a chimeric F(ab) with murine VL and VH domains fused to human CL and CH1 heavy domains.

AspH101 (33, 48). Substitution of lysine for arginine might conceivably alter this salt-bridge and perturb the conformation of CDR-H3.

In the VL domain, only one framework residue had to be changed to murine to optimize the humanization. Position L46 is at the VL-VH interface, where it is buried and interacts directly with CDR-H3 (Fig. 2). The requirement for murine valine (as opposed to human leucine) implies that this residue plays an important role in the conformation of CDR-H3. The necessity of retaining LysH94 in VH, which is also adjacent to CDR-H3, suggests that CDR-H3 plays a major role in the binding of the antibody to VEGF.

The humanized version with optimal binding, 12-IgG1, exhibited only a 2-fold reduction in binding compared to the parent murine antibody (Table 3). An analysis of the binding kinetics of the humanized and chimeric F(ab)s showed that both had similar off-rates but that the humanized F(ab) had a 2-fold slower on-rate (Table 2), which accounts for the 2-fold reduction in binding. However, this modest reduction in on-rate did not result in any decreased ability to antagonize VEGF bioactivity. The two anti-

Table 3 *Binding of anti-VEGF IgG variants to VEGF*[a]

Variant	IgG1/chIgG1[b] Mean	SD	N
chIgG1	1.0		2
murIgG1[c]	0.759	0.001	2
12-IgG1[d]	1.71	0.03	2

[a] Anti-VEGF IgG variants were incubated with biotinylated VEGF and then transferred to ELISA plates coated with KDR-IgG (40).

[b] chIgG1 is chimeric IgG1 with murine VL and VH domains fused to human CL and IgG1 heavy chains; the EC_{50} for chIgG1 was 0.113 ± 0.013 μg/ml (0.75 nM).

[c] murIgG1 is muMAb VEGF A.4.6.1 purified from ascites.

[d] 12-IgG1 is F(ab)-12 VL and VH domains fused to human CL and IgG1 heavy chains.

bodies had essentially identical activity, both in an endothelial cell proliferation assay and in an *in vivo* tumor model.

Interestingly, an alternative approach using monovalent phage display has been also applied to the humanization of muMAb VEGF A.4.6.1. (49). Random mutagenesis of framework residues resulted in selection of variants with significantly improved affinity compared to the initial humanized MAb with no framework changes. However, the best variant obtained by this method had a less complete restoration of the binding affinity of muMAb VEGF A.4.6.1 compared to that reported in this study (49). Clearly, this does not rule out the possibility that other applications of phage display, such as affinity maturation of the CDRs (50), may result in variants with even higher affinity.

In conclusion, protein engineering techniques resulted in virtually complete acquisition by a human immunoglobulin framework of the binding properties and biological activities of a high-affinity murine anti-VEGF MAb. In view of the nearly ubiquitous up-regulation of VEGF mRNA in human tumors (12–16) and the ability of muMAb VEGF A.4.6.1 to inhibit the *in vivo* growth of a broad spectrum of tumor cell lines (20–23), VEGF is a major target of anticancer therapy. Clinical trials using rhuMAb VEGF should allow us to test the hypothesis that inhibition of VEGF-mediated angiogenesis is an effective strategy for the treatment of several solid tumors in humans. Such trials are already under way. Other important clinical applications of rhuMAb VEGF include the prevention of blindness secondary to proliferative diabetic retinopathy (17) or AMD (18). Clearly, the success of the humanization can be ultimately judged by the degree of anti-human globulin response and and by the clinical response in patients. However, the recent report of a Phase II study where rhuMAb HER2, a humanized MAb with the same framework as rhuMAb VEGF, did not induce any anti-globulin response in breast cancer patients and also demonstrated clinical efficacy (51), makes one optimistic. The results of this (51) as well as other (52) trials raise hope that, after many disappointing results (53), progress in antibody technology, coupled with selection of better targets, will bring therapy with MAbs closer to fulfilling its promises.

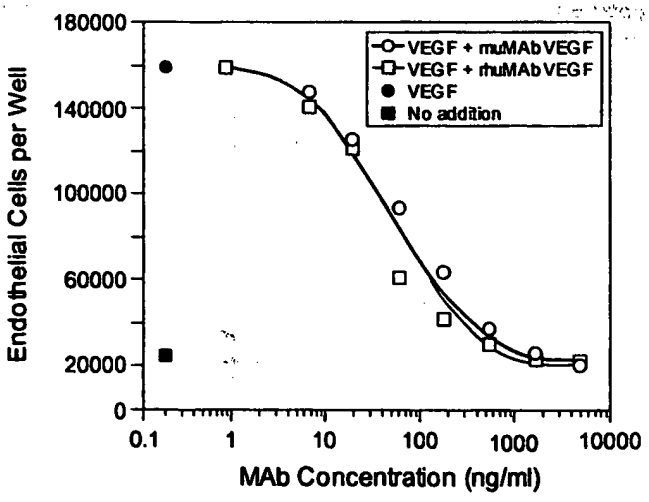

Fig. 3. Inhibition of VEGF-induced mitogenesis. Bovine adrenal cortex-derived capillary endothelial cells were seeded at the density of 6×10^3 cells/well in six-well plates, as described in "Materials and Methods." Either muMAb VEGF A.4.6.1 or rhuMAb VEGF (IgG1) was added at the indicated concentrations. After 2–3 h, $rhVEGF_{165}$ was added at the final concentration of 3 ng/ml. After 5 or 6 days, cells were trypsinized and counted. Values shown are means of duplicate determinations. The variation from the mean did not exceed 10%.

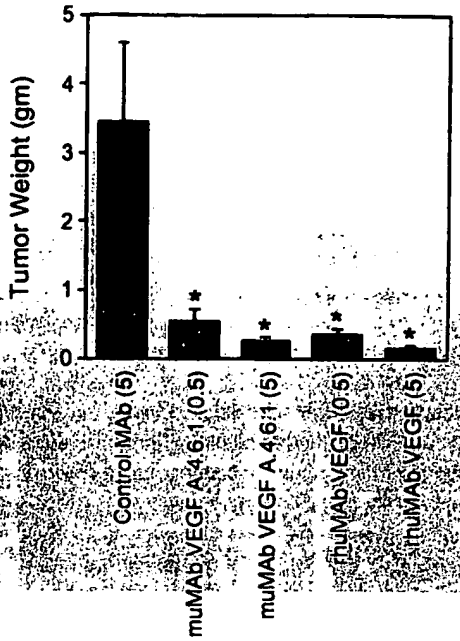

Fig. 4. Inhibition of tumor growth *in vivo*. A673 rhabdomyosarcoma cells were injected in BALB/c nude mice at the density of 2×10^6 per mouse. Starting 24 h after tumor cell inoculation, animals were injected with a control MAb, muMAb VEGF A.4.6.1, or rhuMab VEGF (IgG1) twice weekly, i.p. The dose of the control MAb was 5 mg/kg; the anti-VEGF MAbs were given at 0.5 or 5 mg/kg, as indicated ($n = 10$). Four weeks after tumor cell injection, animals were euthanized, and tumors were removed and weighed. * significant difference when compared to the control group by ANOVA ($P < 0.05$).

ACKNOWLEDGMENTS

We thank K. Garcia for performing the VEGF binding ELISA, W. Henzel for protein microsequencing, A. Padua for amino acid analysis, J. Bourell for mass spectrometry, and J. Silva for animal studies. We are grateful to the DNA synthesis and the DNA sequencing groups at Genentech. We also thank C. Adams, J. Kim, B. Fendly, B. Keyt, and M. Beresini for helpful comments and advice.

REFERENCES

1. Folkman, J., and Shing, Y. Angiogenesis. J. Biol. Chem., *267:* 10931–10934, 1992.
2. Klagsbrun, M., and D'Amore, P. A. Regulators of angiogenesis. Annu. Rev. Physiol., *53:* 217–239, 1991.
3. Garner, A. Vascular diseases. *In:* A. Garner and G. K. Klintworth (eds.), Pathobiology of Ocular Disease. A Dynamic Approach, Ed. 2, pp. 1625–1710. New York: Marcel Dekker, 1994.
4. Weidner, N., Semple, P., Welch, W., and Folkman, J. Tumor angiogenesis and metastasis. Correlation in invasive breast carcinoma. N. Engl. J. Med., *324:* 1–6, 1991.
5. Horak, E. R., Leek, R., Klenk, N., Lejeune, S., Smith, K., Stuart, M., Greenall, M., and Harris, A. Quantitative angiogenesis assessed by anti-PECAM antibodies: correlation with node metastasis and survival in breast cancer. Lancet, *340:* 1120–1124, 1992.
6. Macchiarini, P., Fontanini, G., Hardin, M. J., Squartini, F., and Angeletti, C. A. Relation of neovascularization to metastasis of non-small cell lung carcinoma. Lancet, *340:* 145–146, 1992.
7. Good, D., Polverini, P., Rastinejad, F., Beau, M., Lemons, R., Frazier, W., and Bouck, N. A tumor suppressor-dependent inhibitor of angiogenesis is immunologically and functionally indistinguishable from a fragment of thrombospondin. Proc. Natl. Acad. Sci. USA, *87:* 6624–6628, 1990.
8. Clapp, C., Martial, J. A., Guzman, R. C., Rentier-Delrue, F., and Weiner, R. I. The 16-kilodalton N-terminal fragment of human prolactin is a potent inhibitor of angiogenesis. Endocrinology, *133:* 1292–1299, 1993.
9. O'Reilly, M. S., Holmgren, L., Shing, Y., Chen, C., Rosenthal, R. A., Mosem, M., Lane, W. S., Cao, Y., Sage, E. H., and Folkman, J. Angiostatin. A novel angiogenesis inhibitor that mediates the suppression of metastasis by a Lewis lung carcinoma. Cell, *79:* 315–328, 1994.
10. O'Reilly, M. S., Boehm, T., Shing, Y., Fukai, N., Vasios, G., Lane, W. S., Flynn, E., Birkhead, J. R., Olsen, B. R., and Folkman, J. Endostatin. An endogenous inhibitor of angiogenesis and tumor growth. Cell, *88:* 277–285, 1996.
11. Ferrara, N., and Davis Smyth, T. The biology of vascular endothelial growth factor. Endocr. Rev., *18:* 4–25, 1997.

12. Berkman, R. A., Merrill, M. J., Reinhold, W. C., Monacci, W. T., Saxena, A., Clark, W. C., Robertson, J. T., Ali, I. U., and Oldfield, E. H. Expression of the vascular permeability/vascular endothelial growth factor gene in central nervous system neoplasms. J. Clin. Invest., *91:* 153–159, 1993.
13. Brown, L. F., Berse, B., Jackman, R. W., Guidi, A. J., Dvorak, H. F., Senger, D. R., Connolly, J. L., and Schnitt, S. J. Expression of vascular permeability factor (vascular endothelial growth factor) and its receptors in breast cancer. Hum. Pathol., *26:* 86–91, 1995.
14. Brown, L. F., Berse, B., Jackman, R. W., Tognazzi, K., Manseau, E. J., Senger, D. R., and Dvorak, H. F. Expression of vascular permeability factor (vascular endothelial growth factor) and its receptors in adenocarcinomas of the gastrointestinal tract. Cancer Res., *53:* 4727–4735, 1993.
15. Mattern, J., Koomagi, R., and Volm, M. Association of vascular endothelial growth factor expression with intratumoral microvessel density and tumour cell proliferation in human epidermoid lung carcinoma. Br. J. Cancer, *73:* 931–934, 1996.
16. Dvorak, H. F., Brown, L. F., Detmar, M., and Dvorak, A. M. Vascular permeability factor/vascular endothelial growth factor, microvascular permeability and angiogenesis. Am. J. Pathol., *146:* 1029–1039, 1995.
17. Aiello, L. P., Avery, R., Arrigg, R., Keyt, B., Jampel, H., Shah, S., Pasquale, L., Thieme, H., Iwamoto, M., Park, J. E., Nguyen, H., Aiello, L. M., Ferrara, N., and King, G. L. Vascular endothelial growth factor in ocular fluid of patients with diabetic retinopathy and other retinal disorders. N. Engl. J. Med., *331:* 1480–1487, 1994.
18. Lopez, P. F., Sippy, B. D., Lambert, H. M., Thach, A. B., and Hinton, D. R. Transdifferentiated retinal pigment epithelial cells are immunoreactive for vascular endothelial growth factor in surgically excised age-related macular degeneration-related choroidal neovascular membranes. Invest. Ophthalmol. Visual Sci., *37:* 855–868, 1996.
19. Kim, K. J., Li, B., Houck, K., Winer, J., and Ferrara, N. The vascular endothelial growth factor proteins: identification of biologically relevant regions by neutralizing monoclonal antibodies. Growth Factors, *7:* 53–64, 1992.
20. Kim, K. J., Li, B., Winer, J., Armanini, M., Gillett, N., Phillips, H. S., and Ferrara, N. Inhibition of vascular endothelial growth factor-induced angiogenesis suppresses tumour growth *in vivo*. Nature (Lond.), *362:* 841–844, 1993.
21. Warren, R. S., Yuan, H., Matli, M. R., Gillett, N. A., and Ferrara, N. Regulation by vascular endothelial growth factor of human colon cancer tumorigenesis in a mouse model of experimental liver metastasis. J. Clin. Invest., *95:* 1789–1797, 1995.
22. Borgstrom, P., Hillan, K. J., Sriramarao, P., and Ferrara, N. Complete inhibition of angiogenesis and growth of microtumors by anti-vascular endothelial growth factor neutralizing antibodies: Novel concepts of angiostatic therapy from intravital videomicroscopy. Cancer Res., *56:* 4032–4039, 1996.
23. Melnyk, O., Schuman, M. A., and Kim, K. J. Vascular endothelial growth factor promotes tumor dissemination by a mechanism distinct from its effect on primary tumor growth. Cancer Res., *56:* 921–924, 1996.
24. Adamis, A. P., Shima, D. T., Tolentino, M., Gragoudas, E., Ferrara, N., Folkman, J., D'Amore, P. A., and Miller, J. W. Inhibition of VEGF prevents retinal ischemia-associated iris neovascularization in a primate. Arch. Ophthalmol., *114:* 66–71, 1996.
25. Miller, R. A., Oseroff, A. R., Stratte, P. T., and Levy, R. Monoclonal antibody therapeutic trials in seven patients with T-cell lymphoma. Blood, *62:* 988–995, 1983.
26. Schroff, R. W., Foon, K. A., Beatty, S. M., Oldham, R. K., and Morgan, A. C. Jr. Human anti-murine immunoglobulin response in patients receiving monoclonal antibody therapy. Cancer Res., *45:* 879–885, 1985.
27. Neuberger, M. S., Williams, G. T., Mitchell, E. B., Jouhal, S. S., Flanagan, J. G., and Rabbits, T. H. A hapten-specific chimaeric IgE antibody with human physiological effector function. Nature (Lond.), *314:* 268–270, 1985.
28. Jones, P. T., Dear, P. H., Foote, J., Neuberger, M. S., and Winter, G. Replacing the complementarity-determining regions in a human antibody with those from a mouse. Nature (Lond.), *321:* 522–525, 1986.
29. Riechman, L., Clark, M., Waldmann, H., and Winter, G. Reshaping human antibodies for therapy. Nature (Lond.), *332:* 323–327, 1988.
30. Kabat, E. A., Wu, T. T., Perry, H. M., Gottesmann, K. S., and Foeller, C. Sequences of proteins of immunological interest, Ed. 5. Public Health Service, National Institutes of Health, Bethesda, MD, 1991.
31. Werther, W. A., Gonzalez, T. N., O'Connor, S. J., McCabe, S., Chan, B., Hotaling, T., Champe, M., Fox, J. A., Jardieu, P. M., Berman, P. W., and Presta, L. G. Humanization of an anti-lymphocyte function-associated antigen (LFA)-1 monoclonal antibody and reengineering of the humanized antibody for binding to rhesus LFA-1. J. Immunol., *157:* 4986–4995, 1996.
32. Carter, P., Presta, L., Gorman, C. M., Ridgway, J. B. B., Henner, D., Wong, W. L. T., Rowland, A. M., Kotts, C., Carver, M. E., and Shepard, H. M. Humanization of an anti-p185HER2 antibody for human cancer therapy. Proc. Natl. Acad. Sci. USA, *89:* 4285–4289, 1992.
33. Eigenbrot, C., Randal, M., Presta, L., and Kossiakoff, A. A. X-ray structures of the antigen-binding domains from three variants of humanized anti-p185HER2 antibody 4D5 and comparison with molecular modeling. J. Mol. Biol., *229:* 969–995, 1993.
34. Kunkel, T. A. Rapid and efficient site-specific mutagenesis without phenotypic selection. Proc. Natl. Acad. Sci. USA, *82:* 488–492, 1985.
35. Eaton, D. L., Wood, W. I., Eaton, D., Hass, P. E., Hollingshead, P., Wion, K., Mather, J., Lawn, R. M., Vehar, G. A., and Gorman, C. Construction, and characterization of an active factor VIII variant lacking the central one-third of the molecule. Biochemistry, *25:* 8343–8347, 1986.
36. Graham, F. L., Smiley, J., Russell, W. C., and Nairn, R. Characteristics of a human cell line transformed by DNA from human adenovirus type 5. J. Gen. Virol., *36:* 59–74, 1977.
37. Gorman, C. M., Gies, D. R., and McCray, G. Transient production of proteins using an adenovirus transformed cell line. DNA Prot. Eng. Tech., *2:* 3–10, 1990.
38. Lucas, B. K., Giere, L. M., DeMarco, R. A., Chisholm, V., and Crowley, C. W. High-level production of recombinant proteins in CHO cells using a dicistronic DHFR intron expression vector. Nucleic Acids Res., *24:* 1774–1779, 1996.
39. Chisholm, V. High efficiency gene transfer in mammalian cells. *In:* D. M. Glover and B. D. Hames (eds.), DNA Cloning 4: Mammalian systems, pp. 1–41. Oxford: Oxford University Press, 1996.
40. Park, J. E., Chen, H., Winer, J., Houck, K. A., and Ferrara, N. Placenta growth factor. Potentiation of VEGF bioactivity, *in vitro* and *in vivo*, and high affinity binding to Flt-1 but not to Flk-1/KDR. J. Biol. Chem., *269:* 25646–25645, 1994.
41. Karlsson, R., Roos, H., Fagerstam, L., and Persson, B. Kinetic and concentration analysis using BIA technology. Methods: A Companion to Methods in Enzymology, Vol. 6, pp. 97–108, 1994.
42. Leung, D. W., Cachianes, G., Kuang, W-J., Goeddel, D. V., and Ferrara, N. Vascular endothelial growth factor is a secreted angiogenic mitogen. Science (Washington DC), *246:* 1306–1309, 1989.
43. Presta, L. G., Lahr, S. J., Shields, R. L., Porter, J. P., Gorman, C. M., Fendly, B. M., and Jardieu, P. M. Humanization of an antibody directed against IgE. J. Immunol., *151:* 2623–2632, 1993.
44. Eigenbrot, C., Gonzalez, T., Mayeda, J., Carter, P., Werther, W., Hotaling, T., Fox, J., and Kessler, J. X-ray structures of fragments from binding and nonbinding versions of a humanized anti-CD18 antibody: structural indications of the key role of VH residues 59 to 65. Proteins, *18:* 49–62, 1994.
45. Chothia, C., Lesk, A. M., Tramontano, A., Levitt, M., Smith-Gill, S. J., Air, G., Sheriff, S., Padlan, E. A., Davies, D., Tulip, W. R., Colman, P. M., Spinelli, S., Alzari, P. M., and Poljak, R. J. Conformations of immunoglobulin hypervariable regions. Nature (Lond.), *342:* 877–883, 1989.
46. Xiang, J., Sha, Y., Jia, Z., Prasad, L., and Delbaere, L. T. Framework residues 71 and 93 of the chimeric B72.3 antibody are major determinants of the conformation of heavy-chain hypervariable loops. J. Mol. Biol., *253:* 385–390, 1995.
47. Tramontano, A., Chothia, C., and Lesk, A. M. Framework residue 71 is a major determinant of the position and conformation of the second hypervariable region in the VH domains of immunoglobulins. J. Mol. Biol., *215:* 175–182, 1990.
48. Fischmann, T. O., Bentley, G. A., Bhat, T. N., Boulot, G., Mariuzza, R. A., Phillips, S. E. V., Tello, D., and Poljak, R. J. Crystallographic refinement of the three-dimensional structure of the FabD1.3-lysozyme complex at 2.5-Å resolution. J. Biol. Chem., *266:* 12915–12920, 1994.
49. Baca, M., Presta, L. G., O'Connor, S. J., and Wells, J. A. Antibody humanization using monovalent phage display. J. Biol. Chem., *272:* 10678–10684, 1997.
50. Barbas, C. F., III. Selection and evolution of high-affinity anti-viral antibodies. Trends Biotechnol., *14:* 230–234, 1996.
51. Baselga, J., Tripathy, D., Mendelsohn, J., Baughman, S., Benz, C. C., Dantis, L., Sklarin, N. T., Seidman, A. D., Hudis, C. A., Moore, J., Rosen, P. P., Twaddell, T., Henderson, I. C., and Norton, L. Phase II study of weekly intravenous recombinant humanized anti-p185^{HER2} monoclonal antibody in patients with HER2/neu overexpressing metastatic breast cancer. J. Clin. Oncol., *14:* 737–744, 1996.
52. von Mehren, M., and Weiner, L. M. Monoclonal antibody-based therapy. Curr. Opin. Oncol., *8:* 493–498, 1996.
53. Riethmuller, G., Schneider-Gadicke, E., and Johnson, J. P. Monoclonal antibodies in cancer therapy. Curr. Opin. Immunol., *5:* 732–739, 1993.